

ספריות הטכניון *The Technion Libraries*

בית הספר ללימודים מוסמכים ע"ש ארוין וג'ואן ג'ייקובס
Irwin and Joan Jacobs Graduate School

©
All rights reserved to the author

This work, in whole or in part, may not be copied (in any media), printed, translated, stored in a retrieval system, transmitted via the internet or other electronic means, except for "fair use" of brief quotations for academic instruction, criticism, or research purposes only. Commercial use of this material is completely prohibited.

©
כל הזכויות שמורות למחבר/ת

אין להעתיק (במדיה כלשהי), להדפיס, לתרגם, לאחסן במאגר מידע, להפיצו באינטרנט, חיבור זה או כל חלק ממנו, למעט "שימוש הוגן" בקטעים קצרים מן החיבור למטרות לימוד, הוראה, ביקורת או מחקר. שימוש מסחרי בחומר הכלול בחיבור זה אסור בהחלט.

Study of the Dynamics of the Quantum Vacuum using Ramsey Interference

Research thesis

In Partial Fulfillment of the Requirements
for the Degree of Doctor of Philosophy

Tal Goren

Submitted to the Senate of the Technion - Israel Institute of Technology

Iyar, 5774 Haifa July, 2016

The research thesis was done
under the supervision of Professor Eric Akkermans
in the Department of Physics

The generous financial help of the technion is gratefully
acknowledged

Contents

List of Figures	iii
Abstract	1
Abbreviations and Notations	3
1 Introduction	5
2 Ramsey interference – Introduction	7
2.1 Ramsey interference in two-level systems	7
2.2 Ramsey interference as a two slit experiment	10
3 Ramsey interference in mesoscopic physics	13
3.1 Quantum interference in a mesoscopic conductor	13
3.2 The tunnel junction – the simplest mesoscopic conductor	16
3.3 Probability for the creation of $e\text{-}h$ pairs	17
3.4 Current noise – Relation to the probability for the creation of $e\text{-}h$ pairs	19
3.5 Ramsey interference in the probability for the creation of $e\text{-}h$ pairs . . .	21
3.6 A recent experiment – Measurement of the second derivative of the shot noise	24
3.7 Ramsey interference in the presence of disorder	25
3.8 The effect of an electromagnetic environment	28
3.8.1 Quantum circuit theory	29
3.8.2 Tunnel junction embedded in an electric circuit	31
3.8.3 Probability for the creation of $e\text{-}h$ pairs in the presence of an environment	33
3.8.4 The effect of an electromagnetic environment on Ramsey interference	35
3.8.5 Current noise in the presence of an environment	37
3.8.6 Ohmic environment - Crossover from ballistic to diffusive regimes	38
4 Ramsey interference and Schwinger effect	43
4.1 Introduction to Schwinger physics	44
4.1.1 “in/out” spinors	45
4.1.2 Adiabatic spinors	46
4.2 Description of Schwinger effect as a TLS	47
4.2.1 Two-level system	48
4.2.2 The mapping	48
4.3 Ramsey interference	49
4.3.1 Scattering approach	50
4.3.2 Adiabatic-impulse approximation	53

5 Ramsey interference and dynamical Casimir effect	55
5.1 Introduction to the dynamical Casimir effect	56
5.2 Ramsey interference and number of photons	57
6 Summary	61
A Scattering approach to transport	63
A.1 Photon-assisted transport	64
A.2 Photon-assisted noise	66
A.3 Levitov-Lesovik approach	67
B Probability for the creation of $e-h$ pairs – Derivation	68
C Relation of the current noise to the probability for the creation of $e-h$ pairs – Derivation	71
D Tunnel junction phase as a quantum Brownian particle	74
D.1 Ohmic environment	74
D.1.1 High temperature limit	75
Bibliography	77

List of Figures

2.1	Ramsey probability for a TLS	9
2.2	Ramsey interference as a Young two slit experiment	11
3.1	Generating Ramsey interference in a tunnel junction	14
3.2	Illustration of a $e\text{-}h$ creation in a tunnel junction by a voltage pulse	16
3.3	Ramsey interference in the $e\text{-}h$ creation probability in a tunnel junction	23
3.4	Recent experiment - shot noise of a tunnel junction under bi-harmonic modulation	25
3.5	Illustration of the interfering trajectories	28
3.6	LC circuit	29
3.7	Tunnel junction in a linear electromagnetic environment	32
3.8	Illustration of a $e\text{-}h$ creation in a tunnel junction in a linear environment by a voltage pulse	35
3.9	Ramsey interference for the probability of a $e\text{-}h$ pair creation in the Coulomb blockade regime for different temperatures	41
3.10	Crossover between ballistic and diffusive regimes	42
4.1	$e\text{-}p$ creation in Schwinger effect vs. $e\text{-}h$ creation in a tunnel junction	44
4.2	Symmetric and anti-symmetric electric field modulation	50
4.3	Scattering problem for the symmetric and anti-symmetric electric field modulation	52
4.4	The symmetric and anti-symmetric adiabatic energies	53
5.1	Dynamical Casimir effect as a scattering problem	59
A.1	Scattering operators	63
A.2	Redistribution of the electrons in the photon assisted transport description	66
A.3	A $e\text{-}h$ creation process in the photon assisted transport and the tunneling descriptions	67

Abstract

We have generalized the Ramsey interference effect, a widely used spectroscopic tool in atomic physics, to quantum systems with a continuous frequency/energy spectrum. This generalization provides a method to probe new dynamical features of quantum mesoscopic systems by monitoring the time delay between two identically shaped pulses. By exploring the contrast of the Ramsey interference pattern, we have been able to access various dephasing processes affecting the quantum behavior of quasiparticles in mesoscopic conductors.

We have shown how the Ramsey interference pattern modifies the probability to create electron-hole pairs for the specific case of a tunnel junction as a working example of mesoscopic conductor. We have established a useful connection between this probability and the measurable power spectrum (shot noise).

Those general results have been implemented in the case of the dephasing induced on electron-hole pairs by an ohmic environment. We have found that the crossover between high and low impedances (e.g. between Coulomb blockade regime and Johnson noise) can be described using the corresponding behavior of a quantum Brownian particle, and it can be monitored by means of the time delay between the pulses in the Ramsey experimental setup.

Furthermore, we have implemented the Ramsey interference setup in order to investigate the dynamical amplification of vacuum fluctuations in the Schwinger and the dynamical Casimir effects, thus showing that Ramsey interference is useful to study a wide range of driven quantum systems beyond two-level systems as used in atomic spectroscopy.

Finally, we have found that the Schwinger effect can be understood as a two-level system which can be realized, for instance, by means of a NMR setup. This allows for further investigations of the so far, elusive Schwinger effect.

Abbreviations and Notations

TLS two-level system

QED quantum electrodynamics

NMR nuclear magnetic resonance

PDF probability distribution function

e-h electron-hole

e-p electron-positron

T tunneling matrix element

V_{dc} dc voltage

$V(t)$ time dependent voltage

$\phi(t)$ phase of the tunnel junction $\phi(t) = \frac{e}{\hbar} \int^t V(t') dt'$

ρ density of states

$S(\Omega)$ current noise at frequency Ω

shot noise current noise at zero frequency $S(\Omega) \rightarrow 0$

$P_{LR}(\Delta\epsilon)$ probability to create an electron in the left lead and a hole in the right lead as a function of the *e-h* pair energy $\Delta\epsilon$

$P_{RL}(\Delta\epsilon)$ probability to create an electron in the right lead and a left in the right lead as a function of the *e-h* pair energy $\Delta\epsilon$

ϵ_{Lk} energy of an electron in the left lead with momentum k

ϵ_{Rq} energy of an electron in the right lead with momentum q

$\vec{\sigma}$ vector of the Pauli matrices $\vec{\sigma} = (\sigma^1, \sigma^2, \sigma^3)$

σ^1 first Pauli matrix $\sigma^1 = \begin{pmatrix} 0 & 1 \\ 1 & 0 \end{pmatrix}$

σ^2 second Pauli matrix $\sigma^2 = \begin{pmatrix} 0 & -i \\ i & 0 \end{pmatrix}$

σ^3 third Pauli matrix $\sigma^3 = \begin{pmatrix} 1 & 0 \\ 0 & -1 \end{pmatrix}$

h Planck's constant $h = 6.62 \times 10^{-34} m^2 kg/sec$

\hbar reduced Planck's constant $\hbar = h/2\pi$

$R_K = h/e^2 = 25.8 \text{ k}\Omega$ quantum of resistance

Chapter 1

Introduction

An interesting consequence of quantum field theory is that something can be created from nothing. By dynamically amplifying quantum fluctuations, particles can be created from the vacuum. So far, static quantum effects such as the Casimir force and the Lamb shift have been verified experimentally [13, 14]. Dynamical amplification mechanisms such as the Schwinger [1], Unruh and dynamical Casimir effects are difficult to observe due to the extreme conditions under which they become noticeable. For example, the Schwinger effect requires strong laser intensities (of the order 10^{29} W/cm^2) [19], the Unruh [2, 3] and dynamical Casimir [4] effects require motion with velocities close to the speed of light. Recently, the dynamical Casimir effect was claimed to be demonstrated in a superconducting circuit [17]. In this work we use Ramsey interferometry to explore the dynamical effects of the vacuum.

In this work we use Ramsey interferometry to explore the dynamical effects of the vacuum. Interferometry is a powerful investigative method abundant in many fields of science and engineering. Typically, an interferometer measure the phase difference between two paths. The origin of the phase shift depends on the physical system being studied, thereby providing a probe for the system's parameters and relevant physics. The representative example of a spatial interferometer is the MachZehnder interferometer, in which the interference is between two spatially distinct paths. Its analog in the time domain is the Ramsey interferometer.

Ramsey experiments are commonly used in atomic systems to perform accurate spectroscopy [18]. Here, we generalize Ramsey interference to quantum fields, i.e. to systems with a continuous energy spectrum. Hence, we show that Ramsey interference is a generic effect for driven quantum systems, not only for two-level systems (TLS), and that it is a manifestation of the interference between two quantum amplitudes. Moreover, we implement Ramsey interferometry in systems where the amplification effect is measurable.

Chapter 2 is an introduction to Ramsey interference in two-level systems. It presents an intuitive picture as a two slit experiment in time instead of space. This picture will guide us throughout the work.

Chapter 3 is the main part of this work. We implement Ramsey interference in quantum mesoscopic systems. It provides a method to probe dynamics in quantum mesoscopic systems which yields new results. Using Ramsey interference allows us to explore the time-dependence of dephasing effects of quasi-particles in a mesoscopic conductor. We investigate the dephasing effects of an ohmic environment on an electron-hole pair in a tunnel junction and find that the crossover between high and low impedance corresponds to the crossover between the ballistic and diffusive motion of a quantum brownian particle.

In the remaining chapters we implement the concept of Ramsey interference to two

completely different systems, thus demonstrating the generality of the effect. Chapter 4 considers the Schwinger effect i.e. the creation of electron-positron pairs from the QED vacuum by a strong electric field. We demonstrate how the Schwinger effect can be described by a TLS with time-dependent energy bias. Thus, we show that the Schwinger effect can be modeled by a simple TLS such as used in NMR. We make use of our knowledge from NMR physics to generate Ramsey interference in the probability to create electron-positron pairs and to elucidate its intricate nature [19].

In Chapter 5 we consider the dynamical Casimir effect in the creation of photons from the QED vacuum by a time-dependent boundary condition. We show how Ramsey interference can be induced in the number of photons. This serves as a simple example for a generalization of Ramsey interference to quantum fields.

Chapter 2

Ramsey interference – Introduction

2.1 Ramsey interference in two-level systems

Ramsey experiments are commonly used in atomic systems to perform accurate spectroscopy. In this section we review the usual description of Ramsey interference for two-level systems (TLS) [18]. Consider a TLS with energy bias ω_0 perturbed by a field with frequency ω . The amplitude of the driving field is ω_1 . It is described by the Hamiltonian

$$H = \frac{\hbar}{2} \begin{pmatrix} \omega_0 & 2\omega_1(t) \cos \omega t \\ 2\omega_1(t) \cos \omega t & -\omega_0 \end{pmatrix}. \quad (2.1)$$

The original Ramsey experiment consisted of a spin $\frac{1}{2}$ in a constant magnetic field in the z direction, thus ω_0 is the Larmor frequency. The spin propagates at a constant velocity v through two consequent RF cavities with an identical (in phase and amplitude) magnetic field rotating in the xy -plane with frequency ω . Therefore, $\omega_1(t)$ is non zero and equal to ω_1 only at two time intervals:

$$\omega_1(t) = \omega_1 [\Theta(t)\Theta(\tau-t) + \Theta(t-T)\Theta(\tau-t+T)]. \quad (2.2)$$

The intervals duration is $\tau = vl$ and they are separated by $T = vL$, where l is the length of a single cavity and L is the distance between the cavities.

In the rotating wave approximation, we work in a reference frame rotating with the driving field frequency and neglect terms oscillating with the frequency $\omega + \omega_0$. The resulting Hamiltonian is

$$H' = e^{i\frac{\omega t}{2}\sigma^3} H e^{-i\frac{\omega t}{2}\sigma^3} = \frac{\hbar}{2} \begin{pmatrix} \omega_0 - \omega & \omega_1(t) \\ \omega_1(t) & -\omega_0 + \omega \end{pmatrix}. \quad (2.3)$$

The time evolution operator propagates the system from its state at time $t = t_1$ to its state at time $t = t_2$. The time evolution operator from the initial state of the spin at time $t = 0$ to its final state at time $t = 2\tau + T$ can be separated to three parts in the following way

$$U(2\tau + T, 0) = U_1(T + \tau, T)U_0(T, \tau)U_1(\tau, 0) \quad (2.4)$$

where U_1 is the time evolution operator for the spin in the RF cavities and U_0 is the time evolution operator between the RF cavities. In the rotating frame they are given

by :

$$\begin{aligned} U_1(t_2, t_1) &= e^{-\frac{i}{2}[(\omega_0 - \omega)\sigma^3 + \omega_1\sigma^1](t_2 - t_1)} \\ U_0(t_2, t_1) &= e^{-\frac{i}{2}(\omega_0 - \omega)\sigma^3(t_2 - t_1)} \end{aligned} \quad (2.5)$$

and σ^i 's are the Pauli matrices:

$$\sigma^1 = \begin{pmatrix} 0 & 1 \\ 1 & 0 \end{pmatrix} \quad \sigma^2 = \begin{pmatrix} 0 & -i \\ i & 0 \end{pmatrix} \quad \sigma^3 = \begin{pmatrix} 1 & 0 \\ 0 & -1 \end{pmatrix}. \quad (2.6)$$

If the system is initially an eigenstate of σ^3 , the transition probability to the other eigenstate of σ^3 after a single cavity is given by

$$P_1 = |\langle \uparrow |U_1(\tau, 0)| \downarrow \rangle|^2 = \frac{\omega_1^2 \tau^2}{4} \text{sinc}^2 \frac{\Omega \tau}{2} \quad (2.7)$$

where $\Omega = \sqrt{(\omega - \omega_0)^2 + \omega_1^2}$ and $|\uparrow / \downarrow\rangle$ are the eigenstates of σ^3 , i.e. $\sigma^3|\uparrow / \downarrow\rangle = \pm|\uparrow / \downarrow\rangle$. As expected, the maximal transition probability occurs when the magnetic field frequency ω is equal to the energy difference ω_0 . The oscillations with $\Omega\tau$ are known as Rabi oscillations [20]. It demonstrates that the accuracy of a single pulse spectroscopic measurement is controlled by the width τ of the pulse.

The transition probability, e.g. from the ground state $|-\rangle$ to the excited state $|+\rangle$, after two pulses is given by

$$P_2 = |\langle \uparrow |U(2\tau + T, 0)| \downarrow \rangle|^2 = 4(1 - P_1)P_1 \cos^2((\omega_0 - \omega)(T - \tau) + \phi_0) \quad (2.8)$$

where the phase ϕ_0 does not depend on T . For a pulse width much shorter than the time difference between the pulses, i.e. $\tau \ll T$, P_2 exhibits oscillations with $(\omega_0 - \omega)T$ under an envelope function determined by the one pulse transition probability with width $\sim 1/\tau$. This phenomenon is known as Ramsey interference [21]. In the Ramsey (two pulses) set-up the resolution of the spectroscopic measurement (determination of ω_0) is improved by a factor T/τ over the Rabi (single pulse) set-up.

In the limit of small perturbation, i.e. $\omega_1 \ll \omega_0$, the Rabi term (2.7) is much smaller than 1 ($P_1 \ll 1$) and the Ramsey probability is given by

$$P_2 = 4P_1 \cos^2((\omega_0 - \omega)(T - \tau) + \phi_0) \quad (2.9)$$

where the Rabi term is

$$P_1 = \frac{\omega_1^2}{|\omega_0 - \omega|^2} \sin^2\left(\frac{\omega_0 - \omega}{2}\tau\right) \quad (2.10)$$

In Figure 2.1 the Ramsey probability is plotted as a function of ω .

The Hamiltonian (2.1) describes a general two-level system. For example, it can describe the interaction of an atom with classical light field with frequency ω [22]. The ground state $|g\rangle$ and excited state $|e\rangle$ of the atom are separated by the energy $\hbar\omega_0$ so that the atomic Hamiltonian is

$$H_A = \frac{\hbar\omega_0}{2} (|e\rangle\langle e| - |g\rangle\langle g|). \quad (2.11)$$

The atomic states are conjugated by the interaction of the atomic dipole \vec{D} to the

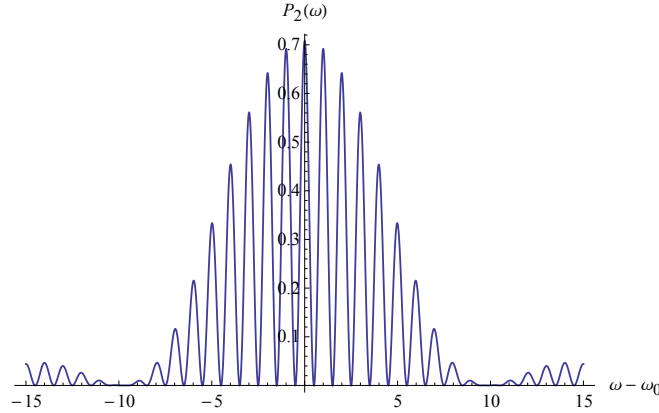


Figure 2.1: The transition probability P_2 after two pulses, is plotted as a function of $\omega - \omega_0$ and in units of π/T , where T is the time difference between the pulses. The width of a single pulse is $\tau = T/5$. The perturbation amplitude is $\omega_1 = 5/T$.

electric field of the light $\vec{E} = \vec{E}_0(t) \cos \omega t$

$$V_{AL} = -\vec{D} \cdot \vec{E} = -E_0(t) D_z \cos(\omega t) \quad (2.12)$$

where we chose the electric field direction to be z .

In the rotating wave approximation, terms oscillating with the frequency $\omega + \omega_0$ are neglected and the dipole interaction in the rotating frame is given by

$$V'_{AL} = \frac{\hbar \omega_1(t)}{2} (|e\rangle\langle g| + |g\rangle\langle e|) \quad (2.13)$$

where $\omega_1(t) = -\langle e|D_z|g\rangle E_0(t)$ is the strength of the dipole interaction. The total Hamiltonian in the rotating frame is given by (2.3).

In the atomic case, Ramsey interference will be obtained by applying two identical laser pulses of width τ separated by the time T . The shape of the pulses do not have to be rectangular like in the original Ramsey experiment (2.2) in order to obtain Ramsey interference. Consider indeed the following Ramsey modulation with an arbitrary pulse shape

$$\omega_1(t) = \omega_1 [f(t) + f(t - T)] \quad (2.14)$$

where the support of $f(t)$ is $[0, \tau]$. The evolution operator of a single pulse U_1 is given by

$$U_1(\tau, 0) = U_1(T + \tau, T) = \mathcal{T} e^{-\frac{i}{2} \int_0^\tau dt [\sigma^3(\omega_0 - \omega) + \sigma^1 \omega_1(t)]}. \quad (2.15)$$

where \mathcal{T} is the time ordering operator. Any 2×2 unitary matrix can be parametrized (up to a global phase) by 3 angles. Thereby, we define the evolution operator of a single pulse as

$$U_1(\tau, 0) = U_1(T + \tau, T) = \begin{pmatrix} e^{i\phi_1} \cos \theta & e^{i\phi_2} \sin \theta \\ -e^{-i\phi_2} \sin \theta & e^{-i\phi_1} \cos \theta \end{pmatrix}. \quad (2.16)$$

The transition amplitude between the atomic states after a single pulse is given by the off-diagonal elements of U_1 . The transition probability after a single pulse is

$$P_1 = \sin^2 \theta. \quad (2.17)$$

The evolution operator after the two pulses is

$$\begin{aligned} U(2\tau + T) &= U_1(T + \tau, T) U_0(T, \tau) U_1(\tau, 0) \\ &= \begin{pmatrix} e^{i\phi_1} \cos \theta & e^{i\phi_2} \sin \theta \\ -e^{-i\phi_2} \sin \theta & e^{-i\phi_1} \cos \theta \end{pmatrix} \begin{pmatrix} e^{-i\frac{(\omega_0 - \omega)(T-\tau)}{2}} & 0 \\ 0 & e^{+i\frac{(\omega_0 - \omega)(T-\tau)}{2}} \end{pmatrix} \begin{pmatrix} e^{i\phi_1} \cos \theta & e^{i\phi_2} \sin \theta \\ -e^{-i\phi_2} \sin \theta & e^{-i\phi_1} \cos \theta \end{pmatrix} \\ &\equiv \begin{pmatrix} B & A \\ A^* & B^* \end{pmatrix} \quad (2.18) \end{aligned}$$

where

$$\begin{aligned} A &= 2 \cos \left[\frac{(\omega_0 - \omega)(T - \tau)}{2} - \phi_1 \right] e^{i\phi_2} \cos \theta \sin \theta \\ B &= e^{-i\frac{(\omega_0 - \omega)(T-\tau)}{2}} e^{2i\phi_1} \cos^2 \theta - e^{+i\frac{(\omega_0 - \omega)(T-\tau)}{2}} \sin^2 \theta. \end{aligned} \quad (2.19)$$

The transition probability between the atomic states after two pulses is given by

$$\begin{aligned} P_2 = |A|^2 &= 4 \sin^2 \theta \cos^2 \theta \cos^2 \left[\frac{(\omega_0 - \omega)(T - \tau)}{2} - \phi_1 \right] \\ &= 4P_1(1 - P_1) \cos^2 \left[\frac{(\omega_0 - \omega)(T - \tau)}{2} - \phi_1 \right] \quad (2.20) \end{aligned}$$

which is exactly the same expression we obtained before (2.8). Therefore, the Ramsey interference does not depend on the shape of the pulses. Only the Rabi term, the envelope of the oscillations, depends on the pulse shape.

Spectroscopic measurements based on Ramsey interferometry are extremely accurate. For example, atomic clocks use this method to gain accuracy of 10^{-15} in the frequency measurements [23]. It is also used in superconducting qubits to determine their coherence time [24, 25], and in nuclear magnetic resonance (NMR) to determine the phase randomization time T_2 [26].

2.2 Ramsey interference as a two slit experiment

The Ramsey effect is generic for many driven quantum systems and not only for two-level systems. It is a manifestation of the interference between two quantum amplitudes [18]. This point will be clarified in this section.

Consider two states of a quantum system $|i\rangle$ and $|f\rangle$ with energies E_i and E_f , the states can be part of a discrete or a continuous energy spectrum. Suppose that perturbing the system by some external modulation can induce a transition between the states, with transition amplitude $A_{if}^{(1)}$. Consider the case where the perturbation occurs only at two times, t_1 and t_2 , separated by T ($T = t_2 - t_1$). To lowest order in perturbation theory, a transition between the states can occur either at t_1 or at t_2 .

If the system was initially in state $|i\rangle$, it has two paths to reach the state $|f\rangle$ (see Figure 2.2). In the first path it stays in state $|i\rangle$ at t_1 and it reaches state $|f\rangle$ at t_2 ; in the second path it reaches state $|f\rangle$ at time t_1 and stays there. Since the states have different energies, the phase accumulated along the two paths is different. Processes where $|i\rangle$ transfers to an intermediate state $|m\rangle$ at t_1 and from there transfers to $|f\rangle$ at t_2 , are higher order in the perturbation theory and are neglected.

Since we consider the lowest order in perturbation theory, the transition probabilities are small $P_{if}^{(1)} = |A_{if}^{(1)}|^2 \ll 1$, and the transition probability at t_2 $P_{if}(t_2) \propto P_{if}^{(1)}(1 - P_{if}^{(1)}) \approx P_{if}^{(1)}$. The transition amplitudes for the different paths can be written

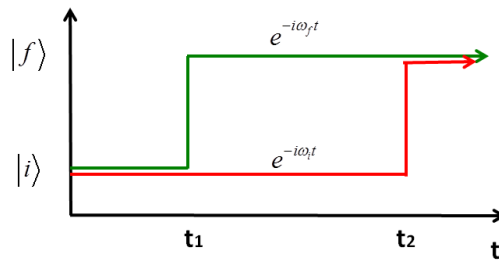


Figure 2.2: Schematic representation of the two paths of the system to go from the initial state $|i\rangle$ to the final state $|f\rangle$ and the phases the system accumulates, $\omega_f = E_f/\hbar$ and $\omega_i = E_i/\hbar$.

as

$$A_1(t_2) = e^{\frac{-iE_i(t_1+T)}{\hbar}} A_{if}^{(1)} \quad (2.21)$$

$$A_2(t_2) = e^{\frac{-iE_i t_1}{\hbar}} e^{\frac{-iE_f T}{\hbar}} A_{if}^{(1)} \quad (2.22)$$

The transition amplitude is a sum of all the possible amplitudes, and the corresponding probability for the transition is

$$P_{if}^{(2)} = |A_1 + A_2|^2 = 4P_{if}^{(1)} \cos^2 \frac{(E_f - E_i)T}{2\hbar}. \quad (2.23)$$

$P_{if}^{(1)}$ is the Rabi term which multiplies the Ramsey oscillations. For a TLS (eq. (2.9)) the energy difference between the initial and final states $E_f - E_i$ is the difference between the energy bias of the TLS $\hbar\omega_0$ and the energy of the field $\hbar\omega$.

This simplified description reveals that the Ramsey setup is a two slit experiment where the phase is accumulated over time instead of space. Equivalently (2.23) is

$$P_{if}^{(2)} = 2P_{if}^{(1)} + 2P_{if}^{(1)} \cos(E_f - E_i)T/\hbar. \quad (2.24)$$

The first term is the classical addition of the transition probability of the two pulses. The second term is the quantum interference between the two amplitudes which is phase sensitive. Therefore, dephasing effects or averaging over energies will diminish the second term. This may seem like an undesirable effect. However, as we will show in section 3.8, the decrease in the amplitude of the interference pattern depends on the dephasing mechanism. Thus, Ramsey experiments can be used to explore some properties of dephasing and test the models describing it.

Chapter 3

Ramsey interference in mesoscopic physics

Here we present a description of Ramsey interference in a mesoscopic system and propose a setup where it can be probed experimentally. Thus, we provide the first proposal to observe the Ramsey interference for a system with a continuum set of states.

One of the most common ways to study a mesoscopic system is by transport experiments. Transport experiments can be described as transition of excitations from one bath to another through the system of interest, where the details of the system are encoded in the scattering matrix [27]. In our case, the transport is driven by a voltage difference between the two baths, thus it is an out of equilibrium process. In this chapter we consider a tunnel junction as a working example to a transport experiment. Our formulation of the problem consists of a tunneling Hamiltonian between the two leads of the system [28]. Another way to describe electrical transport through a phase coherent conductor is by the scattering approach (Landauer approach) [29]. In appendix A we present the basics of the scattering approach with emphasis on transport due to time-dependent voltage (photon assisted transport [29, 30, 31, 32]) and discuss the differences and similarities with our description.

The tunnel junction is subjected to two consequent voltage pulses, an electron-hole (*e-h*) pair can be created at the first or second voltage pulse. The interference between these two quantum amplitudes will induce oscillations in the probability to create a *e-h* pair with the time difference between the pulses, namely Ramsey interference.

In section 3.4 we show a relation between the current noise, which is a measurable quantity, and the probability for the creation of *e-h* pairs, thereby establishing a method to observe Ramsey interference in mesoscopic systems. Ramsey interferometry is a new type of measurement in mesoscopic systems which allows to probe processes in the time domain. In section 3.8 we demonstrate how the dephasing of the *e-h* pairs due to an electromagnetic environment can be investigated by Ramsey interference.

3.1 Quantum interference in a mesoscopic conductor

The basic idea behind quantum interference can be represented by the two slit experiment [27]. Consider a quantum particle which can propagate from an initial point r_1 to a final point r_2 in two different trajectories. The corresponding amplitudes of the trajectories are A_1 and A_2 . The quantum probability that a particle will end up at r_2 is

$$P_q = |A_1 + A_2|^2 = |A_1|^2 + |A_2|^2 + 2\text{Re}A_1A_2^*. \quad (3.1)$$

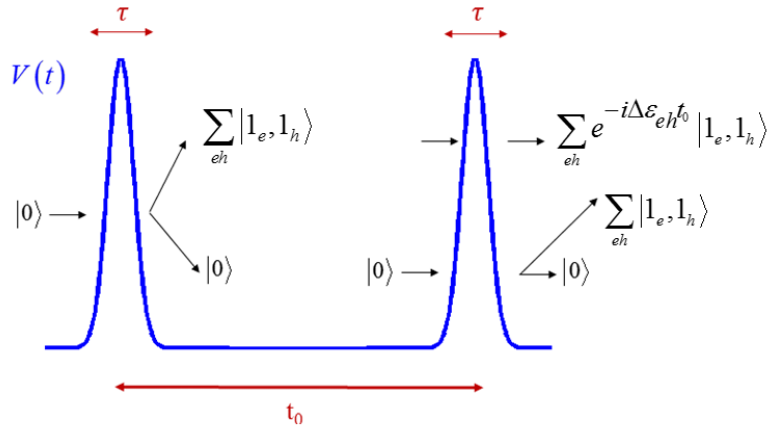


Figure 3.1: *Ramsey setup for the probability for the creation of e-h pairs. Two identical voltage pulses of width τ are applied to the tunnel junction separated by the time delay t_0 . A pair with energy $\Delta\epsilon$ can be created either in the first or in the second pulse. The creation probability will be the interference between these two amplitudes.*

Unlike the classical probability

$$P_{cl} = |A_1|^2 + |A_2|^2 = P_1 + P_2 \quad (3.2)$$

the quantum probability oscillates with the phase difference α between the two amplitudes.

$$P_q = P_{cl} + 2\sqrt{P_1 P_2} \cos \alpha \quad (3.3)$$

Mesoscopic physics is the study of interference effects in disordered systems. In these systems the particles have many possible trajectories between the two points r_1 and r_2 not just two, but the basic principle of interference is the same. Next, we will portray how interference appears in a mesoscopic system.

The propagation of non-interacting electrons in metals in the presence of disorder can be described by the elastic scattering of the electrons from the disorder potential [33]. In the semiclassical approximation, the quantum probability amplitude that an electron will follow a specific trajectory from r_1 to r_2 during the time t is proportional to

$$e^{ikl} e^{-iet} \quad (3.4)$$

where k is the magnitude of wave-vector of the electron, l is the length of the trajectory, t is the time it takes the electron to travel from r_1 to r_2 along the given trajectory and ϵ is the electron's energy. The phase that depends on the trajectory of the electron (and therefore on the disorder potential) kl is called the dynamical phase [27]. Note that the dynamical phase of the time reversed trajectory is equal to the dynamical phase of the forward one.

In the weak disorder limit the mean free path l_e between the scattering events is much larger than the electron's wavelength. The electrons which participate in the transport are close to the Fermi energy, therefore the weak disorder limit is when $k_F l_e \gg 1$, where k_F is the Fermi wave vector. For system size L much larger than the elastic mean free path $L \ll l_e$, the electron scatters many times, each time changing its direction randomly so that its motion can be regarded as diffusive with diffusion coefficient $D = \frac{v_F l_e}{3}$ (in 3d) where v_F is the Fermi velocity. Since the scattering is elastic the energy of the electron and the magnitude of its momentum does not

change.

Consider the quantum interference between two trajectories the electron can take between points r and r' during the time t ,

$$P_q = P_{cl} + 2\sqrt{P_1 P_2} \cos k(l_1 - l_2) \quad (3.5)$$

where l_1 and l_2 are the lengths of the corresponding trajectories and P_1 and P_2 are their probabilities. For different disorder realizations the length of the trajectories l_1 and l_2 changes. Averaging the quantum probability over disorder configurations will yield the classical probability, unless $l_1 = l_2$ for all the disorder realizations. Such situation can occur when the trajectories are a closed loop (i.e. $r_1=r_2$), one trajectory propagates in a clockwise direction and the other in the anti-clockwise direction along the same loop. The dynamical phase of the two trajectories is equal, therefore the phase difference α in (3.3) is zero.

The quantum probability that an electron will propagate from r to r' during time t is the sum over many different scattering trajectories

$$A(r, r', t) = e^{-i\epsilon t} \sum_{N=1}^{\infty} \sum_{r_1 \dots r_N} |A(r, r', \mathcal{C}_N)| e^{ik\mathcal{L}_N} \quad (3.6)$$

where $A(r, r', \mathcal{C}_N)$ is the amplitude associated with a given sequence of N scattering events and \mathcal{L}_N is the length of the trajectory. From the previous simplified example we learned that upon averaging over disorder, interference will remain only between trajectories with equal dynamical phase in each disorder configuration. Mesoscopic physics is the study of coherent effects which survive the disorder averaging, some examples are: universal conductance fluctuations, negative magneto-resistance [33, 27, 34].

The phase coherence of the electrons is, therefore, not limited by the elastic scattering. It is limited by inelastic process such as electron-electron interactions, electron-phonon interactions, interaction with an environment. These processes change the energy of the electrons, thus averaging over all the possible processes randomizes the electron's phase and reduces interference effects. In section 3.8 we consider the dephasing caused by an electromagnetic environment.

In the presence of such inelastic processes, the interference term is reduced by a factor $\langle e^{i\phi(t)} \rangle$, where t is the time of the trajectory. The average $\langle \cdot \rangle$ is over the environment degrees of freedom. The distribution of the phase depends on the origin of the dephasing. In general, it will decay in an exponential manner [33]

$$\langle e^{i\phi(t)} \rangle = e^{-f(t/\tau_\phi)} \quad (3.7)$$

which provides a definition of the phase coherence time τ_ϕ . Beyond τ_ϕ the phase washes out and interference effects are lost.

The phase coherence length is defined as the length the electron passes during the phase coherence time, it is given by $L_\phi = \sqrt{D\tau_\phi}$, where D is the diffusion constant describing the motion of the electrons in the metal. In metals the phase coherence length decreases with temperature, for mK temperatures, L_ϕ is of the order of a few micrometer. In order to observe quantum interference effects the length L of a mesoscopic system should be smaller than the phase coherence length $L < L_\phi$.

One of the common ways of measuring the phase coherence time is by a magneto-transport experiment where it is extracted from the negative maneto-resistance effect [35]. In 1d systems, Mach-Zehnder interferometer has been used to measure the coherence length [36, 37] and study dephasing mechanisms [38, 39, 40, 41, 42, 43].

In this chapter we describe Ramsey interference in a mesoscopic conductor. In order to observe Ramsey interference the electrons should stay coherent longer than the time between pulses t_0 , i.e $t_0 > \tau_\phi$. Therefore, Ramsey interferometry can be used to determine the phase coherence time of the system. Moreover, the way the amplitude of the interference decreases (the function $f(t/\tau_\phi)$ in (3.7)) provides information about the interactions leading to the dephasing. Unlike the Mach-Zehnder interferometer, Ramsey interferometer can be realized also for 2d and 3d systems.

3.2 The tunnel junction – the simplest mesoscopic conductor

As a working example of mesoscopic conductor we consider the simplest one - the tunnel junction. A tunnel junction is composed of two metallic parts separated by a thin insulating barrier. The barrier is thin enough to allow charge transport by tunneling of electrons induced by applying a voltage on the tunnel junction. When an electron tunnels, e.g. from the right lead to the left lead, it leaves a hole in the right lead. Therefore, a tunneling event creates a $e-h$ pair in the tunnel junction. Note, that the electron and the hole are not in the same lead.

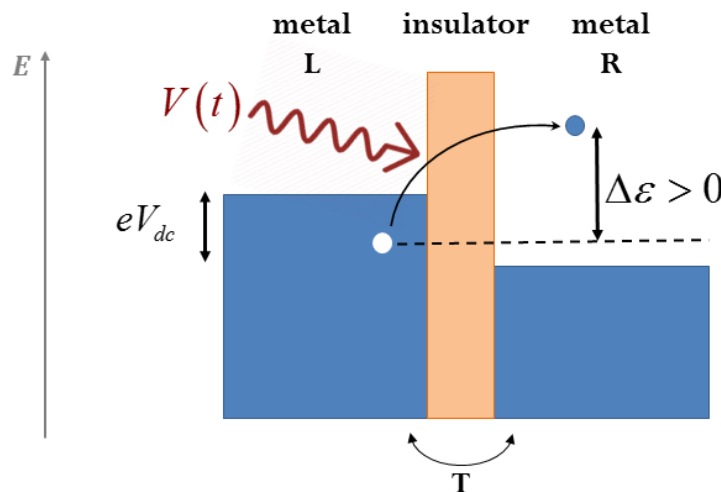


Figure 3.2: A tunnel junction is composed of two metals separated by a thin insulating layer. The insulator is thin enough to allow tunneling of electrons between the two metals. Applying a voltage pulse on the tunnel junction can create $e-h$ pairs within the continuum with energy $\Delta\epsilon > 0$.

The electrons in the two metal electrodes are described by the Hamiltonian

$$H_0 = \sum_k \epsilon_{Lk}(t) c_{Lk}^\dagger c_{Lk} + \sum_q \epsilon_{Rq} c_{Rq}^\dagger c_{Rq} \quad (3.8)$$

where c_{Lk}^\dagger (c_{Rq}^\dagger) creates an electron in the left (right) lead with momentum k (q). For convenience, we choose to include the voltage in the left lead

$$\epsilon_{Lk}(t) = \epsilon_{Lk} - eV_{dc} + eV(t) \equiv \epsilon_{Lk}^0 + eV(t) \quad (3.9)$$

although our results do not depend on the how we distribute the voltage between the leads since the probability of an electron to tunnel depends only on the energy difference between its initial and final states.

Tunneling is described by the Hamiltonian

$$H_T = \sum_{kq} \left[T_{kq} c_{Rq}^\dagger c_{Lk} + T_{kq}^* c_{Lk}^\dagger c_{Rq} \right] \quad (3.10)$$

such that $T_{kq} c_{Rq}^\dagger c_{Lk}$ transfers an electron from the left lead to the right lead. By writing this effective tunneling Hamiltonian [28] we have assumed that the tunneling matrix elements T_{kq} does not depend on the applied voltage. This assumption can be justified when the energy of the tunneling electrons is much smaller than the potential barrier of the insulating layer. In such circumstances, the tunneling between the two sides of the barrier will depend only weakly on the shape of the top of barrier which is changed by the voltage. A rigorous treatment of the effect of the voltage on the tunneling is given in [44, 45]. We assume that the tunneling does not depend on spin, thereby we suppressed the spin index. In general, time reversal symmetry imposes the condition $T_{k\uparrow q\uparrow}^* = T_{-k\downarrow -q\downarrow}$ [46, 47].

The Hamiltonian of the tunnel junction is given by the sum of the Hamiltonians of the leads and the tunneling Hamiltonian

$$H = H_0 + H_T. \quad (3.11)$$

The probability of a tunneling event is assumed to be small, i.e. the tunneling matrix elements are small compared to the Fermi energy ($|T_{kq}| \ll \epsilon_F$). We consider the zero temperature limit, therefore the initial state of the system is a Fermi sea in each lead. The initial state of the system is given by

$$|FS\rangle = \prod_{\substack{k > k_F \\ q < k_F}} c_{Lk}^\dagger c_{Rq}^\dagger |0\rangle \quad (3.12)$$

where k_F is the Fermi wave-vector. This corresponds to the initial state in Fig. 3.2

Tunneling from the right lead to the left lead is allowed only for electrons with initial wave-vector $q < k_F$ and final wave-vector $k > k_F$. Such a tunneling event creates a $e-h$ pair with energy $\Delta\epsilon = +(\epsilon_{Lk}^0 - \epsilon_{Rq})$. In the same way, a tunneling event from the left lead to the right lead is allowed only for $k < k_F$ and $q > k_F$ and creates a $e-h$ pair with energy $\Delta\epsilon = -(\epsilon_{Lk}^0 - \epsilon_{Rq})$. These $e-h$ states correspond to

$$\begin{aligned} |1_{e_{Lk}}, 1_{h_{R,-q}}\rangle &= c_{Lk}^\dagger c_{Rq}^\dagger |FS\rangle \\ |1_{e_{Rq}}, 1_{h_{L,-k}}\rangle &= c_{Rq}^\dagger c_{Lk}^\dagger |FS\rangle. \end{aligned} \quad (3.13)$$

Note that the initial state of the system (3.12) corresponds to the vacuum state of the electrons and holes.

3.3 Probability for the creation of $e-h$ pairs

In this section we find the probability to create $e-h$ pairs by a time dependent voltage modulation. A detailed derivation is given in Appendix B. The probability $P_{LR}^{k,-q}$ ($P_{RL}^{q,-k}$) to create an electron with momentum k (q) in the left (right) lead and a hole

with momentum $-q$ ($-k$) in the right (left) lead from the vacuum is

$$\begin{aligned} P_{LR}^{k,-q} &= |\langle 1_{e_{Lk}}, 1_{h_{R,-q}} | U(\infty, -\infty) | 0_{e_{Lk}}, 0_{h_{R,-q}} \rangle|^2 \\ P_{RL}^{q,-k} &= |\langle 1_{e_{Rq}}, 1_{h_{L,-k}} | U(\infty, -\infty) | 0_{e_{Rq}}, 0_{h_{L,-k}} \rangle|^2 \end{aligned} \quad (3.14)$$

where $U(t_f, t_i)$ is the evolution operator which satisfies $i \frac{d}{dt} U(t) = H(t) U(t)$ and the $|00\rangle$ state correspond to the Fermi sea in both leads, which is the vacuum state for the electrons and holes.

The probability to create a e - h pair to second order in T_{kq} can be expressed as

$$P_{LR}^{k,-q} = \frac{1}{\hbar^2} \int_{-\infty}^{\infty} dt_1 dt_2 \langle 0_{e_{Lk}}, 0_{h_{R,-q}} | \tilde{H}_T(t_1) | 1_{e_{Lk}}, 1_{h_{R,-q}} \rangle \langle 1_{e_{Lk}}, 1_{h_{R,-q}} | \tilde{H}_T(t_2) | 0_{e_{Lk}}, 0_{h_{R,-q}} \rangle \quad (3.15)$$

where the time evolution of \tilde{H}_T is with respect to the Hamiltonian H_0 (3.8)

$$\tilde{H}_T = \sum_{kq} \left[T_{kq} e^{-i\phi(t)} e^{-\frac{i}{\hbar}(\epsilon_{Lk}^0 - \epsilon_{Rq})t} c_{Rq}^\dagger c_{Lk} + h.c. \right] \quad (3.16)$$

and we define the time dependent phase $\phi(t) \equiv \frac{e}{\hbar} \int_{-\infty}^t V(t') dt'$. We obtain that the probability to create a e - h pair is the Fourier transform of $g(t) = e^{-i\phi(t)}$ at frequency $(\epsilon_{Lk}^0 - \epsilon_{Rq})/\hbar$

$$P_{LR}^{k,-q} = \Theta(\epsilon_{Lk} - \epsilon_F) (1 - \Theta(\epsilon_{Rq} - \epsilon_F)) \times \left| \frac{T_{kq}}{\hbar} \int_{-\infty}^{\infty} e^{-i\phi(t)} e^{-\frac{i}{\hbar}(\epsilon_{Lk}^0 - \epsilon_{Rq})t - 0^+|t|} dt \right|^2 \quad (3.17)$$

where $\Theta(\epsilon)$ is the heaviside function and we have regularized the integral by $e^{-0^+|t|}$. In the absence of a time dependent voltage modulation ($V(t) = 0$), the probability is given by Fermi golden rule and only e - h pairs with energy $\Delta\epsilon = 0$ can be created since $P_{LR}^{k,-q} \propto \delta(\epsilon_{Lk}^0 - \epsilon_{Rq})$. We are interested in e - h pairs that are created by the time dependent voltage, i.e with energy $\Delta\epsilon \neq 0$.

In the same way,

$$P_{RL}^{q,-k} = \Theta(\epsilon_{Rq} - \epsilon_F) (1 - \Theta(\epsilon_{Lk} - \epsilon_F)) \times \left| \frac{T_{kq}}{\hbar} \int_{-\infty}^{\infty} e^{+i\phi(t)} e^{-\frac{i}{\hbar}(\epsilon_{Rq} - \epsilon_{Lk}^0)t - 0^+|t|} dt \right|^2 \quad (3.18)$$

The probability for the creation of a e - h pair with energy difference between the initial and final states $\Delta\epsilon = \pm(\epsilon_{Lk}^0 - \epsilon_{Rq})$ vanishes for $\Delta\epsilon \rightarrow \pm\infty$. Thus, it is negligible outside some ΔE . If the tunneling matrix elements do not change considerably on the energy scale of ΔE , we can approximate them by a constant $T_{kq} = T$. This approximation holds when the energy of the electrons is much smaller than the tunnel barrier potential. In this regime the tunneling probability is small, which is consistent with our assumptions for the perturbative treatment of the tunnel junction. Actually, all we need to assume in order to continue, is that the tunneling matrix elements depend only on the energy difference between the initial and final states $\Delta\epsilon = \pm(\epsilon_{Lk}^0 - \epsilon_{Rq})$. Then the probability for the creation of a e - h pair depends only on $\Delta\epsilon$. Modifying our notations accordingly, we define

$$P_{LR}(\Delta\epsilon) = \left| \frac{T}{\hbar} \int_{-\infty}^{\infty} e^{-i\phi(t)} e^{-\frac{i}{\hbar}\Delta\epsilon t - 0^+|t|} dt \right|^2 \quad (3.19)$$

$$P_{RL}(\Delta\epsilon) = \left| \frac{T}{\hbar} \int_{-\infty}^{\infty} e^{+i\phi(t)} e^{-\frac{i}{\hbar}\Delta\epsilon t - 0^+|t|} dt \right|^2$$

such that

$$P_{LR}^{k,-q} = \Theta(\epsilon_{Lk} - \epsilon_F) (1 - \Theta(\epsilon_{Rq} - \epsilon_F)) P_{LR} (\epsilon_{Lk}^0 - \epsilon_{Rq}) \quad (3.20)$$

$$P_{RL}^{q,-k} = \Theta(\epsilon_{Rq} - \epsilon_F) (1 - \Theta(\epsilon_{Lk} - \epsilon_F)) P_{RL} (\epsilon_{Rq} - \epsilon_{Lk}^0).$$

The symmetry between left and right is indicated by the relation

$$P_{LR}(\Delta\epsilon) = P_{RL}(-\Delta\epsilon). \quad (3.21)$$

The total probability to create a e - h pair to lowest order in T is a sum over all the possible e - h pairs that can be created

$$P_{total} = \sum_{\substack{k > k_F \\ q < k_F}} P_{LR}^{k,-q} + \sum_{\substack{k < k_F \\ q > k_F}} P_{RL}^{q,-k} \quad (3.22)$$

To second order in T_{kq} these processes do not interfere since we consider only process where the electron can tunnel between the leads only once. The tunneling Hamiltonian does not relate $|00\rangle$ with itself, therefore $|11\rangle\langle 11|$ in (3.15) can be replaced by the unity operator so that the total probability to create a e - h pair can be expressed as

$$P_{total} = \frac{1}{\hbar^2} \int_{-\infty}^{\infty} dt_1 dt_2 \langle FS | \tilde{H}_T(t_1) \tilde{H}_T(t_2) | FS \rangle \quad (3.23)$$

3.4 Current noise – Relation to the probability for the creation of e - h pairs

In this section we calculate the current noise and we show how it is related to the probability calculated previously. A detailed derivation is given in Appendix C. The power spectrum (the noise) is defined as the Fourier transform of the current correlation function

$$S(\Omega) = \int_{-\infty}^{\infty} dt_1 \int_{-\infty}^{\infty} dt_2 C(t_1, t_2) e^{i\Omega t_1} e^{-i\Omega t_2} \quad (3.24)$$

$$C(t_1, t_2) = \langle I(t_1)I(t_2) \rangle - \langle I(t_1) \rangle \langle I(t_2) \rangle.$$

In the case of classical transport, $\langle \cdot \rangle$ is a statistical average and the correlation function is $C(t_1, t_2) = \int \mathcal{D}I_1 \mathcal{D}I_2 P(I_1(t_1)I_2(t_2)) I_1 I_2$ where $P(I_1(t_1)I_2(t_2))$ is the probability to find I_1 at time t_1 and I_2 at time t_2 . In the case of quantum transport that we consider here, the currents are operators in the Heisenberg picture and $\langle \cdot \rangle$ is a quantum expectation value with respect to the initial state of the system.

For a system in thermal equilibrium the average current is zero, nevertheless the noise is nonzero due to thermal fluctuations. These fluctuation are known as the

Nyquist-Johnson noise and are present in any system, classical or quantum.

Shot noise is an out of equilibrium noise at zero frequency $S(\Omega \rightarrow 0)$ and at zero temperature. The source of this noise is the discreteness of the electron charge, i.e. electrons pass the conductor one by one. The noise probes the transmission properties of the system in a different way than the average current. For example, in a coherent conductor with small transition probability (like a tunnel junction) where $T \ll 1$, the shot noise is proportional to the average current $S(\Omega \rightarrow 0) = 2q \langle I \rangle$, where q is the charge of the quasiparticles passing through the conductor. Thereby, shot noise is used to determine the charge of quasiparticles [48, 49]. The shot noise is also sensitive to the statistics of the quasiparticles [50, 51, 49]. For a review, see [29].

We expect that higher moments will reveal even more information on the system but they are difficult to measure. The third moment was measured by [52, 53]. The highest moment measured is the forth one [54]. The full information about the system is contained within the full counting statistics of the charge transfer. Expressions for the full counting statistics of transport through a coherent conductor due to a *dc* voltage were obtained by [55, 56].

The current operator in the Heisenberg picture is defined as the change in time of the number of electrons in the left lead.

$$I(t) = e \frac{d}{dt} \sum_k c_{Lk}^\dagger c_{Lk} = -i \frac{e}{\hbar} \sum_k [c_{Lk}^\dagger c_{Lk}, H] = i \frac{e}{\hbar} \sum_{kq} [T_{kq} c_{Rq}^\dagger c_{Lk} - T_{kq}^* c_{Lk}^\dagger c_{Rq}] \quad (3.25)$$

Since we work in the Heisenberg picture the particle operators are time dependent. To second order in T the current correlator is given by

$$C(t_1, t_2) = \langle \tilde{I}(t_1) \tilde{I}(t_2) \rangle \quad (3.26)$$

where the time evolution of \tilde{I} is with respect to the Hamiltonian H_0 (3.8)

$$\tilde{I}(t) = i \frac{e}{\hbar} \sum_{kq} [T_{kq} e^{-i\phi(t)} e^{-\frac{i}{\hbar}(\epsilon_{Lk}^0 - \epsilon_{Rq})t} c_{Rq}^\dagger c_{Lk} - h.c.] \quad (3.27)$$

Examining the tunneling Hamiltonian (3.16) and the current operator (3.27) reveals that they act on the $|00\rangle$ state in the same way up to a factor, thus allowing us to express the total probability to create a *e-h* pair to lowest order in T as

$$P_{total} = \frac{1}{e^2} \int_{-\infty}^{\infty} dt_1 dt_2 \langle i | \tilde{I}(t_1) \tilde{I}(t_2) | i \rangle \quad (3.28)$$

which is just the current noise at zero frequency (shot noise) to second order in T (3.24). To be more explicit,

$$S(\Omega \rightarrow 0) = e^2 \left[\sum_{\substack{k > k_F \\ q < k_F}} P_{LR}^{k,-q} + \sum_{\substack{k < k_F \\ q > k_F}} P_{RL}^{q,-k} \right] \quad (3.29)$$

Similar expressions have been obtained previously, for example see [28].

Taking the continuum limit and assuming that the density of states $\rho(\epsilon)$ changes

slowly on the energy scale of the *dc* voltage, the shot noise can be expressed as

$$S(\Omega \rightarrow 0) = e^2 \rho^2 \left[\int_{\epsilon_F}^{\infty} d\epsilon_L \int_{-\infty}^{\epsilon_F} d\epsilon_R P_{LR} (\epsilon_L^0 - \epsilon_R) + \int_{-\infty}^{\epsilon_F} d\epsilon_L \int_{\epsilon_F}^{\infty} d\epsilon_R P_{RL} (\epsilon_R - \epsilon_L^0) \right] \quad (3.30)$$

Where $\epsilon_L^0 = \epsilon_L - eV_{dc}$ and $\rho = \rho(\epsilon_F)$. Note that changing the integration variable ϵ_L to $\epsilon_L + eV_{dc}$ is equivalent to having a difference of eV_{dc} in the Fermi energy of the electrodes.

By virtue of the singularity of the Fermi distribution at zero temperature $f'(\epsilon) = \delta(\epsilon)$, the second derivative of the shot noise with respect to the *dc* voltage yields the probability for the creation of a *e-h* pair

$$\begin{aligned} \frac{d^2 S(\Omega \rightarrow 0)}{d(eV_{dc})^2} &= e^2 \rho^2 [P_{RL}(\Delta\epsilon = eV_{dc}) + P_{LR}(\Delta\epsilon = -eV_{dc})] \\ &= 2e^2 \rho^2 P_{RL}(\Delta\epsilon = eV_{dc}). \end{aligned} \quad (3.31)$$

For finite temperatures the derivative of the Fermi distribution is peaked at $\epsilon = 0$ with width β_{el}^{-1} , where β_{el} is the inverse temperature of the electrons in the leads. The above relation holds as long as the probability to create a *e-h* pair $P_{RL}(\Delta\epsilon)$ is a smooth function on the order of β_{el}^{-1} , i.e. $\partial_\epsilon P_{RL}(\epsilon) \beta_{el}^{-1} \ll 1$.

We have shown that the second derivative of the shot noise with respect to the *dc* voltage is proportional to the probability of creating a *e-h* pair with energy eV_{dc} . Hence, we have identified a way to measure the probability to create a *e-h* pair with a specific energy in a tunnel junction.

3.5 Ramsey interference in the probability for the creation of *e-h* pairs

In the previous section we have described a method to measure the *e-h* creation probability as a function of energy. In this section we will demonstrate how Ramsey interference can modify this probability.

Applying two voltage pulses on the tunnel junction will give rise to an interference between the amplitudes to create a *e-h* pairs. We consider the case of two identical non-overlapping pulses $V(t) = V_0(t) + V_0(t - t_0)$ where $V_0(t)$ is nonzero only in the time interval $0 < t < \tau$ and $\tau < t_0$. Therefore, the time dependent phase is

$$\phi(t) = \frac{e}{\hbar} \int_{-\infty}^t V(t') dt' = \begin{cases} 0 & t < 0 \\ \varphi(t) & 0 < t < \tau \\ \varphi_0 & \tau < t < t_0 \\ \varphi_0 + \varphi(t - t_0) & t_0 < t < t_0 + \tau \\ 2\varphi_0 & t_0 + \tau < t \end{cases} \quad (3.32)$$

where we denote $\varphi(t) = \frac{e}{\hbar} \int_0^{t < \tau} V_0(t') dt'$ and $\varphi_0 = \frac{e}{\hbar} \int_0^\tau V_0(t) dt$.

Inserting (3.32) into the expression for the probability (3.19) yields

$$P_{LR}^{2-pulses}(\Delta\epsilon) = |T|^2 \left| \left(1 + e^{-i\varphi_0} e^{-\frac{i}{\hbar}\Delta\epsilon t_0}\right) \left[\frac{1 - e^{-i\varphi_0} e^{-\frac{i}{\hbar}\Delta\epsilon\tau}}{-i\Delta\epsilon} + \int_0^\tau dt e^{-i\varphi(t)} e^{-\frac{i}{\hbar}\Delta\epsilon t} \right] + \pi\delta(\epsilon) [1 + e^{-2i\varphi_0}] \right|^2 \quad (3.33)$$

Considering only pairs that are created by the voltage pulses, i.e. with non-zero energy ($\Delta\epsilon \neq 0$) we obtain

$$P_{LR}^{2-pulses}(\Delta\epsilon) = 4 \cos^2 \left(\frac{\Delta\epsilon t_0}{2\hbar} + \frac{\varphi_0}{2} \right) P_{LR}^{1-pulse}(\Delta\epsilon) \quad (3.34)$$

where $P_{LR}^{1-pulse}$ is the probability to create a *e-h* pair after a single voltage pulse

$$\begin{aligned} P_{LR}^{1-pulse}(\Delta\epsilon) &= \left| \frac{T}{\hbar} \int_{-\infty}^{\infty} e^{-i\varphi(t)} e^{-\frac{i}{\hbar}\Delta\epsilon t - 0^+|t|} dt \right|^2 \\ &= |T|^2 \left| \frac{1 - e^{-i\varphi_0} e^{-\frac{i}{\hbar}\Delta\epsilon\tau}}{-i\Delta\epsilon} + \int_0^\tau dt e^{-i\varphi(t)} e^{-\frac{i}{\hbar}\Delta\epsilon t} \right|^2. \end{aligned} \quad (3.35)$$

As expected the probability due to two voltage pulses exhibits Ramsey interference. The probability oscillates with $\frac{\Delta\epsilon t_0}{\hbar} + \varphi_0$, which is the phase accumulated by a *e-h* pair created in the first pulse relative to the phase gained by a pair created in the second pulse. $P_{LR}^{1-pulse}$ corresponds to the Rabi term.

In the same way, the probability to create a *e-h* pair in the right-left leads after two voltage pulses is given by

$$P_{RL}^{2-pulses}(\Delta\epsilon) = 4 \cos^2 \left(\frac{\Delta\epsilon t_0}{2\hbar} - \frac{\varphi_0}{2} \right) P_{RL}^{1-pulse}(\Delta\epsilon) \quad (3.36)$$

where $P_{RL}^{1-pulse}(\Delta\epsilon)$ is obtained from $P_{LR}^{1-pulse}(\Delta\epsilon)$ by substituting $\varphi(t) \rightarrow -\varphi(t)$.

The Ramsey probability to create a *e-h* pair with energy $\Delta\epsilon$ oscillate with $\Delta\epsilon$. Since most measurements involve a contribution from a window of energies ΔE , the Ramsey interference will be washed when integrating over ΔE . By virtue of the second derivative of the shot noise with respect to the *dc* voltage at small temperatures (3.31), we are able to isolate the probability for the creation of *e-h* pairs with a given energy, therefore it can be observed.

In order to connect (3.34) to the Ramsey interference expression for a two-level systems, (2.9), we shall consider a voltage modulation which correspond to (2.2). Hence, we consider two constant voltage pulses of width τ separated by t_0 :

$$V(t) = V_0 [\Theta(t)\Theta(\tau-t) + \Theta(t-t_0)\Theta(\tau-t-t_0)] \quad (3.37)$$

The probability for the creation of *e-h* pairs after two pulses is given by (3.34) where the creation probability after a single pulse is

$$P_{LR}^{1-pulse}(\Delta\epsilon) = |T|^2 \left| \frac{1 - e^{-i\varphi_0 - i\Delta\epsilon\tau/\hbar}}{i\Delta\epsilon} + \frac{e^{-i\varphi_0 - i\Delta\epsilon\tau/\hbar}}{i(\Delta\epsilon - eV_0)} \right|^2 \quad (3.38)$$

In the limit of small perturbation $V_0 \ll \Delta\epsilon$, $P_{LR}^{1-pulse}$ corresponds to the two-level system Rabi term, eq. (2.10):

$$P_{LR}^{1-pulse}(\Delta\epsilon) = \left| \frac{T}{\Delta\epsilon} \right|^2 \sin^2 \left(\frac{\Delta\epsilon\tau/\hbar + \varphi_0}{2} \right). \quad (3.39)$$

Ramsey interference in the probability to create a *e-h* pair is plotted in Fig. 3.3 (solid line) for the case of two Gaussian voltage pulses. The time difference between the pulses is $t_0 = 20\sigma$ (σ being the Gaussian voltage pulse width) so they are well separated. As predicted by (3.34) the envelope of the oscillations is 4 times larger than the probability due to a single pulse.

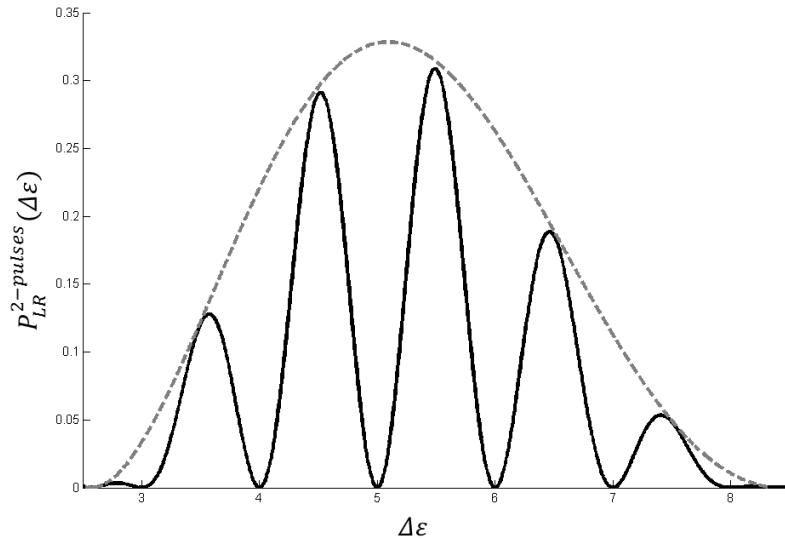


Figure 3.3: *The probability for the creation of a *e-h* pair due to two Gaussian voltage pulses as a function of the energy of the pair (solid line). The envelope function (dashed line) is 4 times the probability due to a single voltage pulse. The time difference between the pulses is $t_0 = 20\sigma$ (σ is the Gaussians width of the pulse). The energy is given in units of $\frac{2\pi\hbar}{t_0}$*

In order to measure the probability for the creation of *e-h* pairs one needs to average over many independent measurements. Typical shot noise measurements involve an average over a long period of time in order to eliminate the stochastic noise of the amplifier. Applying a periodic voltage modulation in which each period is composed of two pulses $V(t) = \sum_n [V_0(t - nT) + V_0(t - t_0 - nT)]$ and averaging the noise over a long period of time (much longer than T) is equivalent to averaging over independent measurements if the period is longer than the coherence time of the electrons in the leads ($T \gg \tau_\phi$) and the time between pulses is shorter than the coherence time ($t_0 \ll \tau_\phi$). Since at times longer than τ_ϕ the phase of the electron is washed out the interference in the probability will arise only from the interference between the two pulses in each period and there will be no interference between the periods.

We have shown how Ramsey interferometry can be implemented in a mesoscopic system. In atomic systems, Ramsey interferometry is used to perform accurate spectroscopy. The advantage of Ramsey in mesoscopics results from its sensitivity to the phase difference, thereby it is sensitive to variations in the energy and/or life time of the particles. Therefore, Ramsey fringes will be sensitive to anything that modifies

the coherence time τ_ϕ , like the finite life-time of the quasi-particles, the temperature of the system, dephasing of the quasi-particles caused by an environment and other time-dependent processes that will affect the energy of the quasi-particles. In section 3.8 , as an example we consider the effect of an electromagnetic environment on the Ramsey fringes.

3.6 A recent experiment – Measurement of the second derivative of the shot noise

In section 3.4 we have shown how the probability for creation of a $e\text{-}h$ pair as a function of energy $P(\Delta\epsilon)$ can be measured by the second derivative of the shot noise with respect to the dc voltage $\frac{d^2S}{dV_{dc}^2}$ as a function of the dc voltage (3.31). In section 3.5 we showed how Ramsey interference can be induced in the probability to create a $e\text{-}h$ pair and we proposed to measure it using the second derivative of the shot noise.

In this section we present a recent experiment [57] which measured this second derivative of the shot noise with respect to a normal dc bias V_{dc} . A tunnel junction composed of Al/Al oxide/Al was subjected to a bi-harmonic voltage modulation

$$V(t) = V_{ac1} \cos(2\pi\nu t) + V_{ac2} \cos(4\pi\nu t + \varphi) \quad (3.40)$$

and its shot noise was measured. Note that this bi-harmonic voltage is not the Ramsey modulation we considered. Nevertheless, the experiment demonstrates the ability to observe interference in a shot noise measurement.

The probability to create a $e\text{-}h$ pair with energy $\Delta\epsilon$ by the bi-harmonic voltage modulation is obtained by inserting the modulation (3.40) in our expression for the probability (3.19) which yields

$$\begin{aligned} P(\Delta\epsilon) &= \left| \int_{-\infty}^{\infty} dt e^{-i\frac{eV_{ac1}}{h\nu} \sin(2\pi\nu t)} e^{-i\frac{eV_{ac2}}{2h\nu} \sin(4\pi\nu t)} e^{-i\Delta\epsilon t} \right|^2 \\ &= \sum_n |C_n|^2 \delta(\Delta\epsilon - nh\nu). \end{aligned} \quad (3.41)$$

C_n is the probability amplitude to create a $e\text{-}h$ pair with energy $nh\nu$, which is given by the Fourier coefficients of the modulation

$$C_n = \sum_{m=-\infty}^{\infty} J_{n-2m} \left(\frac{eV_{ac1}}{h\nu} \right) J_m \left(\frac{eV_{ac2}}{2h\nu} \right) e^{-im\varphi} \quad (3.42)$$

where $J_n(x) = \frac{1}{2\pi} \int_{-\pi}^{\pi} e^{i(ny-x \sin y)} dy$ is the Bessel functions of the first kind. The sum represents interference between all the processes that can create a $e\text{-}h$ pair with energy $nh\nu$, meaning the absorption of m photons of frequency 2ν and $n - 2m$ photons of frequency ν (negative m represents emission).

The experimental results are presented in Fig. 3.4. The intensity is the second derivative of the shot noise with respect to the dc voltage, this correspond to the probability for a $e\text{-}h$ pair creation. The horizontal axis is the dc voltage which corresponds to the energy of the $e\text{-}h$ pair $\Delta\epsilon$. The vertical axis is φ , the phase difference between the two ac modulations. The parameters of the experiment are $eV_{ac1} = 2eV_{ac2} = 5.4h\nu$ with $\nu = 10\text{GHz}$ and the temperature of the electrons in the leads is $0.14h\nu/k_B = 70\text{mK}$. The lower panel is the measurement and upper panel is a theoretical prediction which made use of the photon-assisted transport approach presented in Appendix A. the final expressions for the second derivative of the shot

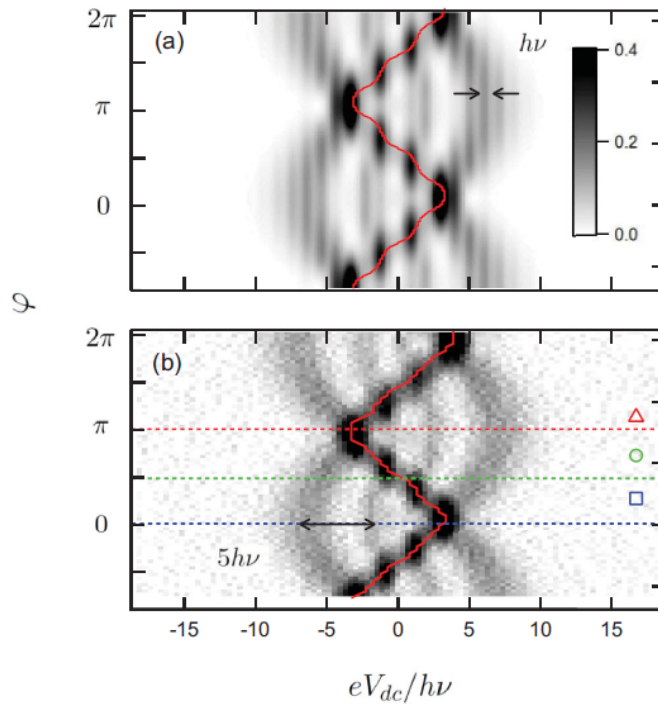


Figure 3.4: calculated (a) and measured (b) second derivative of the bi-harmonic photon-assisted noise as a function of normalized dc bias and phase difference. [57]

noise with respect to the *dc* voltage of our tunneling Hamiltonian approach and of the photon-assisted noise are equal.

Our expression for the *e-h* creation probability for a general time dependent voltage modulation, (3.19), is given for the limit of zero temperature of the leads. Taking into account the finite temperature of the leads (here $70mK$) the delta functions in (3.41) broadens and their width is $\sim k_B T$. This broadening is taken into account in the calculated second derivative of the shot noise presented in the upper panel of Fig. 3.4. The agreement between the experiment and the theory is remarkable.

A reasonable assumption is that τ_ϕ is of the order of the inverse temperature of the electrons in the leads, thereby $\tau_\phi \sim \nu^{-1}$. This explains why the interference features of order ν predicted by the theory, are not observed in the experiment.

The interference observed in this experiment is not a Ramsey interference, since in Ramsey the *e-h* pairs can be created only at two times, separated by t_0 . Here, the *e-h* pairs are created continuously in time. The existence of the time scale t_0 in which the system evolves freely in time is at the origin of the Ramsey interference. As we will show in the next section the introduction of this time scale allows to use Ramsey as a new type of probe in mesoscopic systems.

3.7 Ramsey interference in the presence of disorder

In our description of the tunnel junction the leads were treated as ideal metals. In reality, though , impurities and other defects will introduce disorder to the system. As we discussed in section 3.1 not all interference effects survive the disorder average. Motivated by the observation of interference due to time dependent voltage modulation in the experiment presented in section 3.6, we claim that Ramsey interference can be

obtained in mesoscopic systems. In this section we will advocate this claim from a macroscopic and a microscopic points of view.

From a macroscopic point of view, the Hamiltonian of the two metals (3.8) will keep its structure in the presence of a disorder potential , but the labeling k and q will not stand for momentum anymore but as a labeling of the eigenstates of the disorder Hamiltonian. Since in our derivation we did not specify the relation between k,q and their corresponding eigen-energies ϵ_{Lk} and ϵ_{Rq} , our results hold whatever these energies are, as long as they form a continuum.

For the microscopic point of view we need to consider the motion of the electron in the system. The insulating barrier in a tunnel junction is very thin in order to allow tunneling, typical values are of the order of 10Å. Therefore, we consider the propagation of the electron to be diffusive in the two metals and ballistic in the tunnel barrier. The time the electron spends in the tunnel barrier is negligible with respect to the time it spends in the metal electrodes. Next, we describe the propagation of such an electron due to the Ramsey voltage modulation.

Consider an electron starting from point r_i in the left metal at time t_i and ending at point r_f in the right metal at time t_f . In the Ramsey voltage modulation, the electron can hop through the barrier only at the times of the voltage pulses t_1 or t_2 respectively. We denote the time difference between the pulses by $t_0 = t_2 - t_1$. The probability amplitude for this process is a sum over all the possible trajectories [33]

$$A(r_i, t_i; r_f, t_f) = e^{-\frac{i}{\hbar}\epsilon_L(t_1-t_i)}e^{-\frac{i}{\hbar}\epsilon_R(t_f-t_1)} \sum_{N=1}^{\infty} \sum_{r_1 \dots r_N} |A(r_i, r_f, \mathcal{C}_N | t_1)| e^{ik\mathcal{L}_N} \\ + e^{-\frac{i}{\hbar}\epsilon_L(t_1-t_i)}e^{-\frac{i}{\hbar}\epsilon_L(t_2-t_1)}e^{-i\varphi_0}e^{-\frac{i}{\hbar}\epsilon_R(t_f-t_2)} \sum_{N=1}^{\infty} \sum_{r_1 \dots r_N} |A(r_i, r_f, \mathcal{C}_N | t_2)| e^{ik\mathcal{L}_N} \quad (3.43)$$

where $A(r_i, r_f, \mathcal{C}_N | t)$ is the probability amplitude of the trajectory \mathcal{C}_N such that the electron hops through the barrier at the time t , φ_0 is the phase of a single voltage pulse and \mathcal{L}_N is the length of the path. The probability is given by

$$P(r_i, t_i; r_f, t_f) = \left| \sum_{N=1}^{\infty} \sum_{r_1 \dots r_N} |A(r_i, r_f, \mathcal{C}_N | t_1)| e^{ik\mathcal{L}_N} \right. \\ \left. + e^{-\frac{i}{\hbar}(\epsilon_L-\epsilon_R)t_0}e^{-i\varphi_0} \sum_{N=1}^{\infty} \sum_{r_1 \dots r_N} |A(r_i, r_f, \mathcal{C}_N | t_2)| e^{ik\mathcal{L}_N} \right|^2 \\ = \sum_{N=1}^{\infty} \sum_{r_1 \dots r_N} \sum_{N'=1}^{\infty} \sum_{r'_1 \dots r'_{N'}} |A(r_i, r_f, \mathcal{C}_N | t_1) A(r_i, r_f, \mathcal{C}_{N'} | t_1)| e^{ik(\mathcal{L}_N - \mathcal{L}_{N'})} \\ + \sum_{N=1}^{\infty} \sum_{r_1 \dots r_N} \sum_{N'=1}^{\infty} \sum_{r'_1 \dots r'_{N'}} |A(r_i, r_f, \mathcal{C}_N | t_2) A(r_i, r_f, \mathcal{C}_{N'} | t_2)| e^{ik(\mathcal{L}_N - \mathcal{L}_{N'})} \\ + 2 \sum_{N=1}^{\infty} \sum_{r_1 \dots r_N} \sum_{N'=1}^{\infty} \sum_{r'_1 \dots r'_{N'}} |A(r_i, r_f, \mathcal{C}_N | t_1) A(r_i, r_f, \mathcal{C}_{N'} | t_2)| e^{ik(\mathcal{L}_N - \mathcal{L}_{N'})} \cos \left(\frac{\epsilon_L - \epsilon_R}{\hbar} t_0 + \varphi_0 \right) \quad (3.44)$$

We assume that the probability distribution function of the disorder in the two metals is equal and take the disorder average. As discussed in section 3.1 only terms with $\mathcal{L}_N = \mathcal{L}_{N'}$ survive the average over disorder configurations. For the first two terms in eq. (3.44) this requirement is fulfilled by identical trajectories $\mathcal{C}_N = \mathcal{C}_{N'}$. The

disorder average over the first term is

$$\begin{aligned} & \overline{\sum_{N=1}^{\infty} \sum_{r_1 \dots r_N} \sum_{N'=1}^{\infty} \sum_{r'_1 \dots r'_{N'}} |A(r_i, r_f, \mathcal{C}_N | t_1) A(r_i, r_f, \mathcal{C}_{N'} | t_1)| e^{ik(\mathcal{L}_N - \mathcal{L}_{N'})}} \\ & = \sum_{N=1}^{\infty} \sum_{r_1 \dots r_N} |A(r_i, r_f, \mathcal{C}_N | t_1)|^2 = \sum_{N=1}^{\infty} \sum_{r_1 \dots r_N} P(r_i, r_f, \mathcal{C}_N | t_1) \equiv P_1 \quad (3.45) \end{aligned}$$

Thus, it is given by the incoherent sum over the probabilities of the different trajectories such that the tunneling will happen at time t_1 . A similar expression is obtained for the second term which represents P_2 , the probability to tunnel at time t_2 . Since the voltage pulses are identical the the probability to tunnel at the first pulse and at the second pulse are equal $P_1 = P_2$. These probabilities do not depend on t_0 the time between voltage pulses.

Now, let us consider the third term in eq. (3.44). The trajectories \mathcal{C}_N and $\mathcal{C}_{N'}$ can not be identical since in one of them the electron hops at time t_1 and in the other it hops at t_2 . Nevertheless, there are trajectories such that $\mathcal{L}_N \cong \mathcal{L}_{N'}$ in all the disorder configurations.

Consider the two trajectories illustrated in Fig. 3.5:

$$\begin{aligned} (r_i, t_i) & \rightarrow (r_b, t_1) \rightarrow (r_f, t_f - t_0) \rightarrow (r_f, t_f) \\ (r_i, t_i) & \rightarrow (r_i, t_i + t_0) \rightarrow (r_b, t_2) \rightarrow (r_f, t_f) \end{aligned} \quad (3.46)$$

In the first trajectory the electron starts at point r_i in the left metal at time t_i , it moves along some path such that it reaches point r_b of the barrier at time t_1 of the first voltage pulse where it tunnels to the right lead. From r_b the electron moves along some trajectory and reaches the point r_f at time $t_f - t_0$. At time t_f the electron returns to the point r_f .

In the second trajectory, the electron starts at point r_i in the left metal at time t_i , it returns to r_i after time t_0 , then it moves along the same path of the first trajectory and reaches point r_b at time t_2 of the second voltage pulse where it tunnels to the right metal. From r_b the electron moves along the same path as in the first trajectory and reaches point r_f at time t_f .

Since the electrons have a constant velocity (magnitude) the length of the loops in the two trajectories, l_0 , is determined by t_0 , $l_0 = v_F t_0$. In the multiple scattering regime the length of the loop is much larger than the elastic mean free path and it can be approximated by $l_0 \approx N l_e \gg l_e$. The error in this approximation is of order l_e . In the weak disorder limit $k l_e \ll 1$, so the correction to the dynamical phase $k l_0$ of the loop can be neglected. Therefore, for t_0 much larger than the mean free time between successive scattering events $\tau_e = v_F l_e$ ($t_0 \gg \tau_e$), a loop of length $l_0 = v_F t_0$ exists in any disorder realization.

The probability amplitude for the two trajectories are

$$\begin{aligned} A_1 & \sim e^{ikl_1} e^{-\frac{i}{\hbar} \epsilon_L (t_1 - t_i)} e^{ikl_2} e^{-\frac{i}{\hbar} \epsilon_R (t_f - t_1)} e^{ikl_0} \\ A_2 & \sim e^{ikl_0} e^{ikl_1} e^{-\frac{i}{\hbar} \epsilon_L (t_1 - t_i)} e^{-i\varphi_0} e^{-\frac{i}{\hbar} \epsilon_L (t_2 - t_1)} e^{ikl_2} e^{-\frac{i}{\hbar} \epsilon_R (t_f - t_2)} \end{aligned} \quad (3.47)$$

where φ_0 is the phase of a single voltage pulse, l_1 is the length of the path in the left lead and l_2 is the length of the path in the right lead.

The interference between theses quantum amplitudes is

$$P_q = |A_1 + A_2|^2 = 2P_{cl} \left(1 + \cos \left(\frac{\epsilon_R - \epsilon_L}{\hbar} t_0 - \varphi_0 \right) \right) \quad (3.48)$$

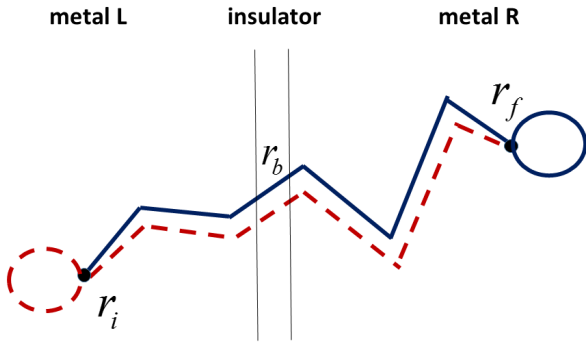


Figure 3.5: Illustration of the interfering trajectories described by (3.46). In the first trajectory (blue) the electron passes the barrier at the first voltage pulse, reaches the final point r_f at $t_f - t_0$ and returns to the final point at t_f . t_0 is the time between the voltage pulses. In the second trajectory, the electron starts at r_i , returns to it after time t_0 and passes through the barrier at the second voltage pulse. Then it reaches the final point r_f at t_f . Since the path the electrons take in the two trajectories between r_i and r_f is equal, the dynamical phase of the corresponding quantum amplitudes is equal and interference between these amplitudes will survive the disorder average.

which is the Ramsey interference in the probability to create a $e-h$ pair in the right-left leads (3.36). Therefore, the disorder average over eq. (3.44) does not wash out the oscillations of the probability with frequency t_0 .

3.8 The effect of an electromagnetic environment

The principle of a Ramsey interferometer can be used to study the dephasing processes of the electrons in a tunnel junction. Here we will consider the dephasing caused by the interaction of the electrons in the tunnel junction with the external electric circuit, i.e. with their electromagnetic environment.

Until now we have considered free electrons in our description of the electrons in the tunnel junction. How does Coulomb interaction affect this description? First, the electrons are fermionic quasi-particles with a finite lifetime [58] which sets an upper bound to the phase coherence time. The quasi-particle lifetime diverges when approaching the Fermi energy and at zero temperature. Thus a description in terms of free particles is valid as long as we consider temperatures and voltages much smaller than the Fermi energy. Second, Coulomb interactions couple the tunnel junction, which may be thought of as a leaky capacitor, to the circuit in which it is embedded. The $P(E)$ theory employed in this section describes the coupling of a small tunnel junction with large resistance compared to the quantum of resistance $R_K = \frac{h}{e^2}$ to a external impedance [59, 60, 61]. The dynamical Coulomb blockade suppression of the tunnel junction conductance at small voltage when it is embedded in a high resistive impedance circuit, predicted by the theory, was verified experimentally [62, 63]. The theory has been extended to low resistance [64] and long tunnel junctions [65] and to a general phase coherent conductors [66, 67]. A relation between the dynamical Coulomb blockade corrections to the conductance of a coherent conductor embedded in small impedance environment and the shot noise of the conductor in the absence of an external impedance was found in [68] and verified experimentally in [69]. A

general relation between the Coulomb blockade corrections to the n th cumulant of the current fluctuations with an external impedance and the $(n + 1)$ th cumulant without the external impedance were derived in [70, 71, 72, 73].

The body of works reviewed above considers transport in the presence of an environment due to a *dc* voltage. Here we consider transport due to a time-dependent voltage. The interplay between the driving force, pumping energy into the system, and the interaction with the environment give rise to complicated dynamics [74]. We concentrate on the Ramsey voltage modulation and find the effect of the environment on the Ramsey fringes.

3.8.1 Quantum circuit theory

We now present a general approach for calculating the quantum behavior of an electric network [75, 76]. A classical Hamiltonian of the circuit which reproduces its classical behavior is defined and quantized by the usual canonical quantization procedure. In this approach the degrees of freedom are the charges and magnetic fluxes stored in the components of the electric circuit and not the electrons of the materials composing the circuit. These are collective degrees of freedom describing the cooperative motion of large number of electrons. Let us first consider a simple circuit consisting of two elements: capacitor (C) and inductor (L), see figure 3.6.

Quantum mechanics of a LC -circuit

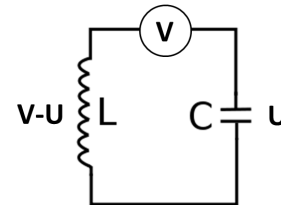


Figure 3.6: *LC* circuit driven by a voltage $V(t)$. The voltage drop on the capacitor is denoted by U and the voltage drop over the inductor is $V - U$.

We are working in the regime where Kirchhoff laws apply. This amounts to the assumption that the size of the circuit is much less than the typical wavelength of the electromagnetic field propagating through it. The dimensions of microelectronic circuits are of the order of a few hundred μm which is much shorter than the wavelength of a microwave signal in the GHz frequencies. Each element b of the circuit is characterized by the voltage across it and the current flowing through it. These variables can be defined from the underlying electromagnetic fields

$$v_b = \int_{\text{beginning of } b}^{\text{end of } b} \vec{E} \cdot \vec{dl} \quad (3.49)$$

$$i_b = \frac{1}{\mu_0} \oint_{\text{around } b} \vec{B} \cdot \vec{dl}. \quad (3.50)$$

In what follows it will be convenient to introduce the phases

$$\phi(t) = \frac{e}{\hbar} \int_{-\infty}^t dt' U(t') \quad (3.51)$$

$$\phi_0(t) = \frac{e}{\hbar} \int_{-\infty}^t dt' V(t') \quad (3.52)$$

where U is the voltage across the capacitor and V is the applied voltage. The equation of motion of the circuit $C\ddot{\phi} = \frac{\phi_0 - \phi}{L}$ can be obtained from the Lagrangian

$$\mathcal{L} = \frac{C}{2} \left(\frac{\hbar}{e} \dot{\phi} \right)^2 - \frac{1}{2L} \left(\frac{\hbar}{e} \right)^2 (\phi - \phi_0)^2. \quad (3.53)$$

This is a classical Lagrangian with no dependence on \hbar here introduced in the definition of ϕ for later convenience. Switching to the Hamilton formalism, we find that the charge Q on the junction is the conjugate variable to $(\hbar/e)\phi$. In the canonical quantization this leads to the commutation relation

$$[\phi, Q] = ie. \quad (3.54)$$

The resulting Hamiltonian is

$$H = \frac{Q^2}{2C} + \frac{1}{2L} \left(\frac{\hbar}{e} \right)^2 (\phi - \phi_0)^2. \quad (3.55)$$

This Hamiltonian is easy to understand. The first term $Q^2/2C$ represents the capacitor energy and the second term is the inductor energy $\frac{1}{2}LI^2$. The current through the inductor can be expressed by phase of the inductor $(\phi - \phi_0)$ as $I = \frac{\hbar}{eL}(\phi - \phi_0)$.

We are interested in the fluctuations of the phase ϕ around ϕ_0 , therefore we redefine the phase operator

$$\phi(t) \rightarrow \phi(t) - \phi_0(t). \quad (3.56)$$

The commutator is still

$$[\phi, Q] = ie \quad (3.57)$$

and the Hamiltonian is given by

$$H = \frac{Q^2}{2C} + \frac{1}{2L} \left(\frac{\hbar}{e} \right)^2 \phi^2. \quad (3.58)$$

The Hamiltonian of LC -circuit is equivalent to that of harmonic oscillator with frequency $\Omega = 1/\sqrt{LC}$, hence it can be written as

$$H = \hbar\Omega \left(a^\dagger a + \frac{1}{2} \right) \quad (3.59)$$

where we have defined the ladder operators $a, a^\dagger = \frac{1}{\sqrt{2}} \left(\left(\frac{\hbar^2 C}{e^4 L} \right)^{\frac{1}{4}} \phi \pm i \left(\frac{L}{\hbar^2 C} \right)^{\frac{1}{4}} Q \right)$, which satisfy the commutation relation $[a, a^\dagger] = 1$.

In order to understand the meaning of these operators we choose a gauge with only vector potential and no electric potential. In such a gauge the longitudinal part of the vector potential is $A_{||}(k) = \vec{A} \cdot \hat{k} = \int^t dt' \frac{i\rho(k)}{k\epsilon_0}$ where ρ is the charge density in the circuit element [77]. We consider the phase of the inductor $\phi \sim (a + a^\dagger)$ and wish to compare it to the vector potential \vec{A} . (3.49) implies that $\phi \propto \int^t dt' \int_{\text{beginning of L}}^{\text{end of L}} \partial_{t'} \vec{A} \cdot d\vec{l} =$

$\int_{\text{beginning of L}}^{\text{end of L}} \vec{A} \cdot d\vec{l}$. Therefore, the phase is proportional to the part of the vector potential propagating along the circuit with frequency $\Omega = 1/\sqrt{LC}$. Thus, a describes a "longitudinal photon" with frequency Ω which propagates along the circuit. The longitudinal vector potential is related to the charge density, hence the "longitudinal photon" describes charge density fluctuations.

Quantum mechanics of a general circuit

In the previous section we have shown that the Hamiltonian of an LC circuit is the sum over the energies stored in the capacitor and inductor. This statement can be generalized to describe an arbitrary circuit. The Hamiltonian of any linear electric circuit is the sum of the energies of its capacitive and inductive elements [75, 76]. In order to describe circuits with linear dissipative elements the Caldeira-Leggett model [78, 79] can be used and the dissipative elements are replaced by a semi-infinite transmission line. The energy loss of the dissipative element is accounted for by the energy sent through the transmission line to infinity. The transmission line is described by a continuum of LC-circuits, the parameters of these LC-circuits are chosen such that the classical equation of motion (with dissipation) of the circuit is recovered.

3.8.2 Tunnel junction embedded in an electric circuit

We consider a tunnel junction connected in series with an external impedance $Z(\omega)$ (see Fig. 3.7) which represents the electrical circuit connected to the tunnel junction. We use the $P(E)$ theory to include the effect of the environment [59].

Tunneling and description of the environment

The $P(E)$ theory [59] described in this section is phenomenological. It treats the electrons in the tunnel junction and the electrons in the electric circuit differently. The electrons in the tunnel junction are described by their fermionic operators while in the circuit the charge fluctuations which incorporate many electrons are described by bosonic operators. A tunneling electron generates electric field fluctuation throughout the circuit, these effects modify the tunneling Hamiltonian within an effective description. The phenomenological description holds when the electric field propagates faster than the electrons in the circuit [59]. The $P(E)$ theory described successfully experiments on tunnel junctions [63, 64, 65, 62], short coherent conductors [69] and Josephson junctions [80] in various external impedances.

As in section 3.2, the electrons in the two metal electrodes are described by the Hamiltonian

$$H_0 = \sum_k \epsilon_{Lk} c_{Lk}^\dagger c_{Lk} + \sum_q \epsilon_{Rq} c_{Rq}^\dagger c_{Rq} \quad (3.60)$$

Tunneling is introduced by the Hamiltonian [59]

$$H_T = \sum_{kq} T c_{Rq}^\dagger c_{Lk} e^{-i\phi_0(t)} \Lambda_e + \text{h.c.} \quad (3.61)$$

such that $T c_{Rq}^\dagger c_{Lk}$ transfers an electron between the electrodes and $\phi_0(t)$ is the time integral over the external voltage applied on the circuit $\phi_0(t) = \frac{e}{\hbar} \int^t V(t') dt'$ as defined in (3.52). Λ_e is an operator changing the charge Q on the junction: $\Lambda_e^\dagger Q \Lambda_e = Q - e$. Therefore, Λ_e represents the coupling to the environment. When an electron tunnels, it changes the charge on the tunnel junction and excites the charge density modes of the electric circuit.

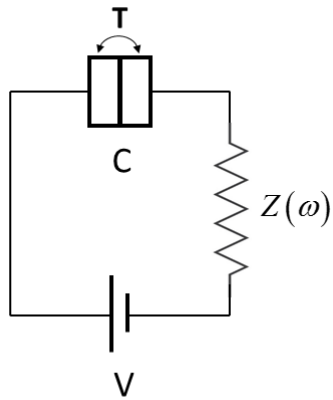


Figure 3.7: A tunnel junction with capacitance C and a constant tunneling matrix element T coupled to a voltage source V via the external impedance $Z(\omega)$.

As in section 3.8.1 we describe the environment phenomenologically by a set of LC -circuits which are bilinearly coupled to the phase of the junction ϕ

$$H_{\text{env}} = \frac{Q^2}{2C} + \sum_{n=1}^N \left[\frac{q_n^2}{2C_n} + \left(\frac{\hbar}{e} \right)^2 \frac{1}{2L_n} (\phi - \phi_n)^2 \right]. \quad (3.62)$$

The first term describes the charging energy of the junction capacitor. In the second term we sum over the degrees of freedom of the external circuit represented by harmonic oscillators of frequency $\tilde{\omega}_n = 1/\sqrt{L_n C_n}$ which are bilinearly coupled to the phase of the tunnel junction. Recall that Q and ϕ represent a multiparticle state of the electrons in the circuit. The Hamiltonian can be diagonalized and written in terms of ladder operators.

$$H_{\text{env}} = \sum_j \hbar \Omega_j \left(a_j^\dagger a_j + \frac{1}{2} \right) \quad (3.63)$$

These operators create/annihilate a photon with frequency Ω_j which represents an excitation of the electromagnetic field propagating along the circuit.

Having a description of the environment, the charge translation operator can be found: $\Lambda_e = e^{-i\phi}$. Since $[\phi, Q] = ie$

$$e^{i\phi} Q e^{-i\phi} = Q - e \quad (3.64)$$

as required. Therefore, tunneling is introduced by the Hamiltonian

$$H_T = \sum_{kq} T c_{Rq}^\dagger c_{Lk} e^{-i\phi - i\phi_0} + \text{h.c.} \quad (3.65)$$

Switching to the diagonalized degrees of freedom of the environment, the phase takes the form

$$\phi = \sum_j b_j (a_j + a_j^\dagger) \quad (3.66)$$

where b_j are constants that result from the diagonalization of (3.62).

Finally, the total Hamiltonian

$$H = H_0 + H_{\text{env}} + H_T \quad (3.67)$$

contains the contributions of the Hamiltonian of the two electrodes (3.60), the Hamiltonian describing the environment including the charge degree of freedom (3.62) and the tunneling Hamiltonian which couples the first two parts (3.65).

It may seem surprising that the external voltage does not enter the energies of the electrons in the electrodes, but it is just a matter of a unitary transformation to the Hamiltonian. Performing the time-dependent unitary transformation

$$U = \prod_k e^{i\phi_0(t)c_{Lk}^\dagger c_{Lk}} \quad (3.68)$$

results in the following quasiparticles and tunneling Hamiltonians

$$\tilde{H}_0 = \sum_k (\epsilon_{Lk} + V(t)) c_{Lk}^\dagger c_{Lk} + \sum_q \epsilon_{Rq} c_{Rq}^\dagger c_{Rq} \quad (3.69)$$

$$\tilde{H}_T = \sum_{kq} T c_{Rq}^\dagger c_{Lk} e^{-i\phi} + \text{h.c.} \quad (3.70)$$

We chose the previous descriptions since for perturbation theory it is convenient to work with a Hamiltonian whose time dependence is in the perturbation and not in the system.

We assume that the initial state of the system is a product state $\rho_i = \rho_{i,e} \otimes \rho_{i,\text{env}}$ where the initial state of the tunnel junction is the vacuum state of electrons and holes $\rho_i = |0\rangle\langle 0|$ and that the environment is in thermal equilibrium with inverse temperature β : $\rho_{i,\text{env}} = Z_\beta^{-1} e^{-\beta H_{\text{env}}}$, $Z_\beta = \text{Tr} e^{-\beta H_{\text{env}}}$. Note that we assume different temperatures for the environment and the leads.

3.8.3 Probability for the creation of e - h pairs in the presence of an environment

The density matrix of the whole system at t_f is given by $\rho(t_f) = U(t_i, t_f) \rho_i U^\dagger(t_i, t_f)$, where $U(t_i, t_f)$ is the time evolution operator. The probability to create a pair is

$$P_{LR}^{k,-q} = \text{Tr}_{\text{env}} \langle 1_{e_{Lk}}, 1_{h_{R,-q}} | \rho(t_f) | 1_{e_{Lk}}, 1_{h_{R,-q}} \rangle \quad (3.71)$$

The probability for the creation of a e - h pair to second order in T , the tunneling matrix element, can be found by expanding U in powers of T

$$\begin{aligned} P_{LR}^{k,-q} &\approx \frac{1}{\hbar^2} \int_{t_i}^{t_f} dt_1 \int_{t_i}^{t_f} dt_2 \text{Tr}_{\text{env}} \langle 1_{e_{Lk}}, 1_{h_{R,-q}} | H_T(t_2) | 0 \rangle \langle 0 | \otimes \rho_{i,\text{env}} H_T(t_1) | 1_{e_{Lk}}, 1_{h_{R,-q}} \rangle \\ &= \frac{T^2}{\hbar^2} \int_{t_i}^{t_f} dt_1 \int_{t_i}^{t_f} dt_2 e^{-i\phi_0(t_1)+i\phi_0(t_2)} e^{-i\frac{\Delta\epsilon_{LR}}{\hbar}t_1} e^{+i\frac{\Delta\epsilon_{LR}}{\hbar}t_2} \text{Tr}_{\text{env}} \left\{ e^{+i\tilde{\phi}(t_2)} e^{-i\tilde{\phi}(t_1)} \rho_{i,\text{env}} \right\} \\ &= \frac{T^2}{\hbar^2} \int_{t_i}^{t_f} dt_1 \int_{t_i}^{t_f} dt_2 e^{-i\phi_0(t_1)+i\phi_0(t_2)} e^{-i\frac{\Delta\epsilon_{LR}}{\hbar}t_1} e^{+i\frac{\Delta\epsilon_{LR}}{\hbar}t_2} e^{J(t_2-t_1)} \end{aligned} \quad (3.72)$$

where the time evolution of \tilde{O} is with respect to the Hamiltonian $H_0 + H_{env}$. Since the thermal state of the environment is Gaussian with respect to the environment operators and stationary, the bath expectation value can be expressed as [59]

$$\text{Tr}_{env} \left\{ e^{\pm i\tilde{\phi}(t_2)} e^{\mp i\tilde{\phi}(t_1)} \rho_{i,env} \right\} = e^{J(t_2-t_1)} \quad (3.73)$$

where we introduce the phase-phase correlation function

$$J(t) = \text{Tr}_{env} \left\{ [\tilde{\phi}(t) - \tilde{\phi}(0)] \tilde{\phi}(0) \rho_{i,env} \right\} \quad (3.74)$$

and the probability of the bath to absorb energy E

$$P(E) = \frac{1}{2\pi\hbar} \int_{-\infty}^{\infty} dt e^{[J(t) + \frac{i}{\hbar} Et]} \quad (3.75)$$

Damping and fluctuations have the same microscopic origin, therefore they are related. This relation is given by the fluctuation-dissipation theorem [81]. The susceptibility is the linear response of the phase to the conjugate force $\frac{e}{\hbar} I(t)$

$$\chi(\omega) = \chi'(\omega) - i\chi''(\omega) = \left(\frac{e}{\hbar}\right)^2 \frac{Z_t(\omega)}{i\omega} \quad (3.76)$$

where Z_t is the total impedance of the electric circuit, i.e. of the tunnel junction capacitance C and the external impedance Z in series $Z_t(\omega) = \frac{1}{Z^{-1} + i\omega C}$.

The fluctuation-dissipation theorem [81] relates the Fourier transform of the correlation function

$$C(\omega) = \int_{-\infty}^{\infty} dt e^{-i\omega t} \langle \tilde{\phi}(0) \tilde{\phi}(t) \rangle \quad (3.77)$$

to the dissipative part of the susceptibility $\chi''(\omega)$

$$C(\omega) = \frac{2\hbar}{1 - e^{-\beta\hbar\omega}} \chi''(\omega) = \frac{2}{1 - e^{-\beta\hbar\omega}} \frac{1}{\omega} \frac{\text{Re}Z_t(\omega)}{R_K} \quad (3.78)$$

where $R_K = \frac{h}{e^2}$ is the quantum resistance. Therefore, the correlation can be expressed as

$$\langle \tilde{\phi}(0) \tilde{\phi}(t) \rangle = \int_{-\infty}^{\infty} d\omega e^{+i\omega t} \frac{2}{1 - e^{-\beta\hbar\omega}} \frac{1}{\omega} \frac{\text{Re}Z_t(\omega)}{R_K} \quad (3.79)$$

Subtracting $\langle \tilde{\phi}^2(0) \rangle$ and using the identity $\frac{1}{1 - e^{-\beta\hbar\omega}} = \frac{1}{2} - \frac{1}{2} \coth(\frac{1}{2}\beta\hbar\omega)$, $J(t)$ is given by [59]

$$J(t) = 2 \int_0^{\infty} \frac{d\omega}{\omega} \frac{\text{Re}Z_t(\omega)}{R_K} \left\{ \coth\left(\frac{\beta\hbar\omega}{2}\right) [\cos(\omega t) - 1] - i \sin(\omega t) \right\}. \quad (3.80)$$

With the help of eqs. (3.74-3.75), the creation probability can be expressed as the sum of all the processes for which a tunneling electron absorbs energy $\Delta\epsilon + E$ from

the time-dependant voltage and emits energy E to the environment

$$P_{LR}^{env}(\Delta\epsilon_{LR}) = \frac{T^2}{\hbar^2} \int_{t_i}^{t_f} dt_1 \int_{t_i}^{t_f} dt_2 e^{-i\phi_0(t_1) + i\phi_0(t_2)} e^{-i\frac{\Delta\epsilon_{LR}}{\hbar}t_1} e^{+i\frac{\Delta\epsilon_{LR}}{\hbar}t_2} \int_{-\infty}^{\infty} dEP(E) e^{-\frac{i}{\hbar}Et} \\ = \int_{-\infty}^{\infty} dEP(E) P_{LR}^0(\Delta\epsilon_{LR} + E). \quad (3.81)$$

$P(E)$ is the probability of the environment to absorb energy E (negative energies correspond to emission) and P_{LR}^0 is the creation probability in the absence of environment (3.19). As in the case without environment, the pair creation probability depends only on the energy difference $\Delta\epsilon_{LR} = \epsilon_{Lk}^0 - \epsilon_{Rq}$. The same expression holds also for P_{RL} with energy difference $\Delta\epsilon_{RL} = \epsilon_{Rq} - \epsilon_{Lk}^0$. This is illustrated in Fig. 3.8.

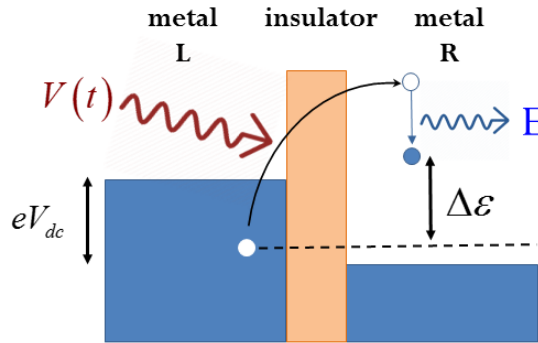


Figure 3.8: In the presence of an environment a tunneling electron can emit energy into the environment. The energy supplied to the electron from the voltage pulse is the final energy of the e - h pair plus the energy the environment absorbed $\Delta\epsilon + E$. This process is described by eq. (3.81)

3.8.4 The effect of an electromagnetic environment on Ramsey interference

The probability for the creation of e - h pairs (3.81) in the presence of an environment is a convolution-like expression between the pair creation probability in the absence of environment and the environment absorption probability. Therefore the Ramsey fringes will be washed out by the environment when the width of $P(E)$ will be comparable to the period $\hbar t_0^{-1}$ of the fringes.

To be more precise, for the Ramsey voltage modulation given by (3.32) the probability for the creation of a e - h pair after two pulses is given by

$$P_{LR,2}^{env}(\Delta\epsilon) = \int_{-\infty}^{\infty} dEP(E) P_{RL,1}^0(\Delta\epsilon + E) \left[2 + 2 \cos \left(\frac{(\Delta\epsilon + E)t_0}{\hbar} + \varphi_0 \right) \right] \quad (3.82)$$

where $P_{RL,1}^0$ is the pair creation probability due to a single pulse in the absence of the environment (3.35).

To better understand the effect of the environment let us consider the probability to create a $e\text{-}h$ pair expressed in the time domain

$$P_{LR}^{env}(\Delta\epsilon_{LR}) = \frac{T^2}{\hbar^2} \int_{t_i}^{t_f} dt_1 \int_{t_i}^{t_f} dt_2 e^{-i\phi_0(t_1)+i\phi_0(t_2)} e^{-i\frac{\Delta\epsilon_{LR}}{\hbar}t_1} e^{+i\frac{\Delta\epsilon_{LR}}{\hbar}t_2} e^{J(t_2-t_1)} \quad (3.83)$$

Using the stationary phase approximation, the main contributions to the integral come from the times where the argument of the exponent is stationary. Assuming that $\dot{J} \ll \dot{\phi}_0$ and $\dot{J} \ll (\epsilon_{Rq} - \epsilon_{Lk})$, the stationary condition is

$$\begin{aligned} \hbar\dot{\phi}_0(t_1) &= \Delta\epsilon_{LR} \\ \hbar\dot{\phi}_0(t_2) &= \Delta\epsilon_{LR} \end{aligned} \quad (3.84)$$

Remember that we consider only cases where $|\Delta\epsilon_{LR}| > 0$, therefore the main contribution to the integral comes from times satisfying

$$V(t_1) = V(t_2) \neq 0. \quad (3.85)$$

Assuming that the two pulses are narrow, i.e. $V(t) \approx \varphi_0\delta(t) + \varphi_0\delta(t-t_0)$, there are only 4 possibilities to satisfy (3.85):

$$\begin{aligned} t_1 &= t_2 = 0 \\ t_1 &= t_2 = t_0 \\ t_1 &= 0 \quad t_2 = t_0 \\ t_1 &= t_0 \quad t_2 = 0 \end{aligned} \quad (3.86)$$

and the $e\text{-}h$ creation probability is approximately given by

$$\begin{aligned} P_{LR}^{env}(\Delta\epsilon_{LR}) &\sim 2e^{J(0)} + e^{J(t_0)} e^{+i\varphi_0} e^{+i\frac{\Delta\epsilon_{LR}t_0}{\hbar}} + e^{J(-t_0)} e^{-i\varphi_0} e^{-i\frac{\Delta\epsilon_{LR}t_0}{\hbar}} \\ &= 2 + 2e^{J_R(t_0)} \cos\left(\frac{\Delta\epsilon_{LR}t_0}{\hbar} + \varphi_0 + J_I(t_0)\right) \end{aligned} \quad (3.87)$$

where we used the time reversal symmetry for the free environment $J(t) = J^*(-t)$ and we defined the real and imaginary part of the correlation function $J(t) = J_R(t) + iJ_I(t)$. This result can be understood in our two-slit description of Ramsey interferometry. The environment dephases the phase of the electron, therefore it reduces only the interference (quantum) part of the probability and keeps the classical sum of the two paths unchanged. Moreover, the amplitude of the Ramsey fringes decays exponentially with the correlation function of the environment $J(t_0)$. Therefore, by measuring it as a function of the time between the pulses, t_0 , we can obtain the correlation function of the bath as a function of time.

In section 3.1 we argued that the effect of an environment on quantum interference will be to reduce exponentially its amplitude (3.7). In this section we consider an example for such an environment - the EM environment. There, the function $f(t)$ in (3.7) which controls the dephasing is just the real part of the correlation function $J_R(t)$. The coherence time τ_ϕ is the characteristic time for the decay of the interference effect. Using Ramsey interferometry, τ_ϕ can be measured in a direct way: the time t_0 between the pulses is increased until the Ramsey interference vanishes.

In the next section we will demonstrate that the $e\text{-}h$ creation probability in the presence of an environment can be measured by the current noise in the same way as without an environment.

3.8.5 Current noise in the presence of an environment

In this section we show that the relation between the current noise and the probability for the creation of $e\text{-}h$ pairs remains unaffected by the environment. Thereby, the creation probability can be measured along the same protocol previously described .

As before, we find the current from the change in time of the number of electrons in the left lead

$$I = i \frac{e}{\hbar} \sum_{kq} \left[T c_{Lk}^\dagger c_{Rq} e^{+i\phi_0(t)+i\phi} - h.c. \right] \quad (3.88)$$

Note that now the current depends also on the bath operators through ϕ . The correlation function of the current is defined as

$$C(t_1, t_2) = \text{Tr} \{ I(t_1) I(t_2) \rho_i \} \quad (3.89)$$

The correlation function, to second order in T , is given by the correlation function of $\tilde{I}(t)$, where $\tilde{I}(t)$ evolve in time with respect to the Hamiltonian $H_0 + H_{env}$

$$\begin{aligned} C(t_1, t_2) &\approx \text{Tr} \left\{ \tilde{I}(t_2) \rho_i \tilde{I}(t_1) \right\} = \text{Tr}_{env} \left\{ \sum_{kq} \langle 11 | \tilde{I}(t_2) | 0 \rangle \langle 0 | \otimes \rho_{i,env} \tilde{I}(t_1) | 11 \rangle \right\} \\ &= \frac{e^2}{\hbar^2} \text{Tr}_{env} \left\{ \sum_{kq} \langle 11 | \tilde{H}_T(t_2) | 0 \rangle \langle 0 | \otimes \rho_{i,env} \tilde{H}_T(t_1) | 11 \rangle \right\} \end{aligned} \quad (3.90)$$

where $|11\rangle$ denotes a state with one $e\text{-}h$ pair and the sum over k, q is over all such possible states. The trace over the electron system is reduced to a trace over one electron-hole states since they are the only states that can be created from the vacuum by \tilde{I} . In order to get the second line of (3.90) we note that the matrix elements of \tilde{I} and \tilde{H}_T differ by a constant only.

The power spectrum of the current is given by the Fourier transform of the correlation function,

$$S(\Omega) = \int_{-\infty}^{\infty} dt_1 \int_{-\infty}^{\infty} dt_2 C(t_1, t_2) e^{i\Omega t_1} e^{-i\Omega t_2}. \quad (3.91)$$

Inserting (3.90) we find that the shot noise is the total probability to create a $e\text{-}h$ pair, as in the absence of the environment.

$$\begin{aligned} S(\Omega \rightarrow 0) &= \int_{-\infty}^{\infty} dt_1 \int_{-\infty}^{\infty} dt_2 \frac{e^2}{\hbar^2} \text{Tr}_{env} \left\{ \sum_{kq} \langle 11 | \tilde{H}_{int}(t_2) | 0 \rangle \langle 0 | \otimes \rho_{i,env} \tilde{H}_{int}(t_1) | 11 \rangle \right\} \\ &= e^2 \left[\sum_{\substack{q > k_F \\ k < k_F}} P_{RL}^{env} (\Delta\epsilon_{RL} = \epsilon_{Rq} - \epsilon_{Lk}^0) + \sum_{\substack{k > k_F \\ q < k_F}} P_{LR}^{env} (\Delta\epsilon_{LR} = \epsilon_{Lk}^0 - \epsilon_{Rq}) \right]. \end{aligned} \quad (3.92)$$

As before, taking the continuum limit and assuming that the density of states and the tunneling matrix element does not depend on energy, the second derivative with

respect to the *dc* voltage yields

$$\frac{d^2S(\Omega \rightarrow 0)}{d(eV_{dc})^2} = e^2\rho^2 [P_{LR}^{env}(\Delta\epsilon_{LR} = -eV_{dc}) + P_{RL}^{env}(\Delta\epsilon_{RL} = eV_{dc})] \quad (3.93)$$

We have demonstrated that the relation between the current noise and the *e-h* creation probability does not depend on the environment. Therefore, the measurement procedure described in section 3.4 can be used to observe the effect of an environment on the tunneling process.

3.8.6 Ohmic environment - Crossover from ballistic to diffusive regimes

For an ohmic environment the classical equation of motion of the phase in the absence of tunneling and external voltage correspond to a free particle with friction [82]

$$\ddot{\phi} + \frac{1}{RC}\dot{\phi}(s) = 0 \quad (3.94)$$

where the friction coefficient is given by $(RC)^{-1}$, C is the tunnel junction capacitance and R is the external resistor. Fluctuation dissipation theorem tells us that the source of friction is the fluctuations of the phase. When the RC circuit is at zero temperature ($\beta \rightarrow \infty$) the origin of the fluctuations will be quantum. In the high temperature limit $\hbar\beta \ll RC$, the fluctuations will be dominated by the thermal ones.

The quantum equation of motion of the phase is analogous to that of a quantum Brownian particle [59, 82], where the phase corresponds to the position of the Brownian particle. In the high temperature limit $\hbar\beta \ll RC$ the limiting behavior of the correlation function $J(t)$ is [82]

$$J(t) = \begin{cases} -\frac{1}{\hbar\beta} \frac{\pi}{R_k C} t^2 - i\pi \frac{1}{R_k C} t & t \ll RC \\ -\frac{R}{R_k} \frac{2\pi}{\hbar\beta} (t - RC) - i\pi \frac{R}{R_k} & t \gg RC \end{cases} \quad (3.95)$$

where we introduce the quantum of resistance $R_K = h/e^2$. The mapping between the tunnel junction phase and the position of a quantum Brownian particle is described in [82] and sketched in appendix D.

The real part of the correlation function $J_R(t)$ corresponds to the mean square displacement of the Brownian particle

$$J_R(t) = -\frac{1}{2} \langle [\tilde{\phi}(t) - \tilde{\phi}(0)]^2 \rangle \sim \begin{cases} t^2 & t \ll RC \\ t & t \gg RC \end{cases} \quad (3.96)$$

where $\langle \cdot \rangle$ represents the trace over the environment degrees of freedom. For $t \ll RC$, the displacement of the Brownian particle is linear in time $\sqrt{\langle [\tilde{\phi}(t) - \tilde{\phi}(0)]^2 \rangle} \sim t$, therefore its motion is ballistic in this regime. For $t \gg RC$, the displacement of the Brownian particle is $\sqrt{\langle [\tilde{\phi}(t) - \tilde{\phi}(0)]^2 \rangle} \sim \sqrt{t}$, therefore its motion is diffusive in that regime. These limits can be understood from noting that RC is the average time between kicks of the Brownian particle. For $t \ll RC$, the Brownian particle did not change its direction, therefore its motion is ballistic. For $t \gg RC$ the Brownian particle has already changed its direction of propagation many times, therefore its motion is diffusive. In both regimes, the correlation decreases linearly with the temperature of the circuit β^{-1} .

The probability for the bath to absorb the energy E for high/low resistance corre-

spond to taking correspondingly the short/long time limits of the correlation function $J(t)$ into the definition of $P(E)$ eq. (3.75)

$$P(E) = \begin{cases} \sqrt{\frac{\beta}{4\pi E_c}} \exp\left[-\beta \frac{(E-E_c)^2}{4E_c}\right] & R \rightarrow \infty \\ \frac{1}{\pi} \frac{2\pi R}{\beta R_K} \frac{1}{(E)^2 + \left(\frac{2\pi R}{\beta R_K}\right)^2} & R \rightarrow 0 \end{cases} \quad (3.97)$$

where $E_c = \frac{e^2}{2C}$ is the charging energy of the tunnel junction. In the high resistance limit the probability of the environment to absorb the energy E is a Gaussian centered at the charging energy of the tunnel junction. This is the Coulomb blockade regime where an electron can tunnel only if it can give the charging energy to the environment. In the low resistance limit the environment probability $P(E)$ is a Lorentzian centered at zero. In both regimes, the width of the probability distribution increases with temperature, indicating that more tunneling processes are allowed as the temperature increases.

Here, we can demonstrate the advantage of the Ramsey interference method. Since Ramsey setup introduces a new time scale t_0 , the time between the voltage pulses, scanning t_0 allows to probe the dynamics at all time scales. Recall that in section 3.8.4 we found how the environment modifies the Ramsey interference pattern (3.87)

$$P_{LR}^{env}(\Delta\epsilon_{LR}) \sim 2 + 2e^{J_R(t_0)} \cos\left(\frac{\Delta\epsilon_{LR}t_0}{\hbar} + \varphi_0 + J_I(t_0)\right) \quad (3.98)$$

where we defined the real and imaginary part of the correlation function $J(t) = J_R(t) + iJ_I(t)$. The correlation function $J_R(t_0)$ can be obtained from the amplitude of the Ramsey fringes. Modifying t_0 allows to probe the crossover between the short (ballistic) and long (diffusive) time limits of the ohmic environment (3.95).

The probability for the creation of a $e-h$ pair in the presence of the ohmic environment (3.82) for $t_0 \gg RC$ is given by

$$P_2^{env}(\Delta\epsilon) = 4 \int_{-\infty}^{\infty} \frac{dE}{\pi} \frac{\frac{2\pi}{\beta\alpha}}{(E)^2 + \left(\frac{2\pi}{\beta\alpha}\right)^2} P_1^0(\Delta\epsilon + E) \cos^2\left(\frac{(\Delta\epsilon + E)t_0}{2\hbar} + \frac{\varphi_0}{2}\right) \quad (3.99)$$

Since the probability to create a $e-h$ pair is a convolution between the bare probability $P^0(\Delta\epsilon)$ and the probability of the environment to absorb energy $P(E)$, the Ramsey interference pattern will be noticeable only when the width of $P(E)$ is smaller than the period of the Ramsey fringes $2\pi\hbar t_0^{-1}$. The width of the one-pulse envelope is much larger than the period of the Ramsey fringes ($\tau^{-1} \gg t_0^{-1}$), therefore we can assume that in the regime we are interested in, the one-pulse envelope varies slowly with respect to the width of $P(E)$

$$\frac{d}{d\Delta\epsilon} P_1^0(\Delta\epsilon) \frac{2\pi R_K}{\beta R} \ll 1 \quad (3.100)$$

and take it as constant over the integration range to obtain a simple expression for the Ramsey interference probability in the diffusive regime

$$P_2^{env}(\Delta\epsilon) \approx 2P_1^0(\Delta\epsilon) \left(1 + \cos\left(\frac{\Delta\epsilon t_0}{\hbar} \pm \varphi_0\right) e^{-\frac{2\pi R}{\hbar\beta R_K} t_0}\right). \quad (3.101)$$

The phase coherence time τ_ϕ is the characteristic time for the decay of the interference effect. In this regime it is given by $\tau_\phi = \hbar\beta R_K/2\pi R$.

In the opposite limit, $t_0 \ll RC$, the probability for the creation of a $e-h$ pair in the

presence of the ohmic environment (3.82) is given by

$$P_2^{env}(\Delta\epsilon) = 4 \int_{-\infty}^{\infty} dE \sqrt{\frac{\beta}{4\pi E_c}} e^{-\beta \frac{(E-E_c)^2}{4E_c}} P_1^0(\Delta\epsilon + E) \cos^2 \left(\frac{(\Delta\epsilon + E)t_0}{2\hbar} + \frac{\varphi_0}{2} \right). \quad (3.102)$$

From the same considerations as before we assume that the one-pulse envelope varies slowly with respect to the width of $P(E)$

$$\frac{d}{d\Delta\epsilon} P_1^0(\Delta\epsilon) \sqrt{\frac{2E_c}{\beta}} \ll 1 \quad (3.103)$$

and take it to be constant over the integration range. The probability for the creation of a $e-h$ pair in the ballistic regime can be expressed as

$$P_2^{env}(\Delta\epsilon) \approx 2P_1^0(\Delta\epsilon + E_c) \left(1 + \cos \left(\frac{(\Delta\epsilon + E_c)t_0}{\hbar} \pm \varphi_0 \right) e^{-\frac{E_c}{\beta\hbar^2}t_0^2} \right) \quad (3.104)$$

Note that in this regime the amplitude of the Ramsey fringes decay as $e^{-\frac{E_c}{\beta\hbar^2}t_0^2}$ where the argument of the exponent decreases quadratically and not linearly in time. The phase coherence time, the characteristic time for the decay of the Ramsey fringes, is now given by $\tau_\phi = \sqrt{\beta\hbar^2/E_c}$. The ballistic regime corresponds to the appearance of Coulomb blockade, the attenuation of the current through the tunnel junction as a consequence of the interaction of the tunneling electron with the EM environment. In the Ramsey interference, Coulomb blockade appears as a shift of the interference pattern by the charging energy E_c (see eq. 3.104 relative to eq. (3.34)). Due to the sensitivity of the Ramsey fringes it can be used to measure the charging energy of the tunnel junction in an accurate way.

Fig. 3.9 shows the probability for the creation of a $e-h$ pair as a function of its energy in the Coulomb blockade regime (3.104) for the same voltage modulation used in Fig. 3.3 where the probability in the absence of environment (3.34) is plotted. The different plots represent different temperatures of the resistor, the temperature is given in units of E_c , the charging energy of the tunnel junction. The figure shows the decrease in the amplitude of the Ramsey fringes with temperature. In all the plots, the time t_0 between the pulses is kept constant. The energy of the $e-h$ pair $\Delta\epsilon$ is given in units of $\frac{2\pi\hbar}{t_0}$ as in Fig. 3.3. In order to clearly see the shift of the interference pattern by E_c relative to Fig. 3.3, we chose, artificially, that the charging energy of the tunnel junction is $E_C = 1$ in units of $\frac{2\pi\hbar}{t_0}$.

The ohmic environment decreases the amplitude of the Ramsey fringes in an exponential manner where the exponent argument is $J_R(t_0)$. Therefore, the quantum Brownian motion of the tunnel junction phase can be explored using Ramsey interference. The crossover between the ballistic and diffusive regimes correspond to having both arguments in the exponents of the functions (3.101), (3.104) small compared to 1 when $t_0 \sim RC$. Therefore, we require $\frac{2\pi^2}{\beta E_C} \frac{R^2}{R_K^2} < 1$. The high temperature limit should also be satisfied. It can be rewritten as $\beta E_C \ll \pi(R/R_K)$.

Fig. 3.10 shows the crossover between the ballistic and diffusive regimes around $t_0 = RC$. The amplitude of the Ramsey fringes in the case of on ohmic environment is plotted as a function of t_0 . The blue dots are numerical data and the red and green lines are the approximations for small and large times of the correlation function $J(t)$ (eqs. 3.101, 3.104). The system parameters are chosen to be $E_c = 10^{-8}eV$, $\beta^{-1} = 10^{-4}eV$, $R_K/R = 750$, $\gamma = 0.005(RC)^{-1}$, this corresponds to resistance of $R = 34.5\Omega$, capacitance of $C = 8pF$ and temperature of $1K$. The voltage pulse is

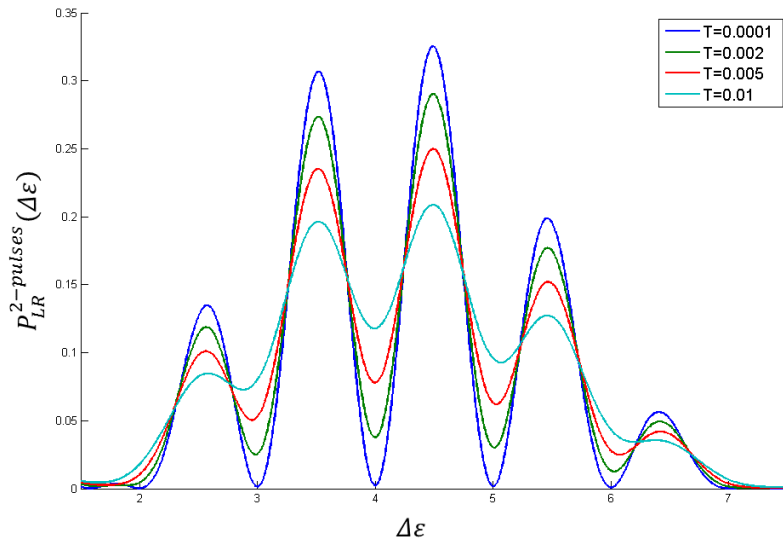


Figure 3.9: *Ramsey interference in the probability for a e-h pair creation in the Coulomb blockade regime as a function of energy for different temperatures of the resistor. The temperatures are given in units of the charging energy E_c . The voltage modulation for all the plots is the same as in Fig. 3.3 and the energy of the e-h pair is given in units of $\frac{2\pi\hbar}{t_0}$ (as in Fig. 3.3). In order to clearly see the shift of the interference pattern by E_c relative to Fig. 3.3, we chose, artificially, that the charging energy of the tunnel junction is $E_C = 1$ in units of $\frac{2\pi\hbar}{t_0}$.*

taken to be a Gaussian with width $\sigma = 0.005RC$ and pulse area $\varphi_0 = 7\pi$.

The numerical data in Fig. 3.10 is calculated in the following way: The environment probability $P(E)$ is calculated from eq. (3.75). The bare creation probability $P^0(\Delta\epsilon)$ after a single Gaussian pulse and after two consequent Gaussian pulses is calculated from eq. (3.19). In order for these integrals to converge we introduce a small imaginary part to the energy γ . Since these integrals oscillate rapidly they are the main source of the numerical errors. The creation probability in the presence of the environment is calculated from eq. (3.81) and fitted to the expression $P_2(\Delta\epsilon) = 2P_1(\Delta\epsilon)(1 + A \cos(\Delta\epsilon t_0/\hbar + b))$. The fitting parameter A is the amplitude of the Ramsey fringes and its logarithm is plotted in Fig. 3.10 as a function of t_0 , the time between the two pulses.

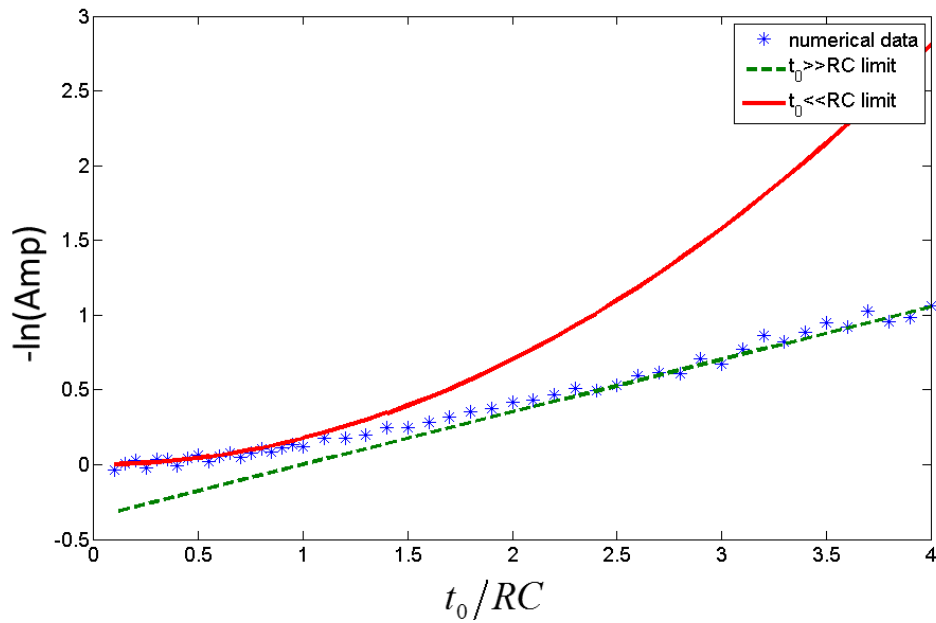


Figure 3.10: The amplitude of the Ramsey fringes in the case of an ohmic environment as a function of the time between the voltage pulses t_0 . The blue dots are numerical data the red and green lines are the approximations for small and large times. The system parameters are chosen to be $E_c = 10^{-8} \text{ eV}$, $\beta^{-1} = 10^{-4} \text{ eV}$, $\frac{R_K}{R} = 750$, $\gamma = 0.005(RC)^{-1}$. The voltage pulse is taken to be a Gaussian with width $\sigma = 0.005RC$ and pulse area $\phi_0 = 7\pi$

Chapter 4

Ramsey interference and Schwinger effect

The Schwinger effect is the creation of electron-positron (*e-p*) pairs from the QED vacuum perturbed by a strong classical external electric field [1, 83, 84, 85]. This fundamental aspect of QED has not yet been observed since it requires strong fields. The critical field strength, for the case of a constant electric field, is of the order of 16^{16} V/cm (the corresponding intensity is 10^{29} W/cm^2).

New theoretical studies, motivated by the experimental developments in ultra-high intensity lasers [86, 87, 88, 89], suggest that by manipulating the shape of the laser pulses the Schwinger effect might become observable at lower intensities ($10^{25} - 10^{26} \text{ W/cm}^2$). Spacial shaping and enhancement of the electric field configuration by simultaneously focusing multiple pulses on one spot was suggested in [90, 91]. Temporal shaping by superimposing a strong and slow pulse with a weak and fast one were considered in [92, 93, 94, 95, 96, 97, 98].

Since the Schwinger effect is non-perturbative, the temporal shape of the laser pulse have a considerable effect on the pair creation rate and momentum distribution [99, 100, 101]. The oscillatory behavior of the momentum distribution is a manifestation of the interference between the multiple laser pulses [102, 103, 104]. Unfortunately, exact analytic solutions of the particle creation probability exist only for a few field configurations, such as a uniform electric field with a time dependence of $\text{sech}(t)$. Hence, optimizing the pulse shape is an intricate problem [105]. We propose that the *e-p* pair creation in the Schwinger effect can be mapped to a simple NMR two-level system. This allows for an experimental study of the optimal time-dependent modulation.

We consider the case of uniform but time-dependent electric fields where the problem can be formulated as a 1d quantum mechanical over the barrier scattering problem. The calculation of the probability to create a *e-p* pair is reduced to finding the reflection and transmission coefficients [106, 107] of the corresponding problem. For adiabatic electric fields, this can be done by the WKB approximation [108, 109]. The scattering formulation sheds light on the origin of the interference effects. In order to take these interference effects into account, extensions to the WKB approximation were made in [102, 103]. Another approach is the quantum kinetic one, where a quantum non-markovian equation is derived for the time evolution of the adiabatic particle number [110, 111, 112, 113, 114, 115, 116]. An extension of this approach to include rotating electric fields was given in [117, 118, 119].

The basic ingredients of the Schwinger effect resemble the components of the tunnel junction (see Fig. 4.1). The rate of *e-h* pairs creation in a tunnel junction is controlled by the enegy scale T , which depends on the classical barrier the electron tunnels

through. In the schwinger effect, the rate of $e\text{-}p$ pairs creation from the Dirac sea is controlled by the energy gap $2mc^2$. Both pairs are excited by perturbing the vacuum state of the system by an electric field. Hence, it is natural to expect that Ramsey interference can be generated in the probability to create an $e\text{-}p$ pair from the QED vacuum in a similar manner to its generation in the probability to create a $e\text{-}h$ pair in the tunnel junction.

Indeed the first generalization of the Ramsey effect to quantum fields was proposed by [19] to the case of Schwinger effect. Here we give a more transparent picture of the mapping between the Schwinger effect and a time-dependent two-level system. The Hamiltonian of any two-level system can be written as $H = \vec{v} \cdot \vec{\sigma}$ where $\vec{\sigma}$ is a vector of the Pauli matrices and \vec{v} is a constant vector. In [19] two of the components of \vec{v} were functions of time, in our description only one component of \vec{v} depends on time making it a simple NMR system.

Unlike the case of a tunnel junction, the Ramsey interference in Schwinger effect appears only for anti-symmetric pulses. This phenomenon can be understood from the analogy to a two-level system as will be presented in section 4.3.

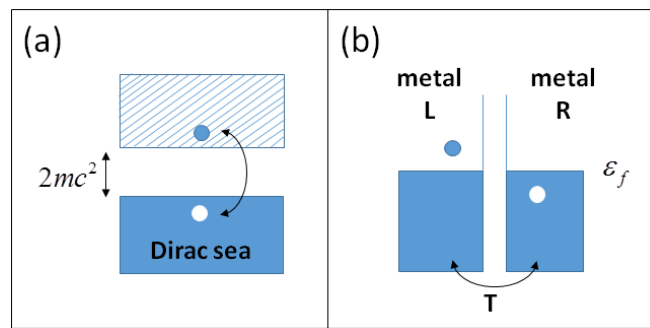


Figure 4.1: a) Schwinger effect. A strong electric field can excite an electron from the dirac sea, thus creating an electron-positron pair. b) Tunnel junction. Tunneling of an electron from the right lead to the left one by an applied voltage.

4.1 Introduction to Schwinger physics

The Dirac Hamiltonian in the presence of a uniform and time dependent electric field can be written in the momentum space as

$$H_D = \int \frac{d^3 k}{(2\pi)^3} \psi^\dagger(k) h_D \psi(k) \quad (4.1)$$

$$h_D = \gamma^0 \left(\vec{\gamma} \cdot (\vec{k} - \vec{A}) + m \right) \quad (4.2)$$

We choose the electric field to be in the z direction $\vec{A} = A(t) \hat{z}$, and the chiral representation for the gamma matrices,

$$\gamma^0 = \begin{pmatrix} 0 & -1 \\ -1 & 0 \end{pmatrix} \quad \gamma^i = \begin{pmatrix} 0 & \sigma^i \\ -\sigma^i & 0 \end{pmatrix}. \quad (4.3)$$

The spinor field ψ can be decomposed as $\psi(k) = \sum_s \psi_s(k) = \sum_s u_{s,p} a_{s,k} + v_{s,-p} b_{s,-k}^\dagger$ where a is the annihilation operator of an electron and b is the annihilation operator of a positron, the sum is over spins.

In QED, a particle is an eigen-state of the Hamiltonian and its energy is the corresponding eigen-value. Since in this problem the Hamiltonian depends on time the notion of a particle is not well defined except in the $t \rightarrow \pm\infty$ limits where we assume the electric field is zero. Since the eigen-states of the Dirac Hamiltonian at $t \rightarrow -\infty$ are different from its eigen-states at $t \rightarrow \infty$, the initial vacuum state is not the final vacuum state, i.e. particles are created.

In order to connect the initial and final states, we consider three bases for the Hilbert space: the "in" basis which diagonalize the Hamiltonian at $t \rightarrow -\infty$, the "out" basis which diagonalize the Hamiltonian at $t \rightarrow \infty$ and the time-dependent adiabatic basis which diagonalizes the Hamiltonian at each moment in time. The adiabatic basis connects the two, it identifies with the "in" basis at $t \rightarrow -\infty$ and with the "out" basis at $t \rightarrow \infty$. The spinor ψ_s can be expanded in each of the basis

$$\psi_s(k, t) = u_{s,p}^{in}(t) a_{s,k}^{in} + v_{s,-p}^{in}(t) b_{s,-k}^{in\dagger} \quad (4.4)$$

$$= u_{s,p}^{out}(t) a_{s,k}^{out} + v_{s,-p}^{out}(t) b_{s,-k}^{out\dagger} \quad (4.5)$$

$$= \tilde{u}_{s,p}(t) \tilde{a}_{s,k}(t) + \tilde{v}_{s,-p}(t) \tilde{b}_{s,-k}^\dagger(t) \quad (4.6)$$

A Bogoliubov transformation relates these basis:

$$\begin{aligned} \tilde{a}_{s,k}(t) &= \alpha_k(t) a_{s,k}^{in} - \beta_k^*(t) b_{s,-k}^{in\dagger} \\ \tilde{b}_{s,-k}^\dagger(t) &= \beta_k(t) a_{s,k}^{in} + \alpha_k^*(t) b_{s,-k}^{in\dagger} \end{aligned} \quad (4.7)$$

In order to satisfy the anti-commutation relation

$$\begin{aligned} a_{s,k} a_{s,k}^\dagger + a_{s,k}^\dagger a_{s,k} &= 1 \\ b_{s,k} b_{s,k}^\dagger + b_{s,k}^\dagger b_{s,k} &= 1 \end{aligned} \quad (4.8)$$

the Bogoliubov coefficients must satisfy $|\alpha|^2 + |\beta|^2 = 1$. Since any measurable physical quantity is expressed by the creation and annihilation operators of the electrons and positrons, all the physical information, e.g. the number of particles created and their correlations, is encompassed in the Bogoliubov coefficients. Hence, they will be our object of interest.

The average number of electron-positron pairs with momentum k created by the electric field from the vacuum is given by the expectation value of the number operator at $t \rightarrow +\infty$ (the "out" basis) with respect to the vacuum at $t \rightarrow -\infty$ (i.e. the vacuum with respect to the "in" basis $|0 : in\rangle$)

$$N_s(k) = \langle 0 : in | a_{s,k}^{out\dagger} a_{s,k}^{out} | 0 : in \rangle = |\beta_k(t \rightarrow +\infty)|^2. \quad (4.9)$$

4.1.1 "in/out" spinors

The spinors $u_{s,k}^{in/out}(t), v_{s,-k}^{in/out}(t)$ are solutions of the Dirac equation

$$\left(i\gamma^0 \partial_t - \vec{\gamma} \cdot (\vec{k} - \vec{A}(t)) - m \right) \Psi = 0. \quad (4.10)$$

Using the chiral representation for the γ matrices we find

$$\begin{aligned} u_{+,p}^{in/out}(t) &= \begin{pmatrix} m \\ 0 \\ -i\partial_t + p_{\parallel}(t) \\ k_1 + ik_2 \end{pmatrix} g_p^{in/out}(t) & v_{+,p}^{in/out}(t) &= \begin{pmatrix} m \\ 0 \\ -i\partial_t + p_{\parallel}(t) \\ k_1 + ik_2 \end{pmatrix} g_{-p}^{in/out*}(t) \\ u_{-,p}^{in/out}(t) &= \begin{pmatrix} -k_1 + ik_2 \\ -i\partial_t + p_{\parallel}(t) \\ 0 \\ m \end{pmatrix} g_p^{in/out}(t) & v_{-,p}^{in/out}(t) &= \begin{pmatrix} -k_1 + ik_2 \\ -i\partial_t + p_{\parallel}(t) \\ 0 \\ m \end{pmatrix} g_{-p}^{in/out*}(t) \end{aligned} \quad (4.11)$$

where the mode function $g_p(t)$ satisfies an oscillator type equation of motion

$$[\partial_t^2 + \omega_p^2(t) + i\partial_t p_{\parallel}(t)] g_p^{in/out}(t) = 0 \quad (4.12)$$

and we define

$$\begin{aligned} \omega_p^2(t) &\equiv p_{\parallel}^2(t) + \epsilon_{\perp}^2 \\ p_{\parallel}(t) &\equiv (k_3 - eA(t)) \\ \epsilon_{\perp}^2 &\equiv k_1^2 + k_2^2 + m^2 \end{aligned} \quad (4.13)$$

The in/out modes correspond to particles in the in/out states. Thus, their time dependence should be of a free particle in the in/out states. This gives the boundary conditions for $g_p^{in/out}(t)$ are

$$\begin{aligned} g_p^{in}(t \rightarrow -\infty) &= \frac{1}{\sqrt{2\omega_p^{in}(\omega_p^{in} - p_{\parallel}^{in})}} e^{-i\omega_p^{in}t} \\ g_p^{out}(t \rightarrow +\infty) &= \frac{1}{\sqrt{2\omega_p^{out}(\omega_p^{out} - p_{\parallel}^{out})}} e^{-i\omega_p^{out}t} \end{aligned} \quad (4.14)$$

where $\omega_p^{in/out} = \sqrt{(k_3 - eA^{in/out})^2 + \epsilon_{\perp}^2}$. Since we consider the case where $E(t \rightarrow \pm\infty) = 0$, $A^{in/out}$ (the vector potential at $\pm\infty$) are constants.

4.1.2 Adiabatic spinors

The adiabatic spinors are the time-dependent spinors which diagonalize the Hamiltonian h_D at each moment in time. They are given by

$$\begin{aligned} \tilde{u}_{+,p}(t) &= \begin{pmatrix} m \\ 0 \\ -\omega_p(t) + p_{\parallel}(t) \\ p_1 + ip_2 \end{pmatrix} \tilde{g}_p(t) & \tilde{v}_{+,p}(t) &= \begin{pmatrix} m \\ 0 \\ \omega_p(t) + p_{\parallel}(t) \\ p_1 + ip_2 \end{pmatrix} \tilde{g}_{-p}^*(t) \\ \tilde{u}_{-,p}(t) &= \begin{pmatrix} -p_1 + ip_2 \\ -\omega_p(t) + p_{\parallel}(t) \\ 0 \\ m \end{pmatrix} \tilde{g}_p(t) & \tilde{v}_{-,p}(t) &= \begin{pmatrix} -p_1 + ip_2 \\ \omega_p(t) + p_{\parallel}(t) \\ 0 \\ m \end{pmatrix} \tilde{g}_{-p}^*(t) \end{aligned} \quad (4.15)$$

where the corresponding eigen-values of $\tilde{u}_{s,p}$ is $+\omega_p(t)$ and of $\tilde{v}_{s,-p}$ is $-\omega(t)$ and the adiabatic mode function is

$$\tilde{g}_p(t) = \frac{1}{\sqrt{2\omega_p(\omega_p - p_{||})}} \exp \left(-i \int_{t_0}^t \omega_p(t') dt' \right) \quad (4.16)$$

In order to find the equation of motion for the Bogoliubov coefficients, lets consider the Bogoliubov transformation between the spinors

$$\begin{aligned} u_{s,p}^{in}(t) &= \alpha_k(t) \tilde{u}_{s,p}(t) + \beta_k(t) \tilde{v}_{s,-p}(t) \\ v_{s,-p}^{in}(t) &= -\beta_k^*(t) \tilde{u}_{s,p}(t) + \alpha_k^*(t) \tilde{v}_{s,-p}(t) \end{aligned} \quad (4.17)$$

Inserting (4.17) in the Dirac equation $i\partial_t u_{s,p}^{in}(t) = h_D u_{s,p}^{in}(t)$ yields equations for the Bogoliubov coefficients

$$\begin{aligned} \dot{\alpha}_k(t) &= \frac{\dot{p}_{||}(t)\epsilon_{\perp}}{2\omega_p^2(t)} \beta_k(t) e^{+2i \int_{t_0}^t \omega_p(t') dt'} \\ \dot{\beta}_k(t) &= -\frac{\dot{p}_{||}(t)\epsilon_{\perp}}{2\omega_p^2(t)} \alpha_k(t) e^{-2i \int_{t_0}^t \omega_p(t') dt'} \end{aligned} \quad (4.18)$$

Starting at the vacuum state at $t \rightarrow -\infty$ corresponds to the initial conditions

$$\begin{aligned} \alpha_k(t \rightarrow -\infty) &= 1 \\ \beta_k(t \rightarrow -\infty) &= 0 \end{aligned} \quad (4.19)$$

Exact analytical solution to theses equations is known only for a few field configurations. The optimal pulse modulation is the field modulation $A(t)$ which maximizes the number of electron-positron pairs $N_s(k) = |\beta_k(t \rightarrow +\infty)|^2$.

4.2 Description of Schwinger effect as a TLS

Next we will demonstrate how a two-level system can describe Schwinger effect. As noted in [19], eqns. (4.18) with the normalization constraint $|\alpha|^2 + |\beta|^2 = 1$ correspond to the Schrödinger equation of a two-level system with a time dependent Hamiltonian

$$\begin{aligned} i\partial_t \Psi &= H(t)\Psi \\ H(t) &= \omega_p(t)\sigma^3 + \Omega_p(t)\sigma^2 = \begin{pmatrix} \omega_p(t) & -i\Omega_p(t) \\ i\Omega_p(t) & -\omega_p(t) \end{pmatrix} \\ \Psi &= \begin{pmatrix} \beta(t)e^{+i \int^t \omega_p} \\ \alpha(t)e^{-i \int^t \omega_p} \end{pmatrix} \end{aligned} \quad (4.20)$$

where $\Omega_p(t) = \frac{\dot{p}_{||}(t)\epsilon_{\perp}}{2\omega_p^2(t)}$ and σ^i are the Pauli matrices. In this description the Hamiltonian depends on two time dependent frequencies which are non-trivial functions of the Schwinger physical parameters and the modulation $A(t)$. Nevertheless, from this two level picture, an intuitive picture of interference effects in the probability for creation of $e-p$ pairs can be obtained. Next we will derive a simpler description of Schwinger effect which includes only one time-dependent frequency and is easy to interpret physically. Most importantly, our Hamiltonian is the well known Hamiltonian of NMR systems, making it easy to investigate the optimal pulse shapes for the creation of $e-p$ pairs.

4.2.1 Two-level system

Let us consider a general NMR problem: a two-level system (TLS) with time-dependent energy bias $2\epsilon(t)$ and transition amplitude 2Δ . Its Hamiltonian is given by

$$H_{TLS} = \begin{pmatrix} -\epsilon(t) & -\Delta \\ -\Delta & \epsilon(t) \end{pmatrix} \quad (4.21)$$

The adiabatic basis is the basis which diagonalize the Hamiltonian at each moment in time. The adiabatic eigen-energies are time-dependent

$$\begin{aligned} E_{\pm}(t) &= \pm\Omega(t) \\ \Omega(t) &= \sqrt{\Delta^2 + \epsilon^2(t)} \end{aligned} \quad (4.22)$$

and so are the corresponding adiabatic eigen-states are

$$\varphi_+(t) = \begin{pmatrix} \sqrt{\frac{\Omega-\epsilon}{2\Omega}} \\ -\sqrt{\frac{\Omega+\epsilon}{2\Omega}} \end{pmatrix} \quad \varphi_-(t) = \begin{pmatrix} \sqrt{\frac{\Omega+\epsilon}{2\Omega}} \\ \sqrt{\frac{\Omega-\epsilon}{2\Omega}} \end{pmatrix} \quad (4.23)$$

Note that for $\epsilon \gg \Delta > 0$ the adiabatic states coincide with the eigen-states of σ^3

$$\varphi_+(t) \approx \begin{pmatrix} 0 \\ -1 \end{pmatrix} \quad \varphi_-(t) \approx \begin{pmatrix} 1 \\ 0 \end{pmatrix} \quad (4.24)$$

For large negative bias, $\epsilon < 0$ and $|\epsilon| \gg \Delta$, the adiabatic states coincide with the opposite σ^3 eigen-states

$$\varphi_+(t) \approx \begin{pmatrix} 1 \\ 0 \end{pmatrix} \quad \varphi_-(t) \approx \begin{pmatrix} 0 \\ 1 \end{pmatrix} \quad (4.25)$$

Therefore, a swap between the ground and excited states can be generated by adiabatically switching between positive and negative large bias.

A general state of the two-level system can be written as a sum of the two adiabatic eigenstates.

$$\psi(t) = \alpha(t)\varphi_-(t)e^{-i\int^t \Omega(t')dt'} + \beta(t)\varphi_+(t)e^{+i\int^t \Omega(t')dt'} \quad (4.26)$$

Inserting (4.26) to the Schrodinger eq. $i\partial_t\psi = H_{TLS}(t)\psi$ with H_{TLS} given by (4.21) yields the e.o.m for the adiabatic amplitudes

$$\begin{aligned} \dot{\alpha}(t) &= \beta(t) \frac{\dot{\epsilon}\Delta}{2\Omega^2} e^{+2i\int^t \Omega(t')dt'} \\ \dot{\beta}(t) &= -\alpha(t) \frac{\dot{\epsilon}\Delta}{2\Omega^2} e^{-2i\int^t \Omega(t')dt'} \end{aligned} \quad (4.27)$$

For a system initially at the ground state the initial conditions are given by

$$\begin{aligned} \alpha(t \rightarrow -\infty) &= 1 \\ \beta(t \rightarrow -\infty) &= 0 \end{aligned} \quad (4.28)$$

4.2.2 The mapping

We have shown that the equations of motion of the adiabatic amplitudes of the QED spinors (4.18) are equivalent to the equations of motion of the adiabatic amplitudes of

a two-level system (4.27) under the following substitutions:

$$\begin{aligned}\epsilon(t) &\leftrightarrow p_{\parallel}(t) \\ \Delta &\leftrightarrow \epsilon_{\perp} \\ \varphi_{-}(t) &\leftrightarrow \tilde{u}_{s,k}(t) \\ \varphi_{+}(t) &\leftrightarrow \tilde{v}_{s,k}(t)\end{aligned}\tag{4.29}$$

The adiabatic ground state correspond to the adiabatic electron spinor and the adiabatic excited state correspond to the adiabatic positron spinor. The minimal energy required for a transition between the levels 2Δ correspond to the minimal energy required to create an electron-positron pair $2\epsilon_{\perp}$. The external field $\epsilon(t)$ which controls the transition correspond to parallel momentum $p_{\parallel}(t)$ which controls the creation of the e - p pairs.

Therefore, we have shown that the transition probability from the ground state to the excited state after some modulation of $\epsilon(t)$ is equivalent to the e - p pair creation probability after the same time modulation of $p_{\parallel}(t)$.

The relation between our description and the one given by [19] is by a time dependent unitary transformation. Consider the transformation between the σ^3 (the third Pauli matrix) basis in which H_{TLS} is written and the adiabatic basis:

$$U(t) = \begin{pmatrix} \sqrt{\frac{\Omega-\epsilon}{2\Omega}} & -\sqrt{\frac{\Omega+\epsilon}{2\Omega}} \\ \sqrt{\frac{\Omega+\epsilon}{2\Omega}} & \sqrt{\frac{\Omega-\epsilon}{2\Omega}} \end{pmatrix}.\tag{4.30}$$

The Schrödinger equation for ψ' which is written in the adiabatic basis is

$$i\frac{\partial}{\partial t}\psi' = H'_{TLS}\psi'\tag{4.31}$$

where the Hamiltonian transforms to

$$H'_{TLS} = U H_{TLS} U^{\dagger} - iU \frac{\partial U^{\dagger}}{\partial t} = \begin{pmatrix} \Omega(t) & -i\frac{\Delta}{2\Omega^2}\dot{\epsilon}(t) \\ i\frac{\Delta}{2\Omega^2}\dot{\epsilon}(t) & -\Omega(t) \end{pmatrix}\tag{4.32}$$

This is exactly the Hamiltonian of [19] (eq. 4.20) under the substitutions (4.29).

4.3 Ramsey interference

We have established the equivalence between Schwinger effect and a transition from the ground to excited states of a simple two-level system. Thus, we can use our knowledge and intuition from NMR physics to generate Ramsey interference in the electron-positron creation probability. There is no analytical solution to a general energy bias function $\epsilon(t)$ but some insightful approaches and approximations exist [120].

We wish to find the electric field modulation that will induce Ramsey interference in the probability for creation of e - p pairs in the Schwinger effect. In all the examples we presented until now, Ramsey interference was induced by a modulation of two identical pulses. Next we will see, that contrary to our intuition, in the Schwinger effect Ramsey interference will occur only for anti-symmetric configuration of the electric pulses [19].

In order to understand the difference between a symmetric and anti-symmetric

configuration of the electric pulses, we consider the following modulations:

$$\epsilon_S(t) = \begin{cases} \epsilon_1 & t < 0 \\ \tilde{\epsilon}(t) & 0 < t < \tau \\ -\epsilon_1 & \tau < t < t_0 \\ -\epsilon_1 + \tilde{\epsilon}(t) & t_0 < t < t_0 + \tau \\ -2\epsilon_1 & t > t_0 + \tau \end{cases} \quad \epsilon_{AS}(t) = \begin{cases} \epsilon_1 & t < 0 \\ \tilde{\epsilon}(t) & 0 < t < \tau \\ -\epsilon_1 & \tau < t < t_0 \\ -\epsilon_1 - \tilde{\epsilon}(t) & t_0 < t < t_0 + \tau \\ \epsilon_1 & t > t_0 + \tau \end{cases} \quad (4.33)$$

where $\epsilon_1 \gg \Delta$ and $\tau < t$. The symmetric/anti-symmetric refer to the time derivative of the energy bias, $\dot{\epsilon}(t)$ which correspond to the electric field $\dot{p}_\parallel = -E$ (see Fig. 4.2).

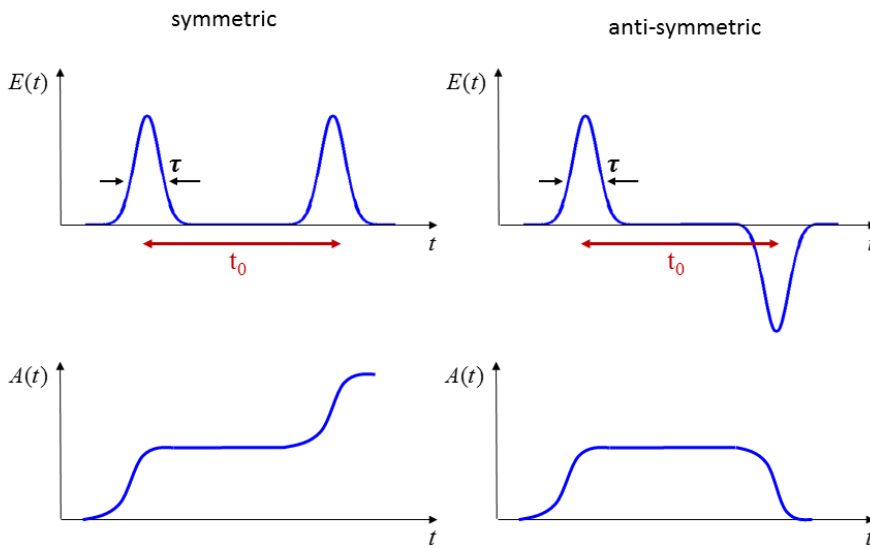


Figure 4.2: The symmetric and anti-symmetric electric field and vector potential modulation described in eq. (4.33).

4.3.1 Scattering approach

Next, we will express the transition problem in a TLS as an over the barrier reflection problem. The time evolution of the eigenstates of σ^3 can be written as uncoupled second order equations for the amplitudes

$$\begin{aligned} (\partial_t^2 + \epsilon^2 + \Delta^2 - i\dot{\epsilon}) c_0 &= 0 \\ (\partial_t^2 + \epsilon^2 + \Delta^2 + i\dot{\epsilon}) c_1 &= 0 \end{aligned} \quad (4.34)$$

The sum of the two amplitudes $Y(t) = c_0(t) + c_1(t)$ satisfies the following equation of motion

$$(\partial_t^2 + \epsilon^2(t) + \Delta^2) Y(t) = 0 \quad (4.35)$$

which is equivalent to an over the barrier scattering problem with potential $-\Omega(t)$ where the energy of the scattered particle is $E = 0$.

We consider a system which is initially in the lower state of σ^3 and assume $\epsilon(t \rightarrow -\infty) \gg \Delta$. Therefore, the ground state of σ^3 coincide with the adiabatic ground state so that

$$Y(t \rightarrow -\infty) = c_0(t \rightarrow -\infty) \sim e^{-\frac{1}{2}\Omega^{int}t} \quad (4.36)$$

These boundary conditions correspond to a back-scattering problem. Therefore,

$$Y(t \rightarrow +\infty) \sim \frac{1}{t} e^{-\frac{1}{2}\Omega^{out}t} + \frac{r}{t} e^{+\frac{1}{2}\Omega^{out}t} \quad (4.37)$$

where r and t are the reflection and transmission coefficients of the potential $-\Omega(t)$. On the other hand

$$Y(t \rightarrow +\infty) = c_0(t \rightarrow +\infty) + c_1(t \rightarrow +\infty) \quad (4.38)$$

For $-\epsilon(t \rightarrow +\infty) \gg \Delta$ (ϵ starts positive and ends negative) the ground state of σ^3 coincide with the excited adiabatic state.

$$\begin{aligned} c_0(t \rightarrow +\infty) &\sim e^{+\frac{1}{2}\Omega^{out}t} \\ c_1(t \rightarrow +\infty) &\sim e^{-\frac{1}{2}\Omega^{out}t} \end{aligned} \quad (4.39)$$

Hence, $c_0(t \rightarrow +\infty)$ is the probability amplitude for the transition from the ground to the excited state in the TLS and it is given by $r/t \approx r$ the reflection over the barrier amplitude.

For $\epsilon(t \rightarrow +\infty) \gg \Delta$ (ϵ starts positive and ends positive), the adiabatic states coincide with σ^3 eigenstates such that

$$\begin{aligned} c_0(t \rightarrow +\infty) &\sim e^{-\frac{1}{2}\Omega^{out}t} \\ c_1(t \rightarrow +\infty) &\sim e^{+\frac{1}{2}\Omega^{out}t} \end{aligned} \quad (4.40)$$

Therefore, the probability amplitude for the transition from the ground to the excited state is $c_1(t \rightarrow +\infty)$. Again, it is given by $r/t \approx r$ the over the barrier reflection coefficient.

In the semi-classical approximation the wave-function of the scattered particle is taken to be a generalization of the free particle wave-function $Y(t) \sim e^{i \int^t \Omega(t') dt'}$. This approximation holds when the wavelength of the particle changes slowly, i.e. when $\left| \frac{d}{dt} \frac{2\pi}{\Omega(t)} \right| \ll 1$. In the semi-classical approximation the reflection amplitude, i.e. the transition amplitude goes like

$$r \sim \sum_{t_p} \exp \left\{ -2i \int_{-\infty}^{t_p} dt \Omega(t) \right\} \quad (4.41)$$

where the turning points t_p are when $\Omega(t_p) = 0$ and the sum is taken over all the turning points in the upper half complex plane [103]. The turning points are solutions to the eq.

$$\epsilon(t_p) = \pm i\Delta \quad (4.42)$$

Since $\epsilon(t)$ is real the turning points come in conjugate pairs. The dominant contribution to the reflection is from the pair closest to the real axis. The contributions of the other turning points will be exponentially smaller. Hence, we expand ϵ around the real axis

$$\epsilon(t_p^R + it_p^I) \approx \epsilon(t_p^R) + i\dot{\epsilon}(t_p^R)t_p^I = \pm i\Delta \quad (4.43)$$

to obtain a simpler equation for the turning points

$$\begin{aligned} \epsilon(t_p^R) &= 0 \\ t_p^I &= \pm \frac{\Delta}{\dot{\epsilon}(t_p^R)} \end{aligned} \quad (4.44)$$

Thus, in the semi-classical approximation reflection occurs only on times such that $\epsilon(t) = 0$.

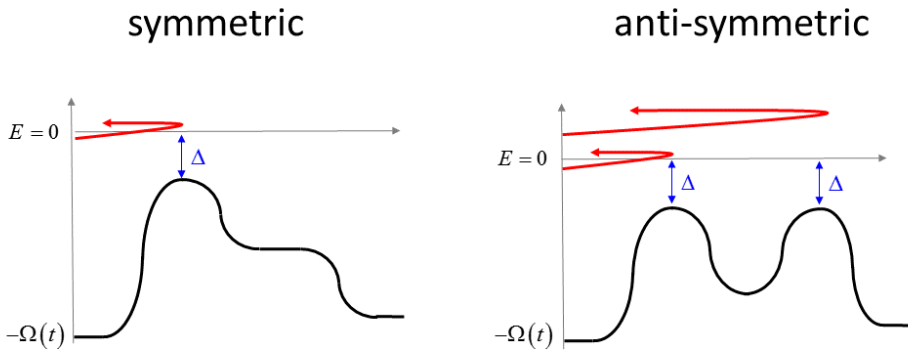


Figure 4.3: The symmetric and anti-symmetric scattering problems for the modulation described in eq. (4.33).

In Figure 4.3 the scattering potentials $-\Omega(t)$ for the two modulations are plotted. From the different shape of the scattering potentials of the symmetric and anti-symmetric electric pulses we can understand why interference will appear only for the anti-symmetric modulation. In the symmetric modulation only one turning point exist, therefore there is only one reflection. In the anti-symmetric modulation there are two turning points, therefore interference between the two reflecting amplitudes will arise. According to (4.41) the reflection probability for the anti-symmetric modulation is

$$P_2 = P_1 \cos^2 \left\{ \int_0^{t_0} dt \Omega(t) \right\} \quad (4.45)$$

as expected from Ramsey interference.

Within the semi-classical approximation the actual shape of the pulses does not matter. All that is need in order to obtain interference is two conjugate pairs of turning points with the same distance from real axis. I.e. that $\epsilon(t = 0) = \epsilon(t = t_0) = 0$ and that the velocity of the transition at these times will be equal and opposite $\dot{\epsilon}(t = 0) = -\dot{\epsilon}(t = t_0)$. In the Schwinger effect it means that at $t = 0$ and $t = t_0$ the vector potential should be equal to momentum $A = k$ and that the electric field at those times should have equal magnitude but opposite sign $E(t = 0) = -E(t = t_0)$.

From the scattering approach we can infer the conditions for the appearance of Ramsey interference in the general case without approximations. Consider a modulation of $\Omega(t)$ composed of two consequent pulses with equal reflection and transmission coefficients r and t . The width of the pulses is much smaller than the separation between them $\tau \ll t_0$. The scattering problem is a Fabri-Perot interferometer. Therefore, as will be shown for the dynamic Casimir effect in section 5.2, the transition probability will be

$$P_2 = \left| \frac{r_T}{t_T} \right|^2 = 4P_1 \cos^2 \{ \Omega_0 t_0 - \theta_t \} \quad (4.46)$$

where r_T and t_T are the total reflection and transmission coefficients, $P_1 = |r/t|^2$ and $\theta_t = \arg\{t\}$.

Although the scattering approach is constructive it is less intuitive to understand the interference stemming from it as Ramsey interference. The connection to our pic-

ture of Ramsey interference as a two slit experiment in time is obtain by the Adiabatic-impulse approximation.

4.3.2 Adiabatic-impulse approximation

The adiabatic impulse approx. is a rephrasing of the semi-classical approx. [120]. It consists of the following assumptions: A transition between the states occurs only at times where $\epsilon(t) = 0$. In all other times the evolution is adiabatic. The transition probability in an impulse is obtained by linearizing $\epsilon(t)$ at the transition time t_p and using Landau-Zener probability for the transition.

$$P_{LZ} = \exp\left(-\frac{\pi\Delta^2}{2|\dot{\epsilon}(t_p)|}\right) \quad (4.47)$$

For the two modulations described by (4.33), the adiabatic energies are plotted in Fig. 4.4. The transition occurs at the minimal adiabatic energy difference. For the

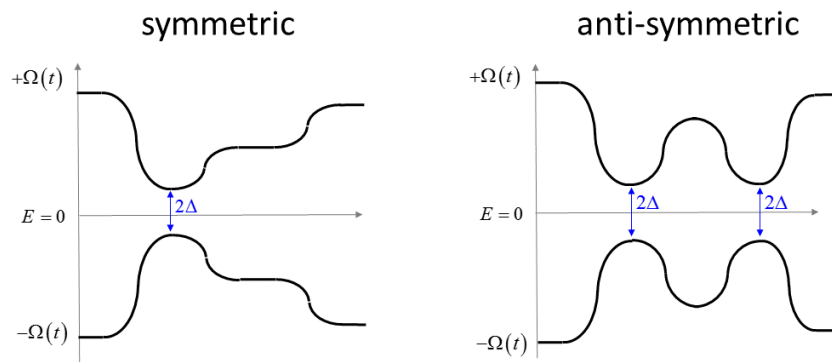


Figure 4.4: The symmetric and anti-symmetric adiabatic energies for the modulation described in eq. (4.33).

symmetric modulation only one such transition occurs. Only for the anti-symmetric modulation the transition can occur at two points in time as required in order to obtain Ramsey interference. Between these times the system evolves adiabatically, so that the adiabatic eigen-states gain the phases $\pm \int_0^t \Omega(t') dt'$. The transition probability after the second pulse will oscillate with the phase difference between the two paths the system can take:

$$P_2 = P_1 \cos^2 \left(\int_0^{t_0} \Omega(t) dt \right) \quad (4.48)$$

where $P_1 = P_{LZ}$. Note that in order to have maximal interference we require that the velocity of the transition through the impulse times will be equal, i.e. $\dot{\epsilon}(t=0) = -\dot{\epsilon}(t=t_0)$. In the Schwinger language this means that the electric field at these times should have equal magnitude.

Chapter 5

Ramsey interference and dynamical Casimir effect

The Schwinger effect is one of the phenomenon where particles are created from the vacuum of a quantum field theory. Such particle creation processes consist of Hawking radiation [5, 6], Unruh [121, 122] and the dynamical Casimir effects [4]. The origin of all these phenomena is the same, the basic mechanism is the dynamical amplification of the vacuum fluctuations. The relation between the dynamical Casimir effect and the parametric down conversion was discussed by [123, 124] and with the Hawking radiation by [125]. Recently the dynamical Casimir effect was reported to be measured in a superconducting circuit [17].

The dynamical Casimir effect describes the generation of photons from the quantum electromagnetic (QED) vacuum by a time dependent boundary conditions imposed by a moving mirror [4, 126, 127]. Due to momentum conservation the photons are created in pairs. The electromagnetic field can be described by the energy-momentum tensor [126, 128, 129] or by the distribution of photons in the Fock state basis [130, 131]. Most of the works consider the creation of photon due to a sinusoidal boundary condition, e.g. [130, 132, 133, 131, 129]. An exact solution for an almost sinusoidal motion of the boundary was obtained by [128].

The frequencies of the modes of an ideal 1d cavity are equidistant. This results in interaction between the different modes [130, 132]. If the cavity has a single mode or the interaction between modes is negligible due to non-equidistant frequencies or by considering adiabatic motion of the boundary, the problem is analog to a harmonic oscillator with time-dependent frequency [134, 129, 135].

Since the effect becomes measurable only at relativistic velocities of the mirrors it is not possible to observe it with a real mirror [136]. In [17], a microwave transmission line was terminated by an effective Josephson junction with tunable josephson energy, thereby allowing for a tunable effective length of the cavity.

In the dynamical Casimir effect the vacuum is perturbed by the moving mirror. In this case, we define a "pulse of width τ " as the displacement of the mirror along some trajectory such that it returns to its original point after a time τ . This "pulse" creates photons from the vacuum by means of the dynamical Casimir effect. Applying two identical pulses separated by a time T will result in Ramsey interference in the number of photons created. The interference will be between a path where the photons are created in the first pulse and the path where they are created in the second one. The energy difference between the vacuum and the photon pair state is twice the frequency of the photons $2\omega_n$, so the number of photons after two pulses will oscillate with $2\omega_n T$.

5.1 Introduction to the dynamical Casimir effect

Consider an electromagnetic field in a 1d cavity with moving walls [4]. For simplicity, we take one wall to be fixed at $x = 0$ while the other one is moving according to $x = z(t)$. In the Coulomb gauge the vector potential $A(x, t)$ satisfies the wave equation

$$\frac{\partial^2 A}{\partial^2 t} = c^2 \frac{\partial^2 A}{\partial^2 x}. \quad (5.1)$$

We consider the case of a linearly polarized electromagnetic field so we can ignore the vector nature of the vector potential. We assume that the walls of the cavity are perfect metals such that they impose the time dependent boundary condition $A(0, t) = A(z(t), t) = 0$.

In the case of static boundary conditions, i.e the cavity length is fixed to be z_0 , the Hamiltonian is given by $H = \sum_n \frac{\hbar n \pi c}{z_0} b_n^\dagger b_n$ and the field can be decomposed as

$$A_{stat}(x, t) = \sum_n \left(\frac{i}{\sqrt{\pi n}} \sin \frac{\pi n x}{z_0} e^{\frac{-i\pi n c t}{z_0}} b_n + h.c. \right) \quad (5.2)$$

where b_n is the annihilation operator of a photon in mode n .

Except for the case of fixed boundary conditions, there is no Hamiltonian which describes this quantum system. If such a Hamiltonian existed it would imply that the field at time t is related to the field at time t_0 by

$$A(x, t) = U^\dagger(t, t_0) A(x, t_0) U(t, t_0) \quad (5.3)$$

where $U(t, t_0) = T \exp \left\{ -\frac{i}{\hbar} \int_{t_0}^t H(t') dt' \right\}$ and T is time-ordering. If we take (x, t_0) to be in the trajectory of the mirror, then $A(x, t_0) = 0$, which means that $A(x, t) = 0$ for all t .

We continue by solving the wave equation with the time dependent boundary condition. The wave equation is invariant under the transformation

$$\begin{aligned} ct - x &\equiv f(cw - s) \\ ct + x &\equiv g(cw + s) \end{aligned} \quad (5.4)$$

If the coordinate transformation will take the boundary condition to be static the EM mode functions will be

$$\psi_n(x, t) = \frac{1}{\sqrt{4\pi n}} \left(e^{-i\pi n f^{-1}(ct-x)} - e^{-i\pi n g^{-1}(ct+x)} \right) \quad (5.5)$$

Mapping $z = 0 \leftrightarrow s = 0$ and $z(t) \leftrightarrow s = 1$ yields the mode functions

$$\psi_n(x, t) = \frac{1}{\sqrt{4\pi n}} \left(e^{-i\pi n R(ct-x)} - e^{-i\pi n R(ct+x)} \right) \quad (5.6)$$

where $R(u) = f^{-1}(u) = g^{-1}(u)$ is a solution of the functional equation (Moore equation)

$$R(ct + z(t)) = R(ct - z(t)) + 2 \quad (5.7)$$

The functions $\psi_n(x, t)$ form a complete orthonormal basis in the interval $(0, z(t))$ with the scalar product $(\psi_n, \psi_m) = -\frac{i}{c} \int_0^{z(t)} dx (\psi_n \partial_t \psi_m^* - \partial_t \psi_n \psi_m^*) = \delta_{nm}$. We proceed in the usual canonical quantization to expand the field in the mode functions and impose

the bosonic commutation relation for the creation and annihilation operators

$$A(x, t) = \sum_n \left(b_n \psi_n + b_n^\dagger \psi_n^* \right) \quad (5.8)$$

$$[b_n, b_m^\dagger] = \delta_{nm} \quad [b_n, b_m] = 0. \quad (5.9)$$

The meaning of these creation and annihilation operators is still unclear at the moment.

Suppose that for $t < 0$ and $t > T$ the walls are at rest at $z = 0$ and $z = z_0$. for $t < 0$ and $t > T$ the field can be decomposed as in the static case (5.2)

$$A(x, t < 0) = \sum_n \left(b_n \psi_n^{(0)} + b_n^\dagger \psi_n^{(0)*} \right) \quad (5.10)$$

$$A(x, t > T) = \sum_n \left(a_n \psi_n^{(0)} + a_n^\dagger \psi_n^{(0)*} \right). \quad (5.11)$$

where the mode functions are

$$\psi_n^{(0)}(x, t) = \frac{i}{\sqrt{\pi n}} \sin \frac{\pi n x}{z_0} e^{\frac{-i\pi n c t}{z_0}}. \quad (5.12)$$

The meaning of the operators b_n and a_n is inherited from the static case, they are the photon operators at $t < 0$ and $t > T$ respectively.

The mode functions of eq. (5.10) evolve in time according to (5.6) with the initial condition (5.12) for $t < 0$. Therefore, at times $t > T$ we can expand the field in two ways:

$$A(x, t) = \sum_n \left(b_n \psi_n + b_n^\dagger \psi_n^* \right) = \sum_n \left(a_n \psi_n^{(0)} + a_n^\dagger \psi_n^{(0)*} \right) \quad (5.13)$$

where ψ_n are given by (5.6) with the initial condition (5.12) for $t < 0$.

Now it is clear why the photonic operators are different, They do not form the same Fock space. Hence, the vacuum state of the two spaces is not necessarily the same. In order to find the transformation between the two sets of operators we expand $\psi_n(x, t)$ using $\psi_n^{(0)}(x, t)$.

$$\psi_n(x, t) = \sum_m \left(\alpha_{nm} \psi_m^{(0)}(x, t) + \beta_{nm} \psi_m^{(0)*}(x, t) \right) \quad (5.14)$$

$$\alpha_{nm} = (\psi_n, \psi_m^{(0)}) \quad \beta_{nm} = -(\psi_n, \psi_m^{(0)*}) \quad (5.15)$$

The resulting Bogoliubov transformation of the operators is:

$$\begin{aligned} a_m &= \sum_n \left(b_n \alpha_{nm} + b_n^\dagger \beta_{nm}^* \right) & b_n &= \sum_m \left(\alpha_{nm}^* a_m - \beta_{nm}^* a_m^\dagger \right) \\ a_m^\dagger &= \sum_n \left(b_n^\dagger \alpha_{nm}^* + b_n \beta_{nm} \right) & b_n^\dagger &= \sum_m \left(\alpha_{nm} a_m^\dagger - \beta_{nm} a_m \right) \end{aligned} \quad (5.16)$$

If the field is in the vacuum state at $t < 0$, then the final number of photons created in mode n by the moving wall is

$$N_n = \langle 0; in | a_n^\dagger a_n | 0; in \rangle = \sum_m |\beta_{nm}|^2. \quad (5.17)$$

5.2 Ramsey interference and number of photons

Finding analytical solutions to the Moore equation (the functions $R(u)$) is difficult. Instead we look for mode functions that satisfy the boundary conditions but are only an

approximate solution to the wave equation. We define the mode frequency $\omega_n(t) = \frac{cn\pi}{z(t)}$, and choose the mode functions

$$\psi_n(x, t) = f_n(t) \frac{i}{\sqrt{n\pi}} \sin \omega_n(t) x \quad (5.18)$$

In the adiabatic approximation we assume that the velocity of the walls is small compared to the mode frequencies, therefore we can neglect the time derivatives of ω_n in the wave equation [137]. We obtain an equation for the slow varying amplitudes $f_n(t)$

$$\frac{d^2}{dt^2} f_n(t) + \omega_n^2(t) f_n(t) = 0 \quad (5.19)$$

The mode functions for $t < 0$ are $\psi_n^{(0)}(x, t) = \frac{i}{\sqrt{\pi n}} \sin \frac{\pi n x}{z_0} e^{-\frac{i\pi n c t}{z_0}}$, hence the initial condition for (5.19) is $f_n(t) = e^{-i\omega_n^{(0)} t}$ for $t < 0$ where $\omega_n^{(0)} = \frac{cn\pi}{z_0}$.

Equation (5.19) is formally identical to a one dimensional Schrödinger equation where the spatial coordinate is replaced by time. It is a scattering problem where $\omega_n^2(t)$ corresponds to $E - V(x)$ (see fig. 5.1). The asymptotic behavior of the backward scattering solution is

$$f_b(t) = \begin{cases} \frac{1}{\sqrt{\omega_n^{(0)}}} t_b e^{-i\omega_n^{(0)} t} & t \rightarrow -\infty \\ \frac{1}{\sqrt{\omega_n^{(0)}}} (e^{-i\omega_n^{(0)} t} + r_f e^{i\omega_n^{(0)} t}) & t \rightarrow \infty \end{cases} \quad (5.20)$$

where t_b and r_f are the transmission and reflection amplitudes of the probability current. From here we can infer that $f_n(t) = \frac{\sqrt{\omega_n^{(0)}}}{t_b} f_b(t)$. In particular for $t > T$ the mode function is

$$\psi_n(t, x) = \frac{1}{t_b} (e^{-i\omega_n^{(0)} t} + r_f e^{i\omega_n^{(0)} t}) \frac{i}{\sqrt{n\pi}} \sin \omega_n^{(0)} x \quad (5.21)$$

In order to find the final number of photons we need to evaluate β_{nm} at $t > T$.

$$\beta_{nm} = \frac{i}{c} \int_0^{z_0} dx \left(\psi_n \partial_t \psi_m^{(0)} - (\partial_t \psi_n) \psi_m^{(0)} \right) = -\frac{r_f}{t_b} \delta_{nm} \quad (5.22)$$

The average number of photons created in mode n is

$$N_n = \frac{R_n}{T_n} \quad (5.23)$$

where $R_n = |r_f|^2$ and $T_n = |t_b|^2$ are the total reflection and transmission coefficient that correspond to scattering by $\omega_n(t)$. The same result was also obtained by [9, 137] for a quantum harmonic oscillator.

Ramsey interference is achieved when we consider two identical pulses separated by T . Namely, the moving mirror trajectory is given by $z(t) = x(t) + x(t - T)$ where $x(t < 0) = x(t > \tau) = z_0$ and $\tau < T$. In the scattering language it is described by two scattering potentials with the same transmission and reflection coefficients T_n and R_n well separated by T . This is a Fabry-Perot set-up and the total reflection and

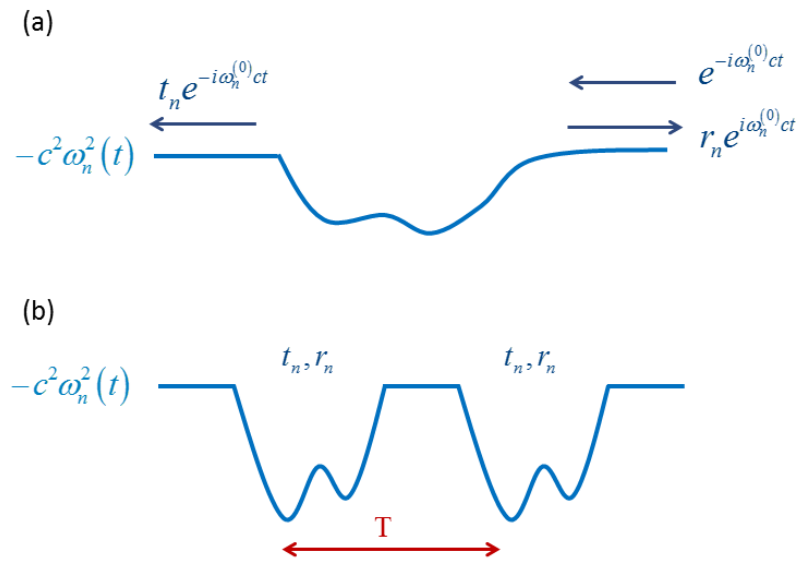


Figure 5.1: Eq. (5.19) describes an over the well scattering problem where the potential is $-c^2\omega_n^2(t)$. (a) The backward scattering solution. (b) Ramsey interference is generated by two identical scattering regimes separated by T .

transmission coefficients of the problem are :

$$R_{tot} = \frac{4R_n \cos^2 x_n}{(1 - R_n)^2 + 4R_n \cos^2 x_n} \quad (5.24)$$

$$T_{tot} = \frac{(1 - R_n)^2}{(1 - R_n)^2 + 4R_n \cos^2 x_n} \quad (5.25)$$

where we have defined $x_n = \omega_n^{(0)}T - \theta_{t_n}$ and $t_n = |t_n|e^{i\theta_{t_n}}$.

As expected, the average number of photons in the mode n produced after two pulses exhibits Ramsey interference

$$N_n^{2-pulse} = \frac{R_{tot}}{T_{tot}} = 4 \frac{R_n}{T_n} \cos^2 x_n = 4N_n^{1-pulse} \cos^2 (\omega_n^{(0)}T - \theta_{t_n}). \quad (5.26)$$

where $N_n^{one-pulse} = \frac{R_n}{T_n}$ is the average number of photons after a single pulse, that is the number of photons produced by the trajectory $x(t)$. $N_n^{1-pulse}$ corresponds to the Rabi term. Comparing the oscillating term to Ramsey (2.23) we see that the energy difference between the initial (vacuum) and final (photon pair) states is indeed twice a photon's energy $2\omega_n^{(0)}$.

Chapter 6

Summary

We have generalized a well-known phenomenon in atomic optics, the Ramsey interference, to quantum fields, thereby to systems with a continuum of energy spectrum. We have demonstrated it in three different physical systems: mesoscopic systems, the Schwinger and dynamical Casimir effects. Thus, we have established a new method to investigate the nature of excitations of a physical systems.

We have presented a new interference phenomenon in mesoscopic systems. We found a way to isolate the e - h pairs with the same energy, i.e. the e - h pairs that will exhibit the same Ramsey interference pattern, so that the interference effects will not be masked by the other e - h pairs.

Since Ramsey interference is sensitive to dephasing it can probe interactions of the quasi-particles. This allows for a new type of measurement of non-equilibrium solid-state systems in the time domain. Ramsey interference can explore, for example: the finite life-time of the quasi-particles, the temperature of the system, dephasing of the quasi-particles caused by an environment and other time-dependent processes that will affect the energy of the quasi-particles.

Applying our method to a tunnel junction in series with a linear impedance, we have shown that the amplitude of the Ramsey fringes decreases exponentially as a result from the interaction of the electrons in the tunnel junction with the electromagnetic environment. The argument of the exponent is the correlation function of the environment at time t_0 , the time between the voltage pulses. Therefore, changing t_0 explores the time dependence of the environment correlation function. For the case of an ohmic environment, changing t_0 can probe the crossover between the ballistic and diffusive regimes of the correlation function.

Appendix A

Scattering approach to transport

Our formulation of the problem consists of a tunneling Hamiltonian between the two leads of the tunnel junction in a similar manner to [28]. Another way to describe electrical transport through a tunnel junction is by the scattering approach (Landauer approach) [29]. Unfortunately, its extensions to time dependent voltage (often called "photon assisted transport") [29, 30, 31] are not gauge invariant, therefore the physical picture provided by them is somewhat misguided. In order to demonstrate this delicate point and the benefit of using the tunneling Hamiltonian approach we give a short review of scattering approach to transport.

Consider a mesoscopic conductor connected to two reservoirs (leads), the conductor is a small perturbation for the reservoirs so the electrons in the reservoirs are in equilibrium and have the Fermi distribution function. We assume that far from the sample the electrons longitudinal (along the leads) and transversal (across the leads) motion in the leads is separable. In the longitudinal direction the system is open and characterized by the continuous wave vector k_l . The motion in the transverse direction is quantized and described by an index n and transverse energy E_n . An electron with longitudinal energy $E_l = \frac{\hbar^2 k_l^2}{2m}$ can have different transverse energies E_n , these transverse degrees of freedom are called channels.

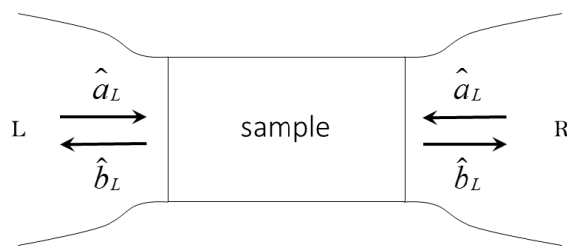


Figure A.1: The operators $\hat{a}_{L/R}^\dagger$ creates an outgoing electron from the left (right) reservoir and the operators $\hat{b}_{L/R,n}^\dagger(E)$ creates an incoming electron to the left (right) reservoir.

We introduce the creation and annihilation operators in the scattering states, $\hat{a}_{L/R,n}^\dagger(E)$ creates an outgoing electron from the left (right) lead with total energy E in the transverse channel n , and $\hat{b}_{L/R,n}^\dagger(E)$ creates an incoming electron to the left (right), see Fig. A.1. The outgoing and incoming operators are connected by the

scattering matrix $S(E)$

$$\begin{pmatrix} b_L(E) \\ b_R(E) \end{pmatrix} = \begin{pmatrix} r^{(n_L \times n_L)}(E) & t^{(n_L \times n_R)}(E) \\ t^{\dagger(n_R \times n_L)}(E) & r^{(n_R \times n_R)}(E) \end{pmatrix} \begin{pmatrix} a_L(E) \\ a_R(E) \end{pmatrix} \quad (\text{A.1})$$

where $n_{L/R}$ is the number of channels in the leads and r and t describe the transmission and reflection matrices of the electrons. For two reservoirs in thermal equilibrium

$$\langle \hat{a}_{L/R}^{\dagger}(E) \hat{a}_{L/R}(E') \rangle = \delta_{LR} \delta(E - E') f_{L/R}(E) \quad (\text{A.2})$$

where $\langle \cdot \rangle$ is a quantum expectation value. Here it is taken with respect to the thermal equilibrium state of the reservoirs, thus $f_{L/R}$ is the Fermi distribution in the left/right lead. The Fermi distribution in left lead is shifted by the applied voltage eV_{dc} with respect to the Fermi distribution in the right lead.

For energies $(E - E')$ small compared to the Fermi energy, the current operator in the left contact of the conductor can be written as

$$\hat{I}_L(t) = \frac{e}{2\pi\hbar} \int dE dE' e^{\frac{i(E-E')t}{\hbar}} [\hat{a}_L^{\dagger}(E) \hat{a}_L(E') - \hat{b}_L^{\dagger}(E) \hat{b}_L(E')] . \quad (\text{A.3})$$

The average current obtained is

$$\langle \hat{I}_L \rangle = \frac{e}{2\pi\hbar} \int dE [f_L(E) - f_R(E)] \text{Tr} [t(E) t^{\dagger}(E)] . \quad (\text{A.4})$$

In the zero temperature limit and for small applied voltage the conductance is given by the Landauer formula

$$G = \frac{d}{dV_{dc}} \langle \hat{I}_L \rangle = \frac{e^2}{h} \text{Tr} [t(E_F) t^{\dagger}(E_F)] = \frac{2e^2}{h} \sum_n T_n(E_F) \quad (\text{A.5})$$

where $T_n(E_F)$ are the transmission probabilities of the eigen-channels obtained by diagonalizing tt^{\dagger} .

A.1 Photon-assisted transport

The scattering approach for electric transport was extended to an ac voltage in [29, 30, 31] and is denoted as "photo-assisted transport". Next, we discuss this method and its physical interpretation.

In this section we restrict ourselves for simplicity to a one channel two terminal conductor. We take the right contact to be under a zero voltage and the left contact to be under a constant voltage V_{dc} plus a time dependent voltage $V(t)$. The scattering states in the left lead gains a time dependent phase.

$$\psi_L(x, E, t) = e^{ik_L x - i\frac{Et}{\hbar}} e^{-i\phi(t)} \quad (\text{A.6})$$

where $\phi(t) = \frac{e}{\hbar} \int_{-\infty}^t dt' V(t')$ as in our notations. If the time dependent voltage $V(t)$ is applied only in the time window $0 < t < T$ (or it is periodic with period T) we can express the function $g(t) = e^{-i\phi(t)}$ as a fourier series

$$g(t) = e^{-i\phi(t)} = \sum_{n=-\infty}^{\infty} C_n e^{in\omega t} \quad (\text{A.7})$$

where $\omega = \frac{2\pi}{T}$ and $C_n = \frac{1}{T} \int_{-\infty}^{\infty} dt g(t) e^{-in\omega t}$.

The scattering wave function then takes the form

$$\psi_L(x, E, t) = \sum_{n=-\infty}^{\infty} C_n e^{ik_l x} e^{-i(\frac{E}{\hbar} + n\hbar\omega)t}. \quad (\text{A.8})$$

Thus, the voltage modulation creates side-bands to the central energy E at $E + n\hbar\omega$. An electron which had energy E can absorb (emit) n modulation quanta with probability $|C_{\pm n}|^2$. Therefore, $|C_n|^2$ is the probability to create a e - h pair in the left lead with energy $n\hbar\omega$ (see Fig A.2). This is similar to the tunneling approach where the probability to create a e - h pair was given by the Fourier transform of $g(t)$, although in the tunneling approach the electron and hole are in different leads (as is expected from a tunneling event) and in the photon-assisted approach the electron and hole are created in the same lead as a result of the illumination of that lead.

Assuming that the voltage applied on the left lead is screened efficiently, there is a section of the lead where there is no potential but also no scattering. An electron with energy E in that part originates from electrons with energies $E - n\hbar\omega$ in the part subjected to the time dependent voltage. The relation between operators in the scattering state (\hat{a}_L) and operators in the state subjected to the time dependent voltage (\hat{a}'_L) is

$$\hat{a}_L(E) = \sum_{n=-\infty}^{\infty} C_n \hat{a}'_L(E - n\hbar\omega) \quad (\text{A.9})$$

up to corrections of the order of $\frac{\hbar\omega}{E_F}$ which arise from the difference in the wave vector of the sidebands and the wave vector at E . We assume that the modulation is slow so that the left lead is still in an equilibrium state, then the averages over the operators \hat{a}'_L are equilibrium averages.

The current operator now reads

$$\begin{aligned} \hat{I}_L(t) = & \frac{e}{2\pi\hbar} \int dE dE' e^{\frac{i(E-E')t}{\hbar}} \left[(1 - r^*(E)r(E')) \sum_{n=-\infty}^{\infty} \sum_{m=-\infty}^{\infty} C_n^* C_m \hat{a}'_L^\dagger(E - n\hbar\omega) \hat{a}'_L(E' - m\hbar\omega) \right. \\ & - t'^*(E)t'(E') \hat{a}_R^\dagger(E) \hat{a}_R(E') - r^*(E)t'(E') \sum_{n=-\infty}^{\infty} C_n^* \hat{a}'_L^\dagger(E - n\hbar\omega) \hat{a}_R(E') \\ & \left. - t'^*(E)r(E') \hat{a}_R^\dagger(E) \sum_{n=-\infty}^{\infty} C_n \hat{a}'_L(E' - n\hbar\omega) \right] \quad (\text{A.10}) \end{aligned}$$

One may point out that adding a constant potential to one lead can not be felt by the electrons in that lead, even if it is time-dependent, since it is just adding a constant to the electron energies. Therefore, the probability distribution of electrons with energy $E_l = \frac{\hbar^2 k_l^2}{2m}$ is the same with the potential or without it. The change in the distribution can be seen only from the point of view of the other lead. There it looks like an electron with wave vector k_l can have energies $E_{l,n} = E_l + \hbar\omega n$ with probabilities $|C_n|^2 f(E_l - n\hbar\omega)$. The probability distribution of the electrons in the left lead as seen from the right lead is $f_L(E) = \sum_n |C_n|^2 f(E - n\hbar\omega)$ (see Fig A.2).

As noted by [29], if the scattering matrix depend on energy, the scattering approach as it is presented here is not gauge invariant. The current correlation depend on how we divide $V(t)$ between the two leads. This is resolved by understanding that the probability distribution of the electrons should be regarded as the distribution of the electrons in the left lead as seen from the right lead. Therefore, there is only one possible gauge choice, where the voltage added to one of the leads.

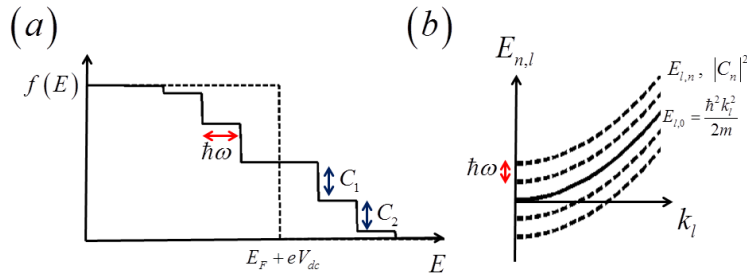


Figure A.2: (a) The probability distribution of the electrons in the left lead as seen from the right lead (solid) and the Fermi distribution function (dashed). The width of the steps is $\hbar\omega$ and the height of the n 'th step is $|C_n|^2$. For $E > E_F + eV_{dc}$ the distribution represents the electrons excited by the time-dependent voltage. For $E < E_F + eV_{dc}$ the space between the new probability distribution and the Fermi distribution represents the holes excited by the time-dependent voltage. (b) The sub-bands created by the time-dependent voltage $E_{l,n} = \frac{\hbar^2 k_l^2}{2m} + n\hbar\omega$. The probability of the electron to be in the n 'th sub-band is $|C_n|^2$.

The *dc* part (the part that is independent on time) of the photo-induced current is

$$I^{dc} = \frac{e}{2\pi\hbar} \int dE |t'(E)|^2 \sum_n |C_n|^2 (f_L(E - n\hbar\omega) - f_R(E)) \quad (\text{A.11})$$

If the scattering matrix does not depend on energy and $V_{dc} = 0$ there is no *dc* current since $\int dE \sum_n |C_n|^2 f_L(E - n\hbar\omega) = \int dE f_R(E)$. However, if the scattering matrix depends on energy a *dc* current exists even at zero bias ($V_{dc} = 0$), this *dc* current is called the "photo-assisted current".

A.2 Photon-assisted noise

Let us now consider our quantity of interest, the second derivative of the shot noise, and investigate its interpretation in the photon-assisted approach. Using expression (A.10) for the current operator under time-dependent voltage and the expectation values (A.2) we calculate the current noise (3.24). For energy-independent scattering matrix and at zero temperature the second derivative of the shot noise with respect to V_{dc} have peaks at $V_{dc} = \frac{n\hbar\omega}{e}$, at zero temperature these peaks become delta functions, the power of the n 'th delta function is $|C_n|^2$.

$$\frac{d^2 S(\Omega \rightarrow 0)}{d(eV_{dc})^2} = \left(\frac{e}{\pi\hbar} \right)^2 |rt'|^2 \sum_n |C_n|^2 \delta(n\hbar\omega + eV_{dc}) \quad (\text{A.12})$$

Therefore, measuring the second derivative of the noise as a function of $\frac{eV_{dc}}{\hbar\omega}$ gives the function $|C_{-n}|^2$, which is the probability to excite a *e-h* pair in the left lead with energy eV_{dc} . The interpretation of the the second derivative of the shot noise is similar in the tunneling approach and the photon-assisted scattering approach. The difference lies in the location of the *e-h* pair, in the tunneling scheme they are in different leads and in the photon-assisted one they are in the same lead.

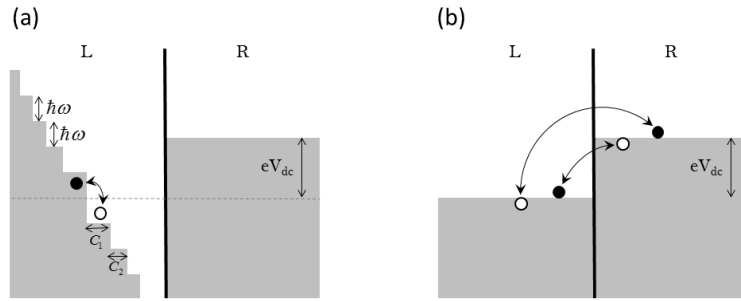


Figure A.3: *Schematic representation of the e-h creation process in (a) the photon-assisted approach and (b) the tunneling approach. In the photon-assisted approach (a) the e-h pairs are created in the left reservoir leading to a steps-like distribution function of the electrons in the left lead. the tunneling then is elastic. In the tunneling approach (b) The electron and hole are created on different sides of the barrier by an electron that tunnels from one of the reservoirs to the other while absorbing or emitting energy due to time dependent voltage.*

A.3 Levitov-Lesovik approach

For completeness we mention another method [32] to incorporate the time dependent voltage into the scattering approach which is to work in the gauge that eliminates the time-dependent electric field from the Hamiltonian. Consequently, the wave function of the electrons gain a phase $\psi(x, t) = \exp \left[i \frac{e}{\hbar} \int_{-\infty}^x A(x', t) dx' \right] \psi_0(x, t)$, where A is the electromagnetic vector potential. Adding that phase to the scattering wave function, is equivalent to adding a phase to the transmission coefficient $t(E) = \exp \left[i \frac{e}{\hbar} \int_{-\infty}^{\infty} A(x, t) dx \right] t_0(E) = \exp \left[i \frac{e}{\hbar} \int_{-\infty}^t V(t') dt' \right] t_0(E)$ and keeping the wavefunction $\psi_0(x, t)$. Therefore the transport is described by eqns. (A.1 - A.3) with a time-dependent transmission coefficient. The results obtained in this way are similar to the previously discussed approach.

Note that in this picture the electron gains the energy $n\hbar\omega$ as it passes the scatterer and not in the left lead. That interpretation resembles our tunneling approach, in which the time-dependent voltage excites an electron from the left(right) lead with energy E to an electron in the right(left) lead with energy $E + n\hbar\omega$, thus creating a e-h pair between the two leads.

Appendix B

Probability for the creation of e - h pairs – Derivation

Here we give a detailed derivation of the probability to create a e - h pair by the voltage modulation eqs. (3.17), (3.18). In order to describe the system in terms of electrons (above the Fermi sea) and holes (below the Fermi sea) we redefine the electronic operators c_{Lk} , c_{Rq}

$$c_{Lk} = \begin{cases} a_{Lk} & k > k_F \\ b_{L,-k}^\dagger & k < k_F \end{cases} \quad c_{Rq} = \begin{cases} a_{Rq} & q > k_F \\ b_{R,-q}^\dagger & q < k_F \end{cases}. \quad (\text{B.1})$$

The initial state of the electron system is assumed to be a Fermi sea in each lead. Hence, the initial state is the vacuum state for the electrons and holes. The Hamiltonians in the new representation are given by

$$\begin{aligned} H_0 = & \sum_{k>k_F} \epsilon_{Lk} a_{Lk}^\dagger a_{Lk} + \sum_{k< k_F} (-\epsilon_{Lk}) b_{L,-k}^\dagger b_{L,-k} \\ & + \sum_{q>k_F} \epsilon_{Rq} a_{Rq}^\dagger a_{Rq} + \sum_{q< k_F} (-\epsilon_{Rq}) b_{R,-q}^\dagger b_{R,-q} \end{aligned} \quad (\text{B.2})$$

$$\begin{aligned} H_T = & \sum_{\substack{k < k_F \\ q < k_F}} T_{kq} b_{R,-q} b_{L,-k}^\dagger e^{-i\phi_0(t)} + \sum_{\substack{k > k_F \\ q > k_F}} T_{kq} a_{Rq}^\dagger a_{Lk} e^{-i\phi_0(t)} \\ & + \sum_{\substack{k < k_F \\ q > k_F}} T_{kq} a_{Rq}^\dagger b_{L,-k}^\dagger e^{-i\phi_0(t)} + \sum_{\substack{k > k_F \\ q < k_F}} T_{k,q} b_{R,-q} a_{Lk} e^{-i\phi_0(t)} + H.C. \end{aligned} \quad (\text{B.3})$$

The probability to create a pair $a_{Rq}^\dagger b_{L,-k}^\dagger |0\rangle = |1_{Rq}, 1_{L,-k}\rangle = c_{Rq}^\dagger c_{Lk} |FS\rangle$ is given by

$$P_{RL}^{q,-k} (\Delta\epsilon_{RL} = \epsilon_{Rq} - \epsilon_{Lk} - eV_{dc}) = \langle 1_{Rq}, 1_{L,-k} | \rho(t_f) | 1_{Rq}, 1_{L,-k} \rangle \quad (\text{B.4})$$

where $\rho(t_f)$ is the density matrix at time t_f which is related to the initial density matrix $\rho_i = |0\rangle\langle 0|$ by

$$\rho(t_f) = U(t_f, t_i) \rho_i U^\dagger(t_f, t_i) \quad (\text{B.5})$$

where $U(t, t_i)$ is the evolution operator which satisfies $i\frac{d}{dt}U(t, t_i) = H(t)U(t, t_i)$. The

evolution operator , to second order in T , is given by

$$U(t_f, t_i) \approx e^{-iH_0(t_f - t_i)} \left[1 - \frac{i}{\hbar} \int_{t_i}^{t_f} \tilde{H}_T(t) dt - \frac{1}{\hbar^2} \int_{t_i}^{t_f} dt_1 \tilde{H}_T(t_1) \int_{t_i}^{t_1} dt_2 \tilde{H}_T(t_2) \right] \quad (\text{B.6})$$

where $\tilde{o}(t) = U_0^\dagger(t) O U_0(t)$ and $U_0(t) = e^{-iH_0 t}$ is the evolution operator with respect to the bare Hamiltonian H_0 . Therefore, the density matrix at t_f to second order in T is

$$\begin{aligned} \rho(t_f) &= U(t) \rho_i U^\dagger(t) = U_0(t_f) \rho_i U_0^\dagger(t_f) - U_0(t_f) \frac{i}{\hbar} \int_{t_i}^{t_f} [\tilde{H}_T(t) \rho_i - \rho_i \tilde{H}_T(t)] dt U_0^\dagger(t_f) \\ &\quad + U_0(t_f) \frac{1}{\hbar^2} \int_{t_i}^{t_f} \tilde{H}_T(t_1) dt_1 \rho_i \int_{t_i}^{t_f} \tilde{H}_T(t_2) dt_2 U_0^\dagger(t_f) \\ &\quad - U_0(t_f) \frac{1}{\hbar^2} \int_{t_i}^{t_f} dt_1 \tilde{H}_T(t_1) \int_{t_i}^{t_1} dt_2 \tilde{H}_T(t_2) \rho_i U_0^\dagger(t_f) - U_0(t_f) \rho_i \frac{1}{\hbar^2} \int_{t_i}^{t_f} dt_1 \tilde{H}_T(t_1) \int_{t_i}^{t_1} dt_2 \tilde{H}_T(t_2) U_0^\dagger(t_f) \end{aligned} \quad (\text{B.7})$$

Since the tunneling Hamiltonian can only create or annihilate a $e-h$ pair, the only term which contributes to the probability to create a $e-h$ pair is the one in the second line of (B.7). So the probability is

$$\begin{aligned} P_{RL}^{q,-k}(\Delta\epsilon_{RL} = \epsilon_{Rq} - \epsilon_{Lk} - eV_{dc}) &= \langle 1_{Rq}, 1_{L,-k} | \rho(t_f) | 1_{Rq}, 1_{L,-k} \rangle \\ &= \langle 1_{Rq}, 1_{L,-k} | \frac{1}{\hbar^2} \int_{t_i}^{t_f} \tilde{H}_T(t_1) dt_1 | 0 \rangle \langle 0 | \int_{t_i}^{t_f} \tilde{H}_T(t_2) dt_2 | 1_{Rq}, 1_{L,-k} \rangle \\ &= \frac{1}{\hbar^2} \left| \langle 1_{Rq}, 1_{L,-k} | \int_{t_i}^{t_f} \tilde{H}_T(t_1) dt_1 | 0 \rangle \right|^2 \\ &= \frac{1}{\hbar^2} \left| \langle 1_{Rq}, 1_{L,-k} | \int_{t_i}^{t_f} T_{kq} a_{Rq}^\dagger b_{L,-k}^\dagger e^{+i(\epsilon_{Rq} - \epsilon_{Lk})t_1} e^{-i\phi_0(t_1)} dt_1 | 0 \rangle \right|^2 \\ &= \theta(\epsilon_{Rq} - \epsilon_F) \theta(\epsilon_F - \epsilon_{Lk}) \frac{T_{kq}^2}{\hbar^2} \left| \int_{t_i}^{t_f} dt e^{+i\phi(t)} e^{-i\frac{1}{\hbar}\Delta\epsilon_{RL}t - 0^+|t|} \right|^2 \end{aligned} \quad (\text{B.8})$$

where in the last line we introduced the regularization of the integral by $e^{-0^+|t|}$. If the leads were not at zero temperature but at some temperature β_{leads}^{-1} , the initial density matrix would have been $\rho_i = e^{-\beta_{leads} H_0} / \text{Tr}\{e^{-\beta_{leads} H_0}\}$ and the theta functions would be replaced with Fermi distribution functions

$$\theta(\epsilon_{Rq} - \epsilon_F) \theta(\epsilon_F - \epsilon_{Lk}) \rightarrow f(\epsilon_{Lk})(1 - f(\epsilon_{Rq})). \quad (\text{B.9})$$

In the same way, the probability to create a pair $a_{Lk}^\dagger b_{R,-q}^\dagger |0\rangle = |1_{Lk}, 1_{R,-q}\rangle$ is given

by

$$\begin{aligned}
 P_{LR}^{k,-q}(\Delta\epsilon_{LR} = \epsilon_{Lk} + eV_{dc} - \epsilon_{Rq}) &= \langle 1_{Lk}, 1_{R,-q} | \rho(t_f) | 1_{Lk}, 1_{R,-q} \rangle \\
 &= \theta(\epsilon_{Lk} - \epsilon_F) \theta(\epsilon_F - \epsilon_{Rq}) \frac{T_{kq}^2}{\hbar^2} \left| \int_{t_i}^{t_f} dt e^{-i\phi(t)} e^{-\frac{i}{\hbar}\Delta\epsilon_{LR}t} \right|^2 \\
 &= \theta(\epsilon_{Lk} - \epsilon_F) \theta(\epsilon_F - \epsilon_{Rq}) \frac{T_{kq}^2}{\hbar^2} \left| \int_{t_i}^{t_f} dt e^{+i\phi(t)} e^{+\frac{i}{\hbar}\Delta\epsilon_{LR}t} \right|^2 \quad (\text{B.10})
 \end{aligned}$$

Note that there is a symmetry for these probabilities: Changing the sign of the voltage switches between left and right

$$\begin{aligned}
 \phi_0 &\rightarrow -\phi_0 \\
 L &\rightarrow R \\
 R &\rightarrow L. \quad (\text{B.11})
 \end{aligned}$$

Appendix C

Relation of the current noise to the probability for the creation of e - h pairs – Derivation

Here we give a detailed derivation of relation (3.31) between the current noise and the probability to create a e - h pair. The correlation function of the current is defined as

$$C(t_1, t_2) = \text{Tr} \{ I(t_1) I(t_2) \rho_i \} \quad (\text{C.1})$$

the trace is taken over the system degrees of freedom. To second order in T , it is given by the correlation function of the currents in the interaction picture.

$$\begin{aligned} C(t_1, t_2) &\approx \text{Tr} \left\{ \tilde{I}(t_1) \tilde{I}(t_2) \rho_i \right\} = \text{Tr} \left\{ \tilde{I}(t_2) \rho_i \tilde{I}(t_1) \right\} \\ &= \sum_{kq} \langle 11 | \tilde{I}(t_2) | 0 \rangle \langle 0 | \tilde{I}(t_1) | 11 \rangle = \frac{e^2}{\hbar^2} \sum_{kq} \langle 11 | \tilde{H}_T(t_2) | 0 \rangle \langle 0 | \tilde{H}_T(t_1) | 11 \rangle \end{aligned} \quad (\text{C.2})$$

where $\tilde{o}(t) \equiv U_0^\dagger(t) o(t) U_0(t)$. In the second line $|11\rangle$ marks a state with one electron-hole pair. The trace over the electron system is reduced to a trace over one electron-hole states since they are the only states that can be created from the vacuum by \tilde{I} . In order to get the last equality we note that the matrix elements of \tilde{I} and \tilde{H}_{int} differ only by a constant.

The power spectrum of the current is given by the Fourier transform of the correlation function.

$$S(\Omega) = \int_{-\infty}^{\infty} dt_1 \int_{-\infty}^{\infty} dt_2 C(t_1, t_2) e^{i\Omega t_1} e^{-i\Omega t_2} \quad (\text{C.3})$$

Inserting the expression obtained for the correlation function we find that the noise

power is the total probability to create an electron-hole pair with energy shifted by Ω .

$$\begin{aligned}
 S(\Omega) &= \int_{-\infty}^{\infty} dt_1 \int_{-\infty}^{\infty} dt_2 e^{i\Omega(t_1-t_2)} \frac{e^2}{\hbar^2} \left\{ \sum_{kq} \langle 11| \tilde{H}_T(t_2) |0\rangle \langle 0| \tilde{H}_T(t_1) |11\rangle \right\} \\
 &= \int_{-\infty}^{\infty} dt_1 \int_{-\infty}^{\infty} dt_2 \frac{e^2}{\hbar^2} \sum_{kq} \langle 11| \tilde{H}_T(t_2) e^{-i\Omega t_2} |0\rangle \langle 0| \tilde{H}_T(t_1) e^{i\Omega t_1} |11\rangle \\
 &= e^2 \sum_{\substack{q > k_F \\ k < k_F}} \frac{T_{kq}^2}{\hbar^2} \left| \int_{-\infty}^{\infty} dt_2 \langle 1_{Rq}, 1_{L,-k} | a_{Rq}^\dagger b_{L,-k}^\dagger e^{+\frac{i}{\hbar}(\epsilon_{Rq} - \epsilon_{Lk}^0)t_2} e^{-i\Omega t_2} e^{-i\phi(t_2)} |0_{Rq}, 0_{L,-k}\rangle \right|^2 \\
 &\quad + \sum_{\substack{k > k_F \\ q < k_F}} \frac{T_{kq}^2}{\hbar^2} \left| \int_{-\infty}^{\infty} dt_2 \langle 1_{Lk}, 1_{R,-q} | a_{Lk}^\dagger b_{R,-q}^\dagger e^{+\frac{i}{\hbar}(\epsilon_{Lk}^0 - \epsilon_{Rq})t_2} e^{-i\Omega t_2} e^{+i\phi(t_2)} |0_{Lk}, 0_{R,-q}\rangle \right|^2 \\
 &= e^2 \left[\sum_{\substack{q > k_F \\ k < k_F}} P_{RL} (\Delta\epsilon_{RL} = \epsilon_{Rq} - \epsilon_{Lk}^0 - \hbar\Omega) + \sum_{\substack{k > k_F \\ q < k_F}} P_{LR} (\Delta\epsilon_{LR} = \epsilon_{Lk}^0 - \epsilon_{Rq} - \hbar\Omega) \right] \tag{C.4}
 \end{aligned}$$

In order to make the transition to the last line compare with (B.8). Taking the continuum limit

$$\begin{aligned}
 S(\Omega) &= e^2 \rho^2 \int_{\epsilon_F}^{\infty} d\epsilon_{Lk} \int_{-\infty}^{\epsilon_F} d\epsilon_{Rq} P_{LR} (\Delta\epsilon_{LR} = \epsilon_{Lk} + eV_{dc} - \epsilon_{Rq} - \hbar\Omega) \\
 &\quad + e^2 \rho^2 \int_{\epsilon_F}^{\infty} d\epsilon_{Rq} \int_{-\infty}^{\epsilon_F} d\epsilon_{Lk} P_{RL} (\Delta\epsilon_{RL} = \epsilon_{Rq} - \epsilon_{Lk} - eV_{dc} - \hbar\Omega) \tag{C.5}
 \end{aligned}$$

where ρ is the density of states of the leads at the Fermi energy. The probability of the creation of a $e-h$ pair is negligible outside an energy window ΔE around zero. We have assumed that $\Delta E \ll E_F$, so that the density of states in this regime can be approximated by the density of states at the Fermi energy. Changing the integration variable to $\epsilon_{Lk} + eV_{dc}$

$$\begin{aligned}
 S(\Omega) &= e^2 \rho^2 \int_{\epsilon_F + eV_{dc}}^{\infty} d\epsilon_{Lk} \int_{-\infty}^{\epsilon_F} d\epsilon_{Rq} P_{LR} (\Delta\epsilon_{LR} = \epsilon_{Lk} - \epsilon_{Rq} - \hbar\Omega) \\
 &\quad + e^2 \rho^2 \int_{\epsilon_F}^{\infty} d\epsilon_{Rq} \int_{-\infty}^{\epsilon_F + eV_{dc}} d\epsilon_{Lk} P_{RL} (\Delta\epsilon_{RL} = \epsilon_{Rq} - \epsilon_{Lk} - \hbar\Omega) \tag{C.6}
 \end{aligned}$$

Taking the derivative of $S(\Omega)$ with respect to the *dc* voltage

$$\begin{aligned}
\frac{dS(\Omega)}{d(eV_{dc})} &= -e^2 \rho^2 \int_{-\infty}^{\epsilon_F} d\epsilon_{Rq} P_{LR} (\Delta\epsilon_{LR} = \epsilon_F + eV_{dc} - \epsilon_{Rq} - \hbar\Omega) \\
&\quad + e^2 \rho^2 \int_{\epsilon_F}^{\infty} d\epsilon_{Rq} P_{RL} (\Delta\epsilon_{RL} = \epsilon_{Rq} - \epsilon_F - eV_{dc} - \hbar\Omega) \\
&= -e^2 \rho^2 \int_{-\infty}^{-eV_{dc}} d\epsilon_{Rq} P_{LR} (\Delta\epsilon_{LR} = -\epsilon_{Rq} - \hbar\Omega) + e^2 \rho^2 \int_{-eV_{dc}}^{\infty} d\epsilon_{Rq} P_{RL} (\Delta\epsilon_{RL} = \epsilon_{Rq} - \hbar\Omega)
\end{aligned} \tag{C.7}$$

Taking another derivative with respect to the *dc* voltage

$$\frac{d^2S(\Omega)}{d(eV_{dc})^2} = e^2 \rho^2 P_{LR} (\Delta\epsilon_{LR} = eV_{dc} - \hbar\Omega) + e^2 \rho^2 P_{RL} (\Delta\epsilon_{RL} = -eV_{dc} - \hbar\Omega) \tag{C.8}$$

Considering the shot noise, i.e. taking $\Omega \rightarrow 0$, we get relation (3.31) between the shot noise and the probability to create a *e-h* pair.

Appendix D

Tunnel junction phase as a quantum Brownian particle

In order to find the correlation function $J(t)$ we need to solve the equation of motion for the phase of the tunnel junction ϕ at equilibrium without the coupling to the electron system. In this section we show the mapping between the tunnel junction phase and the quantum Brownian particle described in [82].

First, we notice that the Hamiltonian of the environment

$$H_{env} = \frac{Q^2}{2C} + \sum_{n=1}^N \left(\frac{q_n^2}{2C_n} + \left(\frac{\hbar}{e} \right)^2 \frac{1}{2L_n} (\varphi - \varphi_n)^2 \right) \quad (D.1)$$

is that of a Brownian particle given by [82]. The Brownian particle momentum, position and mass are equivalent to the tunnel junction charge, phase and capacitance respectively.

$$\begin{aligned} Q &\leftrightarrow p \\ \varphi &\leftrightarrow x \\ C &\leftrightarrow M \end{aligned} \quad (D.2)$$

The external impedance degrees of freedom correspond the bath of the Brownian particle degrees of freedom in a similar manner

$$\begin{aligned} q_n &\leftrightarrow p_n \\ \varphi_n &\leftrightarrow x_n \\ C_n &\leftrightarrow m_n \\ \frac{1}{\sqrt{L_n C_n}} &\leftrightarrow \omega_n \end{aligned} \quad (D.3)$$

D.1 Ohmic environment

The classical equation of motion for the charge on the capacitor in an RC circuit is

$$\dot{Q} + \frac{1}{RC} Q = 0. \quad (D.4)$$

Since the voltage over the capacitor is $\dot{\varphi} = V = Q/C$, the classical equation of motion for the phase φ is

$$\ddot{\varphi} + \frac{1}{RC} \dot{\varphi}(s) = 0 \quad (D.5)$$

Comparing with eq. 4.46 and 7.2 of [82] we see that $(RC)^{-1}$ is mapped to the friction coefficient of a Brownian particle in an ohmic environment

$$\frac{1}{RC} \leftrightarrow \gamma. \quad (\text{D.6})$$

Our correlation function $J(t)$ corresponds to the correlation function $C^F(t)$ defined in [82] (see eq. (9.8) in [82])

$$\left(\frac{\hbar}{e}\right)^2 J(t) \leftrightarrow C^F(t) = Q^F(t) + iA^F(t) \quad (\text{D.7})$$

Eqns. 10.1 and 10.4 of [82] gives the real and imaginary parts of $C^F(t)$. Mapping to our case, the real and imaginary parts of $J(t)$ are given by

$$J_I(t) = -\frac{e^2 R}{\hbar} \left\{ 1 - e^{-\frac{t}{RC}} \right\} = -\pi \frac{R}{R_K} \left\{ 1 - e^{-\frac{t}{RC}} \right\} \quad (\text{D.8})$$

$$J_R(t) = \frac{e^2}{\hbar^2} \left[-\frac{R}{\beta} t + \frac{R^2 C}{\beta} - \frac{2}{C \beta} \sum_{n=1}^{\infty} \frac{1}{\nu_n^2 + \nu_n \frac{1}{RC}} - \frac{\hbar R}{2} \cot \left(\frac{\hbar \beta}{2RC} \right) e^{-\frac{t}{RC}} \right. \\ \left. + \frac{2}{\beta RC^2} \sum_{n=1}^{\infty} \frac{e^{-\nu_n t}}{\nu_n \left(\frac{1}{R^2 C^2} - \nu_n^2 \right)} \right] \quad (\text{D.9})$$

where ν_n are the Matsubara frequencies $\nu_n = \frac{2\pi n}{\hbar \beta}$ and $R_K = h/e^2$ is the quantum of resistance.

D.1.1 High temperature limit

In the high temperature limit $\frac{\hbar \beta}{RC} \ll 1$, the real part of the correlation function is given by

$$J_R(t) \xrightarrow[\frac{\hbar \beta}{RC} \ll 1]{} -\frac{R}{R_k} \frac{2\pi}{\hbar \beta} t + 2\pi \frac{R}{R_k} \frac{RC}{\hbar \beta} \left(1 - e^{-\frac{t}{RC}} \right) - 2\pi \frac{R}{R_k} \frac{\hbar \beta}{12RC} \quad (\text{D.10})$$

As long as $\frac{R}{R_K}$ does not go to infinity, we can neglect the last term. The imaginary part of the correlation does not depend on temperature.

For times much smaller or larger than the RC time, $J(t)$ can be approximated by

$$J(t) = \begin{cases} -\frac{1}{\hbar \beta} \frac{\pi}{R_k C} t^2 - i\pi \frac{1}{R_k C} t & t \ll RC \\ -\frac{R}{R_k} \frac{2\pi}{\hbar \beta} (t - RC) - i\pi \frac{R}{R_K} & t \gg RC \end{cases} \quad (\text{D.11})$$

which is Eq. (3.95).

Bibliography

- [1] J. Schwinger. On gauge invariance and vacuum polarization. *Phys. Rev.*, 82:664–679, Jun 1951.
- [2] W. G. Unruh. Notes on black-hole evaporation. *Phys. Rev. D*, 14:870–892, Aug 1976.
- [3] P. C. W. Davies and S. A. Fulling. Radiation from moving mirrors and from black holes. *Proceedings of the Royal Society of London A: Mathematical, Physical and Engineering Sciences*, 356(1685):237–257, 1977.
- [4] G. T. Moore. Quantum theory of the electromagnetic field in a variablelength onedimensional cavity. *Journal of Mathematical Physics*, 11(9), 1970.
- [5] S. W. Hawking. Black hole explosions. *Nature*, 248(5443):30–31, 1974.
- [6] S. W. Hawking. Particle creation by black holes. *Communications in Mathematical Physics*, 43(3):199–220, 1975.
- [7] R. Boyd. *Nonlinear Optics*. Nonlinear Optics Series. Elsevier Science, 2008.
- [8] P. D. Nation, J. R. Johansson, M. P. Blencowe, and F. Nori. *Colloquium : Stimulating uncertainty: Amplifying the quantum vacuum with superconducting circuits*. *Rev. Mod. Phys.*, 84:1–24, Jan 2012.
- [9] L. S. Brown and L. J. Carson. Quantum-mechanical parametric amplification. *Phys. Rev. A*, 20:2486–2497, Dec 1979.
- [10] U. Leonhardt. *Essential Quantum Optics: From Quantum Measurements to Black Holes*. Cambridge University Press, 2010.
- [11] P. Milonni. *The Quantum Vacuum: An Introduction to Quantum Electrodynamics*. ACADEMIC PressINC, 1993.
- [12] A. A. Clerk, M. H. Devoret, S. M. Girvin, F. Marquardt, and R. J. Schoelkopf. Introduction to quantum noise, measurement, and amplification. *Rev. Mod. Phys.*, 82:1155–1208, Apr 2010.
- [13] S. K. Lamoreaux. Demonstration of the casimir force in the 0.6 to $6\mu m$ range. *Phys. Rev. Lett.*, 78:5–8, Jan 1997.
- [14] W. E. Lamb and R. C. Rutherford. Fine structure of the hydrogen atom by a microwave method. *Phys. Rev.*, 72:241–243, Aug 1947.
- [15] R. Ghosh and L. Mandel. Observation of nonclassical effects in the interference of two photons. *Phys. Rev. Lett.*, 59:1903–1905, Oct 1987.

- [16] A. Zeilinger. Experiment and the foundations of quantum physics. *Rev. Mod. Phys.*, 71:S288–S297, Mar 1999.
- [17] C. Wilson, G. Johansson, A. Pourkabirian, M. Simoen, J. Johansson, T. Duty, F. Nori, and P. Delsing. Observation of the dynamical casimir effect in a superconducting circuit. *Nature*, 479(7373):376–379, 2011.
- [18] D. Guery-Odelin and C. Cohen-Tannoudji. *Advances in Atomic Physics*. World Scientific Publishing Company, 2011.
- [19] E. Akkermans and G. V. Dunne. Ramsey fringes and time-domain multiple-slit interference from vacuum. *Phys. Rev. Lett.*, 108:030401, Jan 2012.
- [20] I. I. Rabi. Space quantization in a gyrating magnetic field. *Phys. Rev.*, 51:652–654, Apr 1937.
- [21] N. F. Ramsey. A molecular beam resonance method with separated oscillating fields. *Phys. Rev.*, 78:695–699, Jun 1950.
- [22] M. Scully and M. Zubairy. *Quantum Optics*. Cambridge University Press, 1997.
- [23] J. Vanier. Atomic clocks based on coherent population trapping: a review. *Applied Physics B*, 81(4):421–442, 2005.
- [24] D. Vion, A. Aassime, A. Cottet, P. Joyez, H. Pothier, C. Urbina, D. Esteve, and M. H. Devoret. Manipulating the quantum state of an electrical circuit. *Science*, 296(5569):886–889, 2002.
- [25] I. Chiorescu, Y. Nakamura, C. J. P. M. Harmans, and J. E. Mooij. Coherent quantum dynamics of a superconducting flux qubit. *Science*, 299(5614):1869–1871, 2003.
- [26] L. M. K. Vandersypen and I. L. Chuang. Nmr techniques for quantum control and computation. *Rev. Mod. Phys.*, 76:1037–1069, Jan 2005.
- [27] Y. Nazarov and Y. Blanter. *Quantum Transport: Introduction to Nanoscience*. Cambridge University Press, 2009.
- [28] D. Rogovin and D. Scalapino. Fluctuation phenomena in tunnel junctions. *Annals of Physics*, 86(1):1 – 90, 1974.
- [29] Y. Blanter and M. Büttiker. Shot noise in mesoscopic conductors. *Physics Reports*, 336(12):1 – 166, 2000.
- [30] M. H. Pedersen and M. Büttiker. Scattering theory of photon-assisted electron transport. *Phys. Rev. B*, 58:12993–13006, Nov 1998.
- [31] P. K. Tien and J. P. Gordon. Multiphoton process observed in the interaction of microwave fields with the tunneling between superconductor films. *Phys. Rev.*, 129:647–651, Jan 1963.
- [32] G. B. Lesovik and L. S. Levitov. Noise in an ac biased junction: Nonstationary aharonov-bohm effect. *Phys. Rev. Lett.*, 72:538–541, Jan 1994.
- [33] E. Akkermans and G. Montambaux. *Mesoscopic Physics of Electrons and Photons*. Cambridge University Press, 2007. Cambridge Books Online.

- [34] Y. Imry. *Introduction to Mesoscopic Physics*. Mesoscopic physics and nanotechnology. Oxford University Press, 2002.
- [35] J. J. Lin and J. P. Bird. Recent experimental studies of electron dephasing in metal and semiconductor mesoscopic structures. *Journal of Physics: Condensed Matter*, 14(18):R501, 2002.
- [36] P. Roulleau, F. Portier, P. Roche, A. Cavanna, G. Faini, U. Gennser, and D. Mailly. Direct measurement of the coherence length of edge states in the integer quantum hall regime. *Phys. Rev. Lett.*, 100:126802, Mar 2008.
- [37] G. Haack, M. Moskalets, J. Splettstoesser, and M. Büttiker. Coherence of single-electron sources from mach-zehnder interferometry. *Phys. Rev. B*, 84:081303, Aug 2011.
- [38] I. Neder, F. Marquardt, M. Heiblum, D. Mahalu, and V. Umansky. Controlled dephasing of electrons by non-gaussian shot noise. *Nature Physics*, 3(8):534–537, 2007.
- [39] K. Le Hur. Dephasing of mesoscopic interferences from electron fractionalization. *Phys. Rev. Lett.*, 95:076801, Aug 2005.
- [40] G. Seelig and M. Büttiker. Charge-fluctuation-induced dephasing in a gated mesoscopic interferometer. *Phys. Rev. B*, 64:245313, Dec 2001.
- [41] J. T. Chalker, Y. Gefen, and M. Y. Veillette. Decoherence and interactions in an electronic mach-zehnder interferometer. *Phys. Rev. B*, 76:085320, Aug 2007.
- [42] L. V. Litvin, H.-P. Tranitz, W. Wegscheider, and C. Strunk. Decoherence and single electron charging in an electronic mach-zehnder interferometer. *Phys. Rev. B*, 75:033315, Jan 2007.
- [43] I. P. Levkivskyi and E. V. Sukhorukov. Dephasing in the electronic mach-zehnder interferometer at filling factor $\nu = 2$. *Phys. Rev. B*, 78:045322, Jul 2008.
- [44] C. Caroli, R. Combescot, P. Nozieres, and D. Saint-James. Direct calculation of the tunneling current. *Journal of Physics C: Solid State Physics*, 4(8):916, 1971.
- [45] C. Caroli, R. Combescot, D. Lederer, P. Nozieres, and D. Saint-James. A direct calculation of the tunnelling current. ii. free electron description. *Journal of Physics C: Solid State Physics*, 4(16):2598, 1971.
- [46] M. H. Cohen, L. M. Falicov, and J. C. Phillips. Superconductive tunneling. *Phys. Rev. Lett.*, 8:316–318, Apr 1962.
- [47] J. Bardeen. Tunnelling from a many-particle point of view. *Phys. Rev. Lett.*, 6:57–59, Jan 1961.
- [48] M. Dolev, M. Heiblum, V. Umansky, A. Stern, and D. Mahalu. Observation of a quarter of an electron charge at the $\nu = 5/2$ quantum hall state. *Nature*, 452(7189):829–834, 2008.
- [49] M. Reznikov, R. de Picciotto, M. Heiblum, D. Glattli, A. Kumar, and L. Saminadayar. Quantum shot noise. *Superlattices and Microstructures*, 23(3):901 – 915, 1998.

- [50] G. Campagnano, O. Zilberberg, I. V. Gornyi, D. E. Feldman, A. C. Potter, and Y. Gefen. Hanbury Brown–Twiss interference of anyons. *Phys. Rev. Lett.*, 109:106802, Sep 2012.
- [51] I. Neder, N. Ofek, Y. Chung, M. Heiblum, D. Mahalu, and V. Umansky. Interference between two indistinguishable electrons from independent sources. *Nature*, 448(7151):333–337, 2007.
- [52] Y. Bomze, G. Gershon, D. Shovkun, L. S. Levitov, and M. Reznikov. Measurement of counting statistics of electron transport in a tunnel junction. *Phys. Rev. Lett.*, 95:176601, Oct 2005.
- [53] J. Gabelli, L. Spietz, J. Aumentado, and B. Reulet. Electronphoton correlations and the third moment of quantum noise. *New Journal of Physics*, 15(11):113045, 2013.
- [54] J.-C. Forges, F. B. Sane, S. Blanchard, L. Spietz, C. Lupien, and B. Reulet. Noise intensity-intensity correlations and the fourth cumulant of photo-assisted shot noise. *Scientific reports*, 3, 2013.
- [55] D. S. Golubev, A. V. Galaktionov, and A. D. Zaikin. Electron transport and current fluctuations in short coherent conductors. *Phys. Rev. B*, 72:205417, Nov 2005.
- [56] L. S. Levitov, H. Lee, and G. B. Lesovik. Electron counting statistics and coherent states of electric current. *Journal of Mathematical Physics*, 37(10), 1996.
- [57] J. Gabelli and B. Reulet. Shaping a time-dependent excitation to minimize the shot noise in a tunnel junction. *Phys. Rev. B*, 87:075403, Feb 2013.
- [58] P. Nozieres and D. Pines. *Theory Of Quantum Liquids*. Advanced Books Classics Series. Westview Press, 1999.
- [59] G.-L. Ingold and Y. V. Nazarov. *Charge Tunneling Rates in Ultrasmall Junctions*, pages 21–107. Springer US, Boston, MA, 1992.
- [60] M. H. Devoret, D. Esteve, H. Grabert, G.-L. Ingold, H. Pothier, and C. Urbina. Effect of the electromagnetic environment on the coulomb blockade in ultrasmall tunnel junctions. *Phys. Rev. Lett.*, 64:1824–1827, Apr 1990.
- [61] S. M. Girvin, L. I. Glazman, M. Jonson, D. R. Penn, and M. D. Stiles. Quantum fluctuations and the single-junction coulomb blockade. *Phys. Rev. Lett.*, 64:3183–3186, Jun 1990.
- [62] A. N. Cleland, J. M. Schmidt, and J. Clarke. Influence of the environment on the coulomb blockade in submicrometer normal-metal tunnel junctions. *Phys. Rev. B*, 45:2950–2961, Feb 1992.
- [63] T. Holst, D. Esteve, C. Urbina, and M. H. Devoret. Effect of a transmission line resonator on a small capacitance tunnel junction. *Phys. Rev. Lett.*, 73:3455–3458, Dec 1994.
- [64] P. Joyez, D. Esteve, and M. H. Devoret. How is the coulomb blockade suppressed in high-conductance tunnel junctions? *Phys. Rev. Lett.*, 80:1956–1959, Mar 1998.
- [65] F. Pierre, H. Pothier, P. Joyez, N. O. Birge, D. Esteve, and M. H. Devoret. Electrodynamic dip in the local density of states of a metallic wire. *Phys. Rev. Lett.*, 86:1590–1593, Feb 2001.

- [66] Y. V. Nazarov. Coulomb blockade without tunnel junctions. *Phys. Rev. Lett.*, 82:1245–1248, Feb 1999.
- [67] D. S. Golubev and A. D. Zaikin. Coulomb interaction and quantum transport through a coherent scatterer. *Phys. Rev. Lett.*, 86:4887–4890, May 2001.
- [68] A. L. Yeyati, A. Martin-Rodero, D. Esteve, and C. Urbina. Direct link between coulomb blockade and shot noise in a quantum-coherent structure. *Phys. Rev. Lett.*, 87:046802, Jul 2001.
- [69] C. Altimiras, U. Gennser, A. Cavanna, D. Mailly, and F. Pierre. Experimental test of the dynamical coulomb blockade theory for short coherent conductors. *Phys. Rev. Lett.*, 99:256805, Dec 2007.
- [70] A. V. Galaktionov, D. S. Golubev, and A. D. Zaikin. Current fluctuations and electron-electron interactions in coherent conductors. *Phys. Rev. B*, 68:085317, Aug 2003.
- [71] M. Kindermann and Y. V. Nazarov. Interaction effects on counting statistics and the transmission distribution. *Phys. Rev. Lett.*, 91:136802, Sep 2003.
- [72] M. Kindermann, Y. V. Nazarov, and C. W. J. Beenakker. Feedback of the electromagnetic environment on current and voltage fluctuations out of equilibrium. *Phys. Rev. B*, 69:035336, Jan 2004.
- [73] I. Safi and H. Saleur. One-channel conductor in an ohmic environment: Mapping to a tomonaga-luttinger liquid and full counting statistics. *Phys. Rev. Lett.*, 93:126602, Sep 2004.
- [74] E. Shimshoni and Y. Gefen. Onset of dissipation in zener dynamics: relaxation versus dephasing. *Annals of Physics*, 210(1):16–80, 1991.
- [75] M. H. Devoret. Quantum fluctuations in electrical circuits. In S. Reynaud, E. Giacobino, and J. Zinn-Justin, editors, *Les Houches, Session LXIII, 1995: Quantum Fluctuations*, pages 351–385. Elsevier Science, 1997.
- [76] B. Yurke and J. S. Denker. Quantum network theory. *Phys. Rev. A*, 29:1419–1437, Mar 1984.
- [77] C. Cohen-Tannoudji, J. Dupont-Roc, and G. Grynberg. *Photons and Atoms: Introduction to Quantum Electrodynamics*. Wiley, 1989.
- [78] A. Caldeira and A. Leggett. Quantum tunnelling in a dissipative system. *Annals of Physics*, 149(2):374 – 456, 1983.
- [79] R. Feynman and F. Vernon. The theory of a general quantum system interacting with a linear dissipative system. *Annals of Physics*, 24:118 – 173, 1963.
- [80] M. Hofheinz, F. Portier, Q. Baudouin, P. Joyez, D. Vion, P. Bertet, P. Roche, and D. Esteve. Bright side of the coulomb blockade. *Phys. Rev. Lett.*, 106:217005, May 2011.
- [81] R. Kubo. The fluctuation-dissipation theorem. *Reports on Progress in Physics*, 29(1):255, 1966.
- [82] H. Grabert, P. Schramm, and G.-L. Ingold. Quantum brownian motion: The functional integral approach. *Physics Reports*, 168(3):115 – 207, 1988.

- [83] *Introduction*, pages 1–2. Springer Berlin Heidelberg, Berlin, Heidelberg, 2000.
- [84] R. Ruffini, G. Vereshchagin, and S.-S. Xue. Electronpositron pairs in physics and astrophysics: From heavy nuclei to black holes. *Physics Reports*, 487(14):1 – 140, 2010.
- [85] W. Greiner and J. Reinhardt. *Quantum Electrodynamics*. Physics and Astronomy. Springer Berlin Heidelberg, 2008.
- [86] V. G. Dunne. New strong-field qed effects at extreme light infrastructure. *The European Physical Journal D*, 55(2):327–340, 2009.
- [87] A. Di Piazza, C. Müller, K. Z. Hatsagortsyan, and C. H. Keitel. Extremely high-intensity laser interactions with fundamental quantum systems. *Rev. Mod. Phys.*, 84:1177–1228, Aug 2012.
- [88] T. Tajima. Prospect for extreme field science. *The European Physical Journal D*, 55(2):519–529, 2009.
- [89] A. Ringwald. Pair production from vacuum at the focus of an x-ray free electron laser. *Physics Letters B*, 510(14):107 – 116, 2001.
- [90] S. S. Bulanov, V. D. Mur, N. B. Narozhny, J. Nees, and V. S. Popov. Multiple colliding electromagnetic pulses: A way to lower the threshold of e^+e^- pair production from vacuum. *Phys. Rev. Lett.*, 104:220404, Jun 2010.
- [91] N. Narozhny, S. Bulanov, V. Mur, and V. Popov. -pair production by a focused laser pulse in vacuum. *Physics Letters A*, 330(12):1 – 6, 2004.
- [92] R. Schützhold, H. Gies, and G. Dunne. Dynamically assisted schwinger mechanism. *Phys. Rev. Lett.*, 101:130404, Sep 2008.
- [93] A. Di Piazza, E. Lötstedt, A. I. Milstein, and C. H. Keitel. Barrier control in tunneling e^+-e^- photoproduction. *Phys. Rev. Lett.*, 103:170403, Oct 2009.
- [94] G. V. Dunne, H. Gies, and R. Schützhold. Catalysis of schwinger vacuum pair production. *Phys. Rev. D*, 80:111301, Dec 2009.
- [95] A. Monin and M. B. Voloshin. Photon-stimulated production of electron-positron pairs in an electric field. *Phys. Rev. D*, 81:025001, Jan 2010.
- [96] C. Fey and R. Schützhold. Momentum dependence in the dynamically assisted sauter-schwinger effect. *Phys. Rev. D*, 85:025004, Jan 2012.
- [97] M. F. Linder, C. Schneider, J. Sicking, N. Szpak, and R. Schützhold. Pulse shape dependence in the dynamically assisted sauter-schwinger effect. *Phys. Rev. D*, 92:085009, Oct 2015.
- [98] D. A. Panferov, A. S. Smolyansky, A. Otto, B. Kämpfer, B. D. Blaschke, and L. Juchnowski. Assisted dynamical schwinger effect: pair production in a pulsed bifrequent field. *The European Physical Journal D*, 70(3):1–8, 2016.
- [99] T. Heinzl, A. Ilderton, and M. Marklund. Finite size effects in stimulated laser pair production. *Physics Letters B*, 692(4):250 – 256, 2010.
- [100] F. Hebenstreit, R. Alkofer, G. V. Dunne, and H. Gies. Momentum signatures for schwinger pair production in short laser pulses with a subcycle structure. *Phys. Rev. Lett.*, 102:150404, Apr 2009.

- [101] V. S. Popov. Schwinger mechanism of electron-positron pair production by the field of optical and x-ray lasers in vacuum. *Journal of Experimental and Theoretical Physics Letters*, 74(3):133–138, 2001.
- [102] C. K. Dumlu and G. V. Dunne. Stokes phenomenon and schwinger vacuum pair production in time-dependent laser pulses. *Phys. Rev. Lett.*, 104:250402, Jun 2010.
- [103] C. K. Dumlu and G. V. Dunne. Interference effects in schwinger vacuum pair production for time-dependent laser pulses. *Phys. Rev. D*, 83:065028, Mar 2011.
- [104] S. Meuren, C. H. Keitel, and A. Di Piazza. Semiclassical picture for electron-positron photoproduction in strong laser fields. *Phys. Rev. D*, 93:085028, Apr 2016.
- [105] C. Kohlfürst, M. Mitter, G. von Winckel, F. Hebenstreit, and R. Alkofer. Optimizing the pulse shape for schwinger pair production. *Phys. Rev. D*, 88:045028, Aug 2013.
- [106] E. Brezin and C. Itzykson. Pair production in vacuum by an alternating field. *Phys. Rev. D*, 2:1191–1199, Oct 1970.
- [107] M. S. Marinov and V. S. Popov. Electron-positron pair creation from vacuum induced by variable electric field. *Fortschritte der Physik*, 25(1-12):373–400, 1977.
- [108] S. P. Gavrilov and D. M. Gitman. Vacuum instability in external fields. *Phys. Rev. D*, 53:7162–7175, Jun 1996.
- [109] S. P. Kim and D. N. Page. Improved approximations for fermion pair production in inhomogeneous electric fields. *Phys. Rev. D*, 75:045013, Feb 2007.
- [110] Y. Kluger, J. M. Eisenberg, B. Svetitsky, F. Cooper, and E. Mottola. Pair production in a strong electric field. *Phys. Rev. Lett.*, 67:2427–2430, Oct 1991.
- [111] Y. Kluger, J. M. Eisenberg, B. Svetitsky, F. Cooper, and E. Mottola. Fermion pair production in a strong electric field. *Phys. Rev. D*, 45:4659–4671, Jun 1992.
- [112] Y. Kluger, E. Mottola, and J. M. Eisenberg. Quantum vlasov equation and its markov limit. *Phys. Rev. D*, 58:125015, Nov 1998.
- [113] J. Rau. Pair production in the quantum boltzmann equation. *Phys. Rev. D*, 50:6911–6916, Dec 1994.
- [114] J. Rau and B. Mller. From reversible quantum microdynamics to irreversible quantum transport. *Physics Reports*, 272(1):1 – 59, 1996.
- [115] S. Schmidt, D. Blaschke, G. Rpke, S. A. Smolyansky, A. V. Prozorkevich, and V. D. Toneev. A quantum kinetic equation for particle production in the schwinger mechanism. *International Journal of Modern Physics E*, 07(06):709–722, 1998.
- [116] B. D. Blaschke, V. A. Prozorkevich, G. Röpke, D. C. Roberts, M. S. Schmidt, S. D. Shkirmanov, and A. S. Smolyansky. Dynamical schwinger effect and high-intensity lasers. realising nonperturbative qed. *The European Physical Journal D*, 55(2):341–358, 2009.
- [117] A. Blinne and H. Gies. Pair production in rotating electric fields. *Phys. Rev. D*, 89:085001, Mar 2014.

- [118] E. Strobel and S.-S. Xue. Semiclassical pair production rate for rotating electric fields. *Phys. Rev. D*, 91:045016, Feb 2015.
- [119] A. Blinne and E. Strobel. Comparison of semiclassical and wigner function methods in pair production in rotating fields. *Phys. Rev. D*, 93:025014, Jan 2016.
- [120] S. Shevchenko, S. Ashhab, and F. Nori. Landau-Zener-Stckelberg interferometry. *Physics Reports*, 492(1):1 – 30, 2010.
- [121] W. G. Unruh. Notes on black-hole evaporation. *Phys. Rev. D*, 14:870–892, Aug 1976.
- [122] W. G. Unruh. Experimental black-hole evaporation? *Phys. Rev. Lett.*, 46:1351–1353, May 1981.
- [123] F. X. Dezael and A. Lambrecht. Analogue casimir radiation using an optical parametric oscillator. *EPL (Europhysics Letters)*, 89(1):14001, 2010.
- [124] J. R. Johansson, G. Johansson, C. M. Wilson, and F. Nori. Dynamical casimir effect in superconducting microwave circuits. *Phys. Rev. A*, 82:052509, Nov 2010.
- [125] R. Schützhold and W. G. Unruh. Hawking radiation in an electromagnetic waveguide? *Phys. Rev. Lett.*, 95:031301, Jul 2005.
- [126] S. A. Fulling and P. C. W. Davies. Radiation from a moving mirror in two dimensional space-time: Conformal anomaly. *Proceedings of the Royal Society of London A: Mathematical, Physical and Engineering Sciences*, 348(1654):393–414, 1976.
- [127] N. Birrell and P. Davies. *Quantum Fields in Curved Space*. Cambridge Monographs on Mathematical Physics. Cambridge University Press, 1984.
- [128] C. K. Law. Resonance response of the quantum vacuum to an oscillating boundary. *Phys. Rev. Lett.*, 73:1931–1934, Oct 1994.
- [129] O. Méplan and C. Gignoux. Exponential growth of the energy of a wave in a 1d vibrating cavity: Application to the quantum vacuum. *Phys. Rev. Lett.*, 76:408–410, Jan 1996.
- [130] V. Dodonov, A. Klimov, and V. Man'ko. Generation of squeezed states in a resonator with a moving wall. *Physics Letters A*, 149(4):225 – 228, 1990.
- [131] R. Schützhold, G. Plunien, and G. Soff. Trembling cavities in the canonical approach. *Phys. Rev. A*, 57:2311–2318, Apr 1998.
- [132] V. V. Dodonov, A. B. Klimov, and D. E. Nikonov. Quantum phenomena in resonators with moving walls. *Journal of Mathematical Physics*, 34(7), 1993.
- [133] V. V. Dodonov and A. B. Klimov. Generation and detection of photons in a cavity with a resonantly oscillating boundary. *Phys. Rev. A*, 53:2664–2682, Apr 1996.
- [134] V. Dodonov. Photon creation and excitation of a detector in a cavity with a resonantly vibrating wall. *Physics Letters A*, 207(3):126 – 132, 1995.
- [135] E. SASSAROLI, Y. N. SRIVASTAVA, and A. WIDOM. Photon production by the dynamical casimir effect. *Phys. Rev. A*, 50:1027–1034, Aug 1994.

- [136] C. Braggio, G. Bressi, G. Carugno, C. D. Noce, G. Galeazzi, A. Lombardi, A. Palmieri, G. Ruoso, and D. Zanello. A novel experimental approach for the detection of the dynamical casimir effect. *EPL (Europhysics Letters)*, 70(6):754, 2005.
- [137] E. SASSAROLI, Y. N. Srivastava, and A. Widom. Photon production by the dynamical casimir effect. *Phys. Rev. A*, 50:1027–1034, Aug 1994.

שאלקטרוניים יכולים לעבור בין שתי המתוות על ידי מנהור. כאשר אלקטرون עובר מתחת הוא משאיר אחריו חור במתכת שהוא עזב, כך נוצר זוג של אלקטרון-חור.

זוג אלקטרון-חור בעל אנרגיה גדולה מאפשר יכול להיווצר על ידי פולס של מתח חשמלי שמופעל על צומת המנהור. הראנו שניתן ליצור התabcות רמיי בהסתברות היצירה של זוגות אלקטרון-חור ע"י שני פולסים עוקבים זהים של מתח המופרדים ע"י זמן T . ההסתברות ליצירת זוג אלקטרון-חור תתנדנד כפונקציה של האנרגיה של הזוג כפול הזמן בין פולסי המתח T .

פולס מתח יוצר הרבה זוגות של אלקטרונים-חורים בעלי אנרגיות שונות. מצאנו שניתן לבדוק את ההסתברות ליצירת זוג אלקטרון-חור בעל אנרגיה ספציפית ע"י הנזורה השנייה של הרעש של הזרם דרך המוליך המזוסקופי לפי מתח ישיר. בכך אנו מספקים שיטה חדשה למדידה של התabcות במערכות מזוסקופיות.

התabcות רמיי רגישה לאנרגיה ולפאוזה של החלקיקים במוליך המזוסקופי. לכן היא מאפשרת לנו לחקור את התלות הזמנית של תהליכי שימושיים עליוון, כגון: הטמפרטורה של המערכת, זמן חיים סופי של החלקיקים, אינטראקציה של החלקיקים עם סביבה.

כדוגמה לאינטראקציה של חלקיקים עם סביבה חקרונו את האפקט של סביבה אלקטромגנטית ליניארית על הפאוזה של זוג אלקטרון-חור שנוצר בצומת מנהור. הראנו שהאמפליטודה של תבנית התabcות רמיי מונחתת ע"י האינטראקציה של האלקטרונים עם הסביבה. האmplיטודה מונחתת באופן אקספוננציאלי כתלות בפונקציית הקורלציה של הסביבה. מתוך התלות של האmplיטודה בזמן בין פולסי המתח T ניתן למצוא את פונקציית הקורלציה של הסביבה כתלות בזמן.

עבור סביבה אומנית מצאנו כי המעבר בין הגבולות של עכבה גבוהה ונמוכה תואם למעבר בין תנואה בליסטיות ודיפוסיבית של חלקיק בראוני קוונטי. ניתן לראות מעבר זה עבור נגד בעל התנגדות קבועה ע"י שינוי הזמן בין פולסי המתח T . זהה דוגמא לכך שההתabcות רמיי יכולה לספק מידע חדש על מערכות מוכרות.

תקציר

אחרת התופעות המעניינות של תורה שדות קוונטיות היא שימושו יכול להיווצר מותוֹך הריק. על ידי הגברת דינמית של התנודות הקוונטיות של הריק חלקיקים יכולים להיווצר מותוֹך הוואקום. תהליכי יצירת חלקיקים אלו כוללים את קרינת הוקינג, אפקט שוינגר, אונרו וקזימיר דינמי. בעבודה זו אנו משתמשים בתאכבות רשמי ככלי לחקירה האפקטים הדינמיים של הוואקום.

התאכבות רשמי היא כלי ספקטוסקופי נפוץ במערכות בעלות ספקטרום דיגיטלי, כגון מערכות אוטומיות. אנחנו הכלנו את התאכבות רשמי למערכות בעלות ספקטרום רציף. בכך אנו מספקים שיטה חדשה לבדוק דינמיקה במערכות קוונטיות.

התאכבות רשמי היא תופעה של התאכבות בין שתי אמפליטודות הסתברות קוונטיות. נניח והמערכת הקוונטית נמצאת במצב i . ע"י הפרעה חיצונית ניתן להעביר אותה במצב f בהסתברות מסוימת. אם מפעילים את ההפרעה על המערכת בשני זמנים שונים t_1 ו- t_2 , למערכת יש שתי דרכים להגיע מהמצב i למצב f , דרך ההפרעה ב- t_1 או דרך ההפרעה ב- t_2 . התאכבות בין שתי דרכים אלו היא התאכבות רשמי. ההסתברות למעבר בין i ל- f תתנדנד כתלות בהפרש האנרגיה בין המצבים כפול הזמן בין ההפרעות $t_1 - t_2$.

ישמנו את התאכבות רשמי על מנת לחזור את ההגבר הדינמי של פלקטוואציות הוואקום באפקטים שוינגר וקזימיר דינמי. בכך הראנו כי התאכבות רשמי היא גנריית למערכות קוונטיות מאולצות רבות ולא רק למערכות בעליות שתי רמות.

באופן כללי, ההסתברות לייצור חלקיקים מהוואקום היא קטנה ואפקטים אלו נהיים ברוי מדים רק תחת תנאים קיצוניים. יישמו את התאכבות רשמי במערכת מזוסקופית קוונטית שבה אפקט ההגברת מדים. בכך, אנו מספקים את ההצעה הראשונה למדידה של התאכבות רשמי במערכת עם ספקטרום רציף.

כדוגמה למערכת מזוסקופית בחנו את צומת המנהור. צומת מנהור מורכבת משני מוליכים המופרדים על ידי שכבה מבודדת. השכבה המבודדת דקה מאוד כך

המחקר נעשה בהנחיית פרופסור אריק אקרמן בפקולטה לפיזיקה.

אני מודה לטכניון על התמיכה הכספית הנדיבה בהשתלמותי.

התabcות רומי ככלי לחקירה הדינמית של הואקום הקוונטי

חיבור על מחקר
לשם מילוי חלקו של הדרישות לקבלת התואר דוקטור לפילוסופיה

טל גורן

הוגש לסנט הטכניון – מכון טכנולוגי לישראל
תמוז תשע"ו חיפה יולי 2016